United States
Environmental Protection
Agency

Office of Research and
Development
Washington DC 20460

EPA/600/R-95/051
April 1995

EPA

RCRA Subtitle D (258) Seismic Design Guidance for Municipal Solid Waste Landfill Facilities

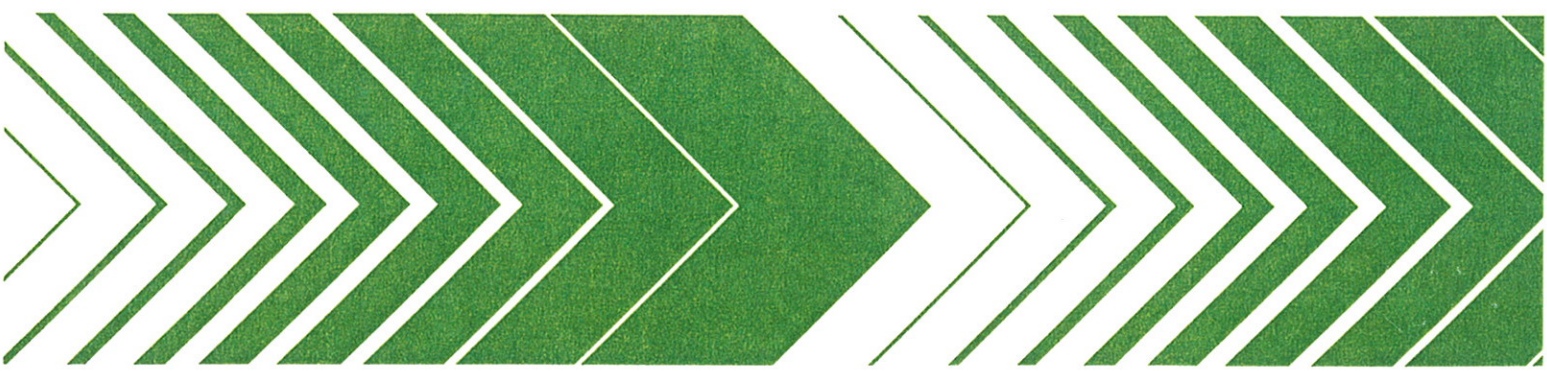

RCRA SUBTITLE D (258) SEISMIC DESIGN GUIDANCE FOR MUNICIPAL SOLID WASTE LANDFILL FACILITIES

By

Gregory N. Richardson
G.N. Richardson & Associates
Raleigh, North Carolina 27603

and

Edward Kavazanjian, Jr.
and
Neven Matasović
GeoSyntec Consultants
Huntington Beach, California 92647

PROJECT MANAGER

Robert Landreth
Waste Minimization, Destruction and
Disposal Research Division
Risk Reduction Engineering Laboratory
Cincinnati, Ohio 45268

Risk Reduction Engineering Laboratory
Office of Research and Development
U.S. Environmental Protection Agency
Cincinnati, Ohio 45268

DISCLAIMER

The information in this document has been funded wholly or in part by the United States Environmental Protection Agency (EPA) under Contract No. 68-C3-0315 WA #05 to Harding Lawson Associates. It has been subjected to the Agency's peer and administrative review, and it has been approved for publication as an EPA document. Mention of trade names or commercial products does not constitute endorsement or recommendation for use.

FOREWORD

Today's rapidly developing technologies, industrial products, and practices frequently carry with them generation of materials that, if improperly dealt with, may threaten both human health and the environment. The United States Environmental Protection Agency (EPA) is charged by Congress with protecting the Nation's land, air, and water resources. Under a mandate of national environmental laws, the Agency strives to formulate and implement actions leading to a compatible balance between human activities and the ability of natural resources to support and nurture life. These laws direct the EPA to conduct research to define our environmental problems, measure the impacts, and search for the solutions.

The Risk Reduction Engineering Laboratory is responsible for planning, implementing, and managing research, development, and demonstration programs. These programs provide an authoritative, defensible engineering basis in support of the policies, programs, and regulations of the EPA with respect to drinking water, wastewater, pesticides, toxic substances, solid and hazardous wastes, and Superfund-related activities. This publication presents information on current research efforts and provides a vital communication link between the researcher and the user community.

Recent RCRA Subtitle D regulations (40 CFR Part 258) establish the requirements that MSW landfills must not be sited where they can be damaged by active ground faulting (258.13) and that they must be designed to resist the effect of regional earthquakes (258.14). This document is intended to provide technical guidance to regulatory reviewers and landfill designers to ensure these objectives are accomplished. It is meant to be a practical design document applicable to the vast majority of MSW landfills.

Further information relative to this document may be obtained by writing Robert Landreth, Risk Reduction Engineering Laboratory, Cincinnati, OH, 45268.

E. Timothy Oppelt, Director
Risk Reduction Engineering Laboratory

ABSTRACT

On October 9, 1993, the new RCRA Subtitle D regulations (40 CFR Part 258) went into effect. These regulations are applicable to landfills receiving municipal solid waste (MSW) and establish minimum Federal criteria for the siting, design, operation, and closure of MSW landfills. These regulations apply to the entire waste containment system, including liners, leachate collection systems, and surface water control systems. This document presents field and design procedures to satisfy the earthquake (or seismic) related criteria contained within these regulations. Sample analyses are provided to evaluate the Subtitle D seismic requirements for a range of site and facility conditions.

Section 258.13 of the regulations requires that new or lateral expansions of existing landfills cannot be sited within 200-feet of a fault that has been active during the Holocene Epoch (past 11,000 years) unless it can be demonstrated that a lesser setback is safe. This document presents field identification methods used to identify active faults. Additionally, the document reviews general tectonic and seismological considerations that strongly suggest that movement of faults during the Holocene Epoch is very rare east of the Rocky Mountains.

Section 258.14 of the regulations identifies seismic impact zones within the United States based on earthquake probability maps prepared by the United States Geological Survey (USGS). Seismic impact zones are defined in the new regulations as those regions having a peak bedrock acceleration exceeding 0.1 g based on a 90% probability of non-exceedance over a 250 year time period. Within seismic impact zones, the regulations require that the waste containment system for new MSW landfills and for lateral expansions of existing MSW landfills be designed to resist the maximum horizontal acceleration in lithified earth material (MHA). The MHA is defined as the maximum expected horizontal acceleration either depicted on a seismic hazard map with a 90 percent probability of non-exceedence in 250 years or based upon a site-specific seismic risk assessment.

This document presents analysis procedures to evaluate the ability of the site subgrade to resist liquefaction and of the waste mass/subgrade to resist slope failure where subjected to the MHA. Sample calculations are provided to demonstrate the analysis techniques for liquefaction and slope stability. Additional discussion is provided regarding more sophisticated deformation analysis methods that may be required for landfills in highly seismic regions.

This report was submitted in fulfillment of Contract No. 68-C3-0315 WA #05 under the sponsorship of the United States Environmental Protection Agency. This report covers a period from November, 1993 to May, 1994, and work was completed as of May, 1994.

TABLE OF CONTENTS

TABLE OF CONTENTS

Appendices

List of Tables

Number

List of Figures

Number

List of Figures (continued)

List of Figures (continued)

List of Figures (continued)

ABBREVIATIONS AND ACRONYMS

ASTM	American Society for Testing and Materials
ATC	Applied Technology Council
CPT	Cone Penetration Test
CSR	Critical Stress Ratio
EERC	Earthquake Engineering Research Center
EERI	Earthquake Engineering Research Institute
EPA	United States Environmental Protection Agency
FSAR	Final Safety Analysis Report
MFZ	Mendocino Fracture Zone
MHA	Maximum Horizontal Acceleration
MM	Modified Mercali (Intensity Scale)
MSW	Municipal Solid Waste
MSWLF	Municipal Solid Waste Landfill Facility
NAPP	National Aerial Photographic Program
NCEER	National Center for Earthquake Engineering Research
NRC	National Research Council
OII	Operating Industries, Inc. (Landfill)
PSAR	Preliminary Safety Analysis Report
RCRA	Resource Conservation and Recovery Act
SDOF	Single Degree of Freedom (System)
SPT	Standard Penetration Test
SSA	Seismological Society of America
USGS	United States Geological Survey

ACKNOWLEDGEMENTS

The authors wish to express their sincere appreciation to the following individuals who reviewed and critiqued drafts of this manuscript: Dr. Rudolph Bonaparte, GeoSyntec Consultants, Professor Jonathan Bray, University of California of Berkeley, Mr. Ron Chaney, Federal Highways Administration, Professor Robert Koerner, Drexel University, Professor Gerald Leonards, Purdue University, Mr. Robert Phaneuf, New York State Department of Environmental Conservation, and Mr. Robert Landreth, United States Environmental Protection Agency. The authors also thank the New York Department of Environmental Conservation for providing case studies used in the sample calculations.

The authors also gratefully acknowledge the many individuals, too numerous to name here, who over the years have shared their experiences and recommendations regarding seismic probability studies, liquefaction analysis, and dynamic stability evaluation.

SECTION 1

INTRODUCTION

On October 9, 1993, the RCRA Subtitle D regulations (40 CFR Part 258) went into effect. These regulations are applicable to landfills receiving municipal solid waste (MSW) and establish minimum Federal criteria for the site location, design, operation, ground-water monitoring, and closure/post closure care of MSW landfills. This document focuses on the earthquake (or seismic) siting and facility design criteria contained within Subtitle D. The document is intended for use by both designers of MSW landfills and the regulatory community that reviews such designs. Where possible, actual landfill situations have been used in the development of example problems to demonstrate the various analysis procedures. Emphasis is placed herein on simple analysis methods that are within the technical capabilities of the general engineering community. The range of applicability and the limitations of these methods are reviewed and more rigorous analysis methods are summarized.

1.1 Introduction to Subtitle D Seismic Criteria

Subtitle D regulations address the potential for damage to a MSW landfill resulting from relative ground displacements (e.g., fault displacement) and from strong ground motions (e.g., ground accelerations) that can accompany an earthquake. Limiting the potential for fault displacement-induced damage is accomplished by siting criteria (258.13) that may preclude the use of a given site for a MSW landfill. The impact of earthquake-induced strong ground motions on a MSW landfill must be addressed by the design engineer. Subtitle D does not specify the required evaluation process but establishes (258.14) the maximum horizontal acceleration (MHA) in lithified earth material based on United States Geological Survey (USGS) earthquake probabilistic studies as the minimum site peak bedrock acceleration that must be considered in the design of landfill containment structures. Landfill containment structures are defined to include liners, leachate collection systems, and surfaces water control systems.

1.1.1 Part 258.13 Fault Zone Siting Criteria

The Federal Subtitle D regulations state that a new MSW landfill or a lateral expansion of an existing landfill may not be located within 200 feet (60 meters) of a fault that has experienced displacement in the Holocene time unless the owner or operator demonstrates to the Director of an approved State Program that an alternative setback distance of less that 200 feet (60 meters) will prevent damage to the structural integrity of the landfill unit and will be protective of human

health and the environment. Within the regulations, a fault means a fracture or zone of fractures along which strata from one side have been displaced with respect to strata on the other side. The Holocene time means the most recent epoch of the Quaternary period, e.g. within the last 10,000 to 12,000 years. This requirement means that MSW landfill site suitability studies must both identify potential fault zones that impact the proposed site and then evaluate whether fault displacement has occurred during the past 10,000 to 12,000 years. Section 2.0 of the document presents the technical methodology for identifying fault zones and for complying with the regulatory criteria.

1.1.2 Part 258.14 Seismic Impact Zones

A seismic impact zone is defined in the Subtitle D regulations as an area having a 10% or greater probability that the peak horizontal acceleration in lithified earth material, expressed as a percentage of the earth's gravitational pull (g), will exceed 0.10 g in 250 years. These zones may be defined using seismic probability maps prepared by the USGS (USGS, 1982 and USGS, 1991) or by more detailed regional or site specific studies. The USGS maps present peak bedrock accelerations and velocities reflecting a 90% probability that the acceleration will not be exceeded over 10, 50 and 250 year interval periods. Seismic impact zones in the United States, defined by application of the Subtitle D criteria to the USGS seismic probability maps, are shown in Figure 1.1.

Section 3.0 of this document provides general background information on the development of the USGS seismic probability maps, some regional alternatives, and a simple interpretation of the meaning and use of the peak bedrock acceleration. Section 4.0 provides methodologies for calculating the peak ground surface acceleration at a landfill site and the peak surface acceleration and peak average acceleration of the waste mass based on site characteristics and peak bedrock acceleration. These peak ground accelerations are then used in Section 5.0 for evaluating the liquefaction potential of a site and in Section 6.0 for evaluating the stability of a landfill foundation, waste mass, and waste slopes. Sections 5.0 and 6.0 present simplified seismic analysis procedures that can typically be performed without the need for supplemental field investigative programs or expensive specialized laboratory and sophisticated dynamic analyses.

1.2 Limitations of this Document

This document presents a set of simplified analyses for seismic performance analysis of the waste mass, liner and cover systems, and foundation of a MSW landfill within a seismic impact

zone. These simplified analyses described herein are presented as an example of one way, but not necessarily the only way, in which such a seismic performance assessment may be conducted.

The simplified analyses presented herein are designed to produce a generally conservative assessment of the seismic resistance of the landfill containment systems. If such simplified analyses indicate potential seismic problems (e.g. results in unacceptable factors of safety), then more sophisticated analysis methods may still demonstrate satisfactory performance of the facility.

This document addresses the seismic design of the landfill waste mass, liner and cover systems, and foundation, only. Additional analyses may be required to assess the performance of other components of the landfill containment systems, including the leachate collection system and surface-water control systems.

1.3 References

EPA (1993), "Technical Manual: Solid Waste Disposal Facility Criteria," United States Environmental Protection Agency, EPA 530-R93-017, Washington, District of Columbia.

USGS (1982), "Probabilistic Estimates of Maximum Acceleration and Velocity in Rock in the Continuous United States," United States Geological Survey, Open-File Report 82-1033.

USGS (1991), "Probabilistic Earthquake Acceleration and Velocity Maps for the United States and Puerto Rico," United States Geological Survey, Miscellaneous Field Studies Map MF-2120.

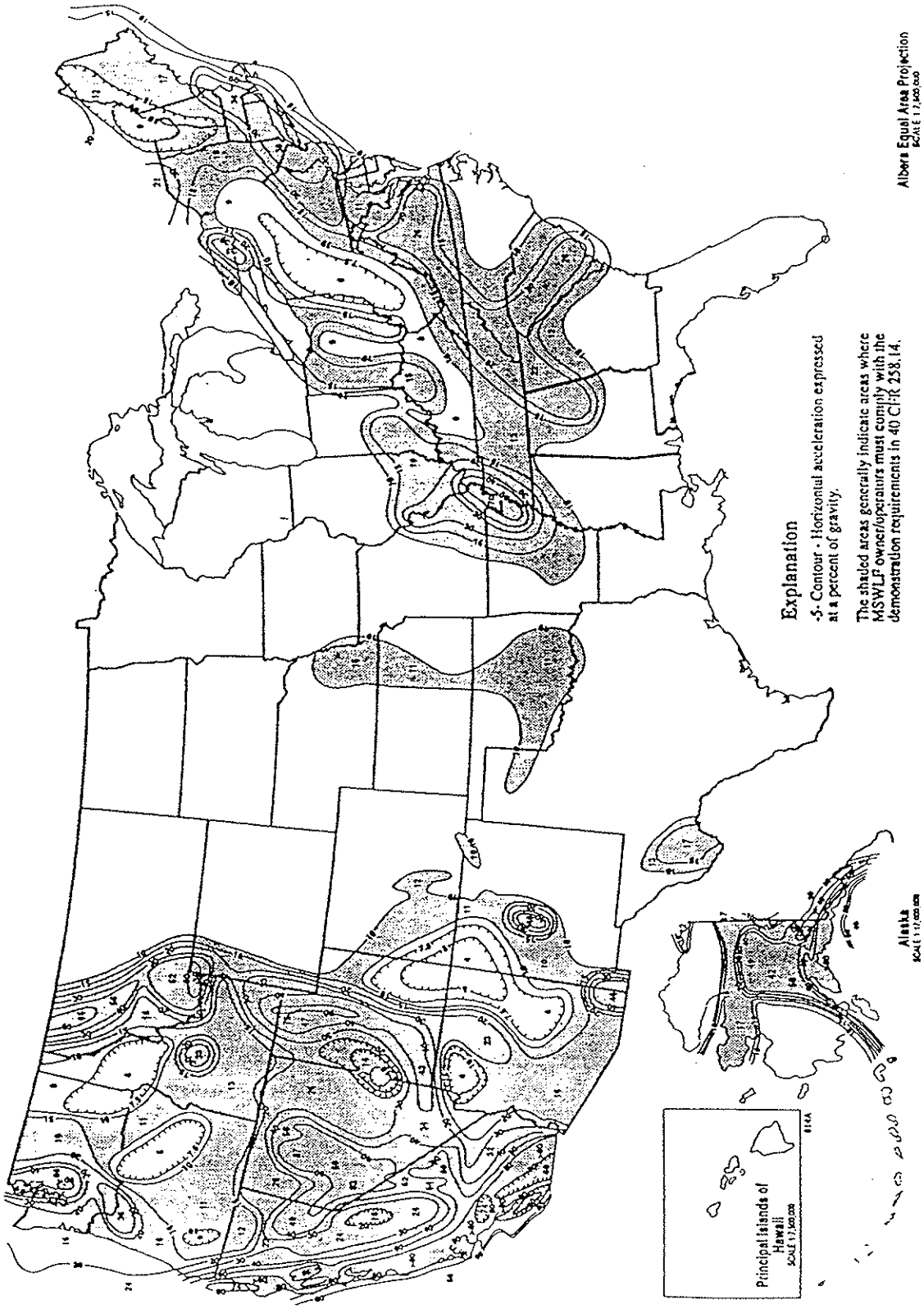

Figure 1.1 Seismic Impact Zones (Areas With a 10% or Greater Probability that the Maximum Horizontal Acceleration Will Exceed 0.10 g in 250 Years) (EPA, 1993).

SECTION 2

258.13 FAULT AREA CONSIDERATIONS

Locating a landfill in the vicinity of faults that have experienced relative movement in recent times poses significant risk to the integrity of the landfill containment system. The impact to the landfill from a seismic event can result directly from ground surface rupture or from deformation, liquefaction, lateral spreading, and differential settlement induced by ground shaking that accompanying the event. The fault area location restrictions imposed by Subtitle D restrict siting of new MSW units or lateral expansions of existing units within 200 feet (60 meters) of a fault that has displaced in Holocene time.

This section of the guidance document reviews methods for evaluating both the presence of faults on-site and the possible movement of a fault within the Holocene Epoch. The section concludes with a discussion regarding the difficulty in applying such methodology to faults located east of the Rocky Mountains.

2.1 Regional Fault Characteristics

Faults are created when the stresses within geologic materials exceed the ability of those materials to withstand the stresses. An understanding of such stresses is aided by a review of current plate tectonics theory. Figure 2.1 shows the major tectonic plates that form the earth's continents and their directions of movement. Along the west coast, earthquakes are the result of two different fault systems that occur along the edge of the Pacific and North American plates. South of the Mendocino Fracture Zone (MFZ) approximately 200 miles (320 kilometers) north of San Francisco, the San Andreas fault system (strike-slip) controls earthquakes. North of the MFZ, earthquakes are controlled by the Cascadia Subduction Zone. The sense of the fault displacement within these fault systems range from horizontal (strike-slip) to vertical (dip-slip) to combinations of these components. These major fault systems and one suggested representation of the major seismic source areas in the United States are shown in Figure 2.2. The Roman numerals on this figure represent the maximum observed (historic) seismic intensity in the region as measured by the Modified Mercali (MM) intensity scale (Richter, 1958).

In contrast to the west coast, earthquakes east of the Rocky Mountains cannot be associated with the relative displacements of edge-plate faults (active margin). Intra-plate (passive margin) earthquakes occur less frequently than the edge-plate associated earthquakes of the west coast but impact a significantly larger geographic area. Table 2.1 presents a summary of significant

earthquakes in Eastern North America in historic time, ordered by decreasing magnitude. As this table shows, the pattern of significant earthquakes east of the Rocky Mountains is broadly dispersed both geographically and temporally.

The differences in the sizes of affected areas may be caused by the differences in stress conditions in the basement rock structure. In the west, the stress condition is predominantly tension, while in the east, stresses in the basement rock are primarily compressional. Whatever the mechanism, the rate of attenuation of earthquake ground motions east of the Rocky Mountains appears to be significantly slower than in the western United States (Nuttli, 1974; 1981), resulting in a much larger impacted area in the eastern U.S. than the western U.S. for earthquakes of the same magnitude. For equivalent historical earthquakes, Figure 2.3 shows the isoseismal contours of MM VI and VII for an event at the plate boundary in the western United States and for two intra-plate events in the eastern United States. Note the small geographic area impacted by the western edge-plate event as compared to the two intra-plate event; one that shook a large portion of the central United States centered around New Madrid and one that shook far beyond Charleston, even into Canada. Another observed difference between earthquakes in the eastern and western U.S. is that eastern earthquakes appear to be enriched in high frequency components compared to western earthquakes (Atkinson, 1987).

The significance of the differences between western edge-plate earthquakes and the intra-plate events that occur east of the Rockies with respect to identification of surface faulting is discussed subsequently within this section. The significance of the differences between western and eastern earthquakes with respect to frequency content is discussed in subsequent sections.

Characterization of the seismicity of the eastern and central U.S. is a topic of much current study and discussion (Applied Technology Council (ATC), 1994). Due to the many ongoing studies, our understanding of the seismicity of the central and eastern United States is evolving rapidly. Prudent investigators should consult current sources of information on local and regional seismicity at the initiation of any project. Sources of current information are discussed subsequently in this section.

2.2 Site Fault Characterization

The principal factors controlling the general characteristics of surface faulting are: (a) the type of fault (reverse, normal, or strike-slip), (b) the inclination of the fault plane, (c) the amount of displacement on the fault, (d) the depth and geometry of the surficial earth materials, and (e) the nature of the overlying earth materials. Strike-slip faults that are not fairly linear may produce

complex surface features. Step-over zones where fault displacement is transferred from adjacent strike-slip faults may be particularly complex. Dip-slip faults, with either normal or reverse motion, typically produce multiple fractures within rather wide and irregular fault zones. These zones generally are confined to the hanging-wall side of the fault leaving the footwall side little disturbed. With respect to fault impacts on a structure, setback requirements for such faults may be rather narrow on the footwall side, depending on the quality of data available, and larger on the hanging wall side of the zone. Some fault zones may contain broad deformational features such as pressure ridges and sags rather than clearly defined fault scarps or shear zones (Hart, 1990).

An investigation to identify faulting at a given site must rely on a review of available data and field geologic reconnaissance methods. Available data may include pertinent technical publications, unpublished reports, maps, aerial photographs, and interviews with experts familiar with the region under study. Pertinent technical publications include maps prepared by the USGS identifying young faults in the western states, publications of the Seismological Society of America, and regional reports from the seismological networks and state geological surveys. A detailed summary of available sources of engineering geologic information is presented by Trautmann and Kulhawy (1983). General sources for such information are indicated on Table 2.2. Table 2.3 provides a listing of addresses of the geological survey offices for all 50 states.

Studies performed for siting of nuclear power plants can be a particularly useful source of information on regional seismicity and geology. All applications for construction permits for nuclear generating stations are required to submit documentation on regional geology, including known faults and observed seismicity, within a 200 mile (320 kilometer) radius of the site. This information can be found in the Preliminary Safety Analysis Report (PSAR) and the Final Safety Analysis Report (FSAR) for the project. These reports are available through the National Technical Information Service (see Table 2.3) for all existing and many proposed nuclear generating stations.

Existing seismic networks provide very detailed identification of recent earthquakes within seismic impact regions. Such information includes the magnitude and epicentral location of all identified events and is commonly available plotted in map form as shown on Figure 2.4. A detailed evaluation of each detected event is also available as shown on Table 2.4. Note that while the presence of micro-seismic activity can be used to infer the location of a subsurface fault, it cannot be directly interpreted as evidence that surface displacement of the fault has taken or will take place. To date, the only known earthquake east of the Rocky Mountains in historic

time that has been accompanied by observations of surface fault rupture is the 1989 Ungava, Quebec earthquake of magnitude 6.3. The Meers fault in Oklahoma, where evidence points to a magnitude 7+ earthquake within the past 1,100 to 1,400 years, is the only other recognized Holocene fault east of the Rocky Mountains.

An interpretation of available stereo aerial photographs is useful in identifying and locating potentially active faults. One source of such photographs is provided in Table 2.3. Other sources are discussed by Trautmann and Kulhawy (1983). Active faults may be indicated in aerial photographs by geomorphic features such as fault scarps, triangular facets, fault scarplets, fault rifts, fault slice ridges, shutter ridges, and fault saddles (Cluff and Etal, 1972). Additional evidence can be provided by ground features such a open fissures, offsets in fence lines, landscape features, mole tracks and furrows, etc., rejuvenated streams, folding or warping of young deposits, ramps, ground water barriers in recent alluvium, echelon faults in alluvium, and fault paths on young surfaces. Usually a combination of such features is generated by recent fault movements at the surface. Note that many of the fault movement indicators require the presence of undisturbed surface soils at the site. Regions that have limited surface soils due to past geologic mechanisms or man's activities can provide a significant challenge in demonstrating the recent activity of existing faults. The aerial photo analysis should include an area within a five-mile radius of the site.

Initial field reconnaissance should be performed at a minimum for the area within approximately 1-kilometer (3300-feet) of the proposed unit. This initial field reconnaissance can include the following:

- walking portions of the site within 1-kilometer (3300 feet) of the unit to identify possible geomorphic or ground features that indicate faulting;

- preparation and interpretation of special aerial photographs such as low sun angle photographs that use shadows to accentuate topographic differences, infrared photos that indicate differences in surface moisture content, and color photographs to study slight color changes.

Section 2.3 discusses the field methods for establishing fault movement.

2.3 Defining Fault Movement in Holocene Epoch

If the site fault characterization study indicates the potential presence of faults on the proposed landfill site, then a detailed geologic reconnaissance may be required for the site of the proposed unit. A detailed geologic surface reconnaissance should be made to identify the best approximation of the fault location on site and the amount of sense of past fault movements. The detailed field site characterization can include the following:

- using geophysical methods such as resistivity, seismic refraction, or magnetic methods to identify specific fault locations;

- excavation of exploratory trenches at an angle to faults identified on the site to allow the detailed examination of the trench walls for evidence of recent fault displacements; and

- subsurface drilling exploration to locate fault zones.

The depth of the subgrade investigated should be sufficient to represent activities within the Holocene Epoch. Radiocarbon dating of carbonaceous material encountered can be used to constrain the age of most recent fault offsets. A detailed description of soil-stratigraphic dating techniques is presented by Shlemon (1985). Sieh et. al (1984) describe the application of high-precision radiocarbon analyses for chronological analysis of active faulting. Note that establishing that recent displacement has occurred is greatly complicated if a limited soil profile over rock exists at the site, e.g., glacially polished regions, or if the Holocene zone of the alluvium is absent or disturbed.

Trenching across a fault through overlying alluvium and colluvium has been the most common tool used to establish both the existence of fault displacement and for dating the displacement. Trench geologic sections established by trenching for portions of the Hayward fault in California are shown on Figure 2.5. These trench sections established that the western trace of the Hayward fault was active (e.g., the fault displacements projected up through the overlying alluvium) and that the eastern trace was not active. These observations are shown on Figure 2.6. Note the distinct stratigraphic displacements that identify the west fault trace. Thus, this study would lead to the requirement that all proposed MSW landfills be located more than 60 meters (200 feet) from the western trace of the Hayward fault. Since the eastern trace of the Hayward fault was found not to be active, there are no regulatory constraints that would exclude siting a MSW landfill adjacent to the eastern trace of the Hayward fault on the basis of faulting.

2.4 Comments on Fault Considerations East of the Rockies

In recent years, seismologists have expressed significant concern regarding our lack of understanding of the source of earthquakes, referred to as seismogenesis, in the eastern United States. Plate tectonic theories are not adequate to explain the mechanisms associated with intra-plate earthquakes. Recent workshops and seminars on the seismogenesis and seismicity of the eastern United States (SSA, 1988; ATC, 1994) have shown that some widely accepted views on earthquake origins are inconsistent with recent observations and that a global perspective may be required to understand intra-plate seismogenesis. Obviously such concerns are beyond the scope of this document. It is, however, important to realize the following observations regarding earthquake/fault considerations east of the Rocky Mountains:

- Earthquake source zones do appear to be related to subsurface crustal structure. However, these source zones do not appear to be related to surface expressions of faulting (ATC, 1994).

- The relationship between intra-plate earthquakes and the potential for surface faulting remains in question. This is in part due to the lack of either accumulated strain or significant seismic events in the eastern and central United States.

- Detailed comparison of earthquake hypocenters and known surface fault locations have failed to provide a correlation (Himes et al., 1988).

- Only two faults that have experienced ground surface displacement during the Holocene Epoch have been identified east of the Rocky Mountains.

Current seismological understanding of seismogenesis east of the Rocky Mountains strongly suggests that significant efforts to define seismically active faults in this region may not be useful. The region of capable faults identified on Figure 2.2 reaches to the Meers fault in Oklahoma but clearly excludes most of the Midwest and all of the Eastern United States.

2.5 References

Adams, J., and Basham, P.W. (1994), "New Knowledge of Northeastern North American Earthquake Potential," Proc. *Seminar on New Developments in Earthquake Ground Motion Estimation and Implications for Engineering Design Practice*, Applied Technology Council, ATC35-1, Redwood City, California, pp. 3-1 - 3-20.

ATC (1994), "Seminar on New Developments in Earthquake Ground Motion Estimation and Implications for Engineering Design Practice," Applied Technology Council, ATC35-1, Redwood City, California.

Atkinson, G.M. (1987), "Implications of Eastern Ground Motion Characteristics for Seismic Hazard Assessment in Eastern North America," Proc. *Symposium on Seismic Hazards, Ground Motions, Soil-Liquefaction and Engineering Practice in Eastern North America*, Tuxedo, New York, NCEER Technical Report No. NCEER-87-0025.

Cluff, L.S, Hansen, W.R., Taylor, C.L., Weaver, K.D., Brogan, G.E., Idriss, I.M., McClure, F.E., and Blayney, J.A. (1972), "Site Evaluation in Seismically Active Regions - An Interdisciplinary Team Approach," Proc. *International Conference on Microzonation for Safety Construction, Research and Application*, Seattle, Washington, Vol. 2, p. 9-57 - 9-87.

Engdahl, E.R., and Rinehard, W.A. (1988), "Seismicity Map of North America," *Geologic Society of America*, Centennial Special Map CSM-4, Scale 1:5,000,000.

Geotimes (1980), "A Directory of Societies in Earth Science," Vol. 25, No. 7, pp. 21-29.

Hart, E.W. (1990), "Fault-Rupture Zones in California," *Special Publication 42*, California Division of Mines and Geology, Sacramento, California.

Himes, L., Stauder, W., and Herrmann, R.B. (1988), "Indication of Active Faults in the New Madrid Seismic Zone from Precise Location of Hypocenters," National Workshop on Seismogenesis in the Eastern United States, A.C. Johnston, et al, Eds. (also presented in Seismological Research Letters, Vol. 59, No. 4, Seismological Society of America).

Johnston, A.C., and Nava, S.J. (1994), "Seismic Hazard Assessment in the Central United States," Proc. *Seminar on New Developments in Earthquake Ground Motion Estimation and Implications for Engineering Design Practice*, Applied Technology Council, ATC35-1, Redwood City, California, pp. 2-1 - 2-12.

Krinitzsky, E.L., Gould, J.P. and Edinger, P.H. (1993), "*Fundamentals of Earthquake-Resistant Construction*," John Wiley & Sons, New York, New York.

Nuttli, O.W. (1974), "Seismic Hazard of the Rocky Mountains," Preprint 2/95, American Society of Civil Engineers, National Structural Engineering Meeting, Cincinnati, Ohio.

Nuttli, O.W. (1981), "Similarities and Differences Between Western and Eastern United States Earthquakes, and their Consequences for Earthquake Engineering," Earthquakes and Earthquake Engineering: The Eastern United States, Vol. 1, Assessing the Hazard - Evaluating the Risk, J.E. Beavers, Ed., Ann Arbor Science Publishers, Inc., Ann Arbor, Michigan, pp. 25-51.

Park, R.G. (1983), *Foundations of Structural Geology*, Blackie Publishing, Chapman and Hall, New York, New York.

Richter, C.F. (1958), *Elementary Seismology*, W.H. Freeman and Company, San Francisco, California.

Shlemon, R.J. (1985), "Application of Soil-Stratigraphic Techniques to Engineering Geology," *Bulletin of the Association of Engineering Geologists*, Vol. XXII, No. 2, pp. 129-142.

Sibol, M.S., Bollinger, G.A., and Mathena, E.C. (1984), "Seismicity of the Southern United States," Southeastern U.S. Seismic Network Bulletin No. 15, Seismologic Observatory, Virginia Polytechnic Institute and State University, Department of Geological Sciences, Blacksburg, Virginia.

Sieh, K., Stuiver, M., and Brillinger, D. (1989), "A More Precise Chronology of Earthquakes Produced by the San Andreas Fault in Southern California," *Journal of Geophysical Research*, Vol. 94, No. B1, pp. 603-623.

SSA (1988), "National Workshop on Seismogenesis in the Eastern United States," A.C. Johnston, A.C. et al., Eds. (presented in Seismological Research Letters, Vol. 59, No. 4, Seismological Society of America).

Trautmann, C.H., and Kulhawy, F.H. (1983), "Data Sources for Engineering Geologic Studies," *Bulletin of the Association of Engineering Geologists*, Vol. XX, No. 4, pp. 439-454.

TABLE 2.1: SIGNIFICANT EARTHQUAKES IN EASTERN NORTH AMERICA
SOURCE: ADAMS AND BUSHAM (1994)

Earthquake	Year	M	Comments
New Madrid Region	1812	8.7	largest stable craton eq.
New Madrid Region	1811	8.6	
New Madrid Region	1812	8.4	
Baffin Bay	1933	7.3	largest Arctic earthquake
Grand Banks	1929	7.2	27 dead from tsunami
Charlevoix, Que	1663	7.0	earliest large earthquake
Charleston, SC	1886	6.9	devastating
Nahanni, N.W.T.	1985	6.9	prior M 6.6 event
Charlevoix, Que	1870	6.5	
Ungava, Que	1989	6.3	10 km surface rupture
Charleston, MO	1895	6.2	
Timiskaming, Que	1935	6.2	Quebec/Ontario border
Charlevoix, Que	1925	6.2	
Cape Ann, offshore	1755	6.1	might be larger
Charlevoix, Que	1791	6.0	
New Madrid Region	1843	6.0	
Charlevoix, Que	1860	6.0	
Franklin L., N.W.T.	1992	6.0	
Saguenay, Quebec	1988	5.9	shaking equivalent to M 6.5
Giles County, VA	1897	5.8	
Massena/Cornwall	1944	5.8	Ontario/NY border
Miramichi, N.B.	1982	5.7	shallow, three M 5 aftershocks
Attica, NY	1929	5.5	western NY

TABLE 2.2: SOURCES OF INFORMATION

Aerial Photographs	National Aerial Photographic Program (NAPP) National High Altitude Program (NHAP) USGS EROS Data Center Sioux Falls, South Dakota (605) 594-6151
Young Fault Maps	United States Geological Survey (USGS) USGS National Center 1-(800) USA-MAPS or USGS Map Sales Center (303) 236-7477
National Seismicity	National Earthquake Information Center United States Geological Survey (USGS) P.O. Box 25046, Denver Federal Center, MS 967 Denver, CO 80225 (800) 525-7848
	Earthquake Engineering Research Institute (EERI) 499 14th Street, Suite 320 Oakland, California 94612 (510) 451-0905
	National Center for Earthquake Engineering Research (NCEER) State University of New York at Buffalo Red Jacket Quadrangle Buffalo, New York 14260 (716) 645-3391
	Seismological Society of America (SSA) National and Eastern Section El Cerrito, California (415) 525-5474
National Technical Information Service	5285 Port Royal Road Springfield, VA 22161 (703) 487-4650 FTS 737-4650

TABLE 2-3: ADDRESSES OF STATE GEOLOGICAL SURVEY OFFICES
SOURCE: GEOTIMES (1980)

Geological Survey of Alabama
Drawer 0, University, Ala., 35486

Alaska Division of Geological & Geophysical Surveys
3001 Porcupine Drive, Anchorage, Alaska, 99501

Arizona Bureau of Geology & Mineral Technology
University of Arizona, Tucson, Ariz., 85721

Arkansas Geological Commission
Vardelle Parham Geology Center, 3815 West Roosevelt Road, Little Rock, Ark., 72204

California Division of Mines & Geology
1416 Ninth St., Room 1341, Sacramento, Calif., 95814

Colorado Geological Survey
1313 Sherman St., Room 715, Denver, Colo., 80203

Connecticut Natural Resources Center
Room 553, State Office Building, 165 Capitol Ave., Hartford, Conn., 06115

Delaware Geological Survey
University of Delaware, Newark, Del., 19711

Florida Bureau of Geology
903 West Tennessee St., Tallahassee, Fla., 32304

Georgia Department of Natural Resources
Earth & Water Division, 19 Hunter St. SW, Room 400, Atlanta, Ga., 30334

Hawaii Division of Water & Land Development
Box 373, Honolulu, Hawaii, 96809

Idaho Bureau of Mines & Geology
Moscow, Idaho, 83843

Illinois Geological Survey
121 Natural Resources Building, Urbana, Ill., 61801

Indiana Geological Survey
611 North Walnut Grove, Bloomington, Ind., 47401

Iowa Geological Survey
123 North Capitol St., Iowa City, Iowa, 52242

Kansas Geological Survey
1930 Avenue A, Campus West, University of Kansas, Lawrence, Kan., 66044

Kentucky Geological Survey
311 Breckinridge Hall, University of Kentucky, Lexington, Ky., 40506

Louisiana Geological Survey
Box G, University Station, Baton Rouge, La., 70803

Maine Bureau of Geology
State Office Building, Room 211, Augusta, Me., 04330

Maryland Geological Survey
Merryman Hall, Johns Hopkins University, Baltimore, Md., 21218

Massachusetts Department of Environmental Quality Engineering
Division of Waterways, 100 Nashua St., Room 532, Boston, Mass., 02114

Michigan Geological Survey Division
Box 30028, Lansing, Mich., 48909

Minnesota Geological Survey
1633 Eustis St., St Paul, Minn., 55108

Mississippi Geologic, Economic & Topographic Survey
Box 4915, Jackson, Miss., 39216

Missouri Division of Geological & Land Survey
Box 250, Rolla, Mo., 65401

Montana Bureau of Mines & Geology
Montana College of Mineral Science & Technology, Butte, Mont., 59701

Nebraska Conservation & Survey Division
University of Nebraska, Lincoln, Neb., 68508

Nevada Bureau of Mines & Geology
University of Nevada, Reno, Nev., 89557

New Hampshire Department of Resources & Economic Development
James Hall, University of New Hampshire, Durham, N.H., 03824

New Jersey Bureau of Geology & Topography
Box 1390, Trenton, N.J., 08625

New Mexico Bureau of Mines & Mineral Resources
Socorro, N.M., 87801

New York State Geological Survey
New York State Education Building, Room 973, Albany, N.Y., 12224

North Carolina Department of Natural Resources & Community Development
Geological Survey Section, Box 27687, Raleigh, N.C., 27611

North Dakota Geological Survey
University Station, Grand Forks, N.D., 58202

Ohio Division of Geological Survey
Fountain Square, Building 6, Columbus, Ohio, 43224

Oklahoma Geological Survey
830 Van Vleet Oval, Room 163, Norman, Okla., 73069

Oregon Department of Geology & Mineral Industries
1069 State Office Building, 1400 SW Fifth Ave., Portland, Ore., 97201

Pennsylvania Bureau of Topographic & Geologic Survey
Department of Environmental Resources, Box 2357, Harrisburg, Pa., 17120

Puerto Rico Service Geologico
Apartado 5887, Puerta de Tierra, San Juan, P.R., 00906

South Carolina Geological Survey
State Development Board, Harbison Forest Road, Columbia, S.C., 29210

South Dakota Geological Survey
Science Center, University of South Dakota, Vermillion, S.D., 57069

Tennessee Division of Geology
G-5 State Office Building, Nashville, Tenn., 37219

Texas Bureau of Economic Geology
University of Texas, Box X, University Station, Austin, Tex., 78712

Utah Geological & Mineral Survey
606 Black Hawk Way, Salt Lake City, Utah, 84108

Vermont Geological Survey
Agency of Environmental Conservation, Montpelier, Vt., 05602

Virginia Division of Mineral Resources
Box 3667, Charlottesville, Va., 22903

Washington Division of Geology & Earth Resources
Olympia, Wash., 98504

West Virginia Geological & Economic Survey
Box 879, Morgantown, W. Va., 26505

Wisconsin Geological & Natural History Survey
1815 University Ave., Madison, Wis., 53706

Wyoming Geological Survey
Box 3008, University Station, University of Wyoming, Laramie, Wyo., 82071

TABLE 2-4: DETAILED SEISMIC EVENT DATA AVAILABLE FROM USGS NATIONAL EARTHQUAKE INFORMATION CENTER

AUGUST 1988

KEY	DAY	ORIGIN TIME UTC HR	MN	SEC	GEOGRAPHIC COORDINATES LAT		LONG		DEPTH	MAGNITUDES GS MB	Msz	SD	NO. STA USED	REGION, CONTRIBUTED MAGNITUDES AND COMMENTS
	01	00	16	25.5%	34.940	N	139.169	E	10 G			0.2	5	NEAR S. COAST OF HONSHU, JAPAN. Felt (II JMA) on Os and (I JMA) at Ajiro.
	01	01	12	03.47	34.92	N	139.14	E	10 G			0.2	4	NEAR S. COAST OF HONSHU, JAPAN. Felt (I JMA) at Aji Mishima and on Oshima.
	01	01	16	27.1	34.949	N	139.161	E	10 G	4.5		0.6	21	NEAR S. COAST OF HONSHU, JAPAN. Felt (III JMA) at Ajiro; (II JMA) at Toteyama and on Oshima; (I JMA) Mishima and Yokohama.
	01	01	34	25.0%	34.918	N	139.142	E	10 G			0.2	6	NEAR S. COAST OF HONSHU, JAPAN. Felt (II JMA) at Aj and (I JMA) at Mishima, Tokyo and on Oshima.
	01	01	39	21.6	34.849	N	139.279	E	10 G	4.9	4.5	1.3	106	NEAR S. COAST OF HONSHU, JAPAN. Felt (IV JMA) at Aj (III JMA) at Toteyama, Mishima, Yokohama and on Osh (II JMA) at Nagaisuro and Tokyo; (I JMA) at Kawaguchi-ko.
	01	02	03	48.3	19.812	S	68.861	W	117 D	4.4		1.0	29	CHILE-BOLIVIA BORDER REGION
	01	02	12	49.9	45.145	N	6.678	E	5 G			1.1	15	FRANCE. ML 2.5 (GEN), 2.3 (LDG).
	01	02	46	58.5	17.632	S	178.782	W	561	4.9		0.9	118	FIJI ISLANDS REGION
	01	02	58	28.1%	34.988	N	139.148	E	10 G			0.4	7	NEAR S. COAST OF HONSHU, JAPAN. Felt (II JMA) on Oshima; (I JMA) at Ajiro.
	01	03	04	45.8%	34.932	N	139.144	E	10 G			0.2	6	NEAR S. COAST OF HONSHU, JAPAN. Felt (II JMA) at Aj (I JMA) at Mishima and on Oshima.
	01	03	07	52.3*	52.138	N	158.596	E	46 D	4.7		0.6	9	NEAR EAST COAST OF KAMCHATKA
	01	04	39	53.8	18.022	S	177.031	W	389	4.8		0.8	82	FIJI ISLANDS REGION
	01	04	39	57.3	1.663	N	125.867	E	222 *	5.8		0.9	22	MOLUCCA PASSAGE
	01	04	53	36.5*	34.944	N	139.883	E	10 G			1.5	5	NEAR S. COAST OF HONSHU, JAPAN. Felt (I JMA) at Aji Mishima and on Oshima.
	01	05	13	07.3	34.896	N	139.165	E	10 G			0.3	7	NEAR S. COAST OF HONSHU, JAPAN. Felt (II JMA) on Oshima; (I JMA) at Ajiro, Mishima and Toteyama.
	01	06	23	24.9*	34.931	N	139.184	E	10 G			0.4	5	NEAR S. COAST OF HONSHU, JAPAN. Felt (I JMA) on Osh
	01	06	27	07.27	5.18	S	150.55	E	164 ?	3.5		1.5	8	NEW BRITAIN REGION
	01	06	28	47.6*	51.251	N	176.039	W	33 H	4.5		1.0	15	ANDREANOF ISLANDS, ALEUTIAN IS. ML 4.1 (PMR).
	01	06	47	55.9	53.618	N	163.516	W	33 H	4.8		0.9	68	UNIMAK ISLAND REGION. ML 4.5 (PMR).
	01	06	02	28.4	34.928	N	139.172	E	10 G			0.2	7	NEAR S. COAST OF HONSHU, JAPAN. Felt (II JMA) at Aj and on Oshima; (I JMA) at Toteyama.
	01	06	12	14.6*	34.917	N	139 155	E	10 G			0.2	5	NEAR S. COAST OF HONSHU, JAPAN. Felt (I JMA) at Aji
	01	06	23	09.5	34.929	N	139.160	E	10 G	4.2		0.9	11	NEAR S. COAST OF HONSHU, JAPAN. Felt (II JMA) at Aj and on Oshima; (I JMA) at Mishima.
	01	06	24	56.3*	40.893	N	122 211	W	15 G			1.2	7	NORTHERN CALIFORNIA. ML 2.6 (BRK).
	01	06	35	03.6	34.919	N	139.165	E	10 G			0.2	7	NEAR S. COAST OF HONSHU, JAPAN. Felt (II JMA) on Os and (I JMA) at Ajiro.
	01	06	51	54.4*	34.841	N	139.121	E	10 G			1.1	6	NEAR S. COAST OF HONSHU, JAPAN. Felt (I JMA) at Aji and on Oshima.
	01	09	13	31.4*	58.164	N	143.233	W	10 G			0.4	7	GULF OF ALASKA. ML 3.4 (PMR).
	01	10	22	30.37	7.35	S	129.46	E	203 ?	3.8		1.3	8	BANDA SEA
	01	10	24	26.4*	39.565	N	29.334	E	10 G			1.4	5	TURKEY
	01	11	19	03.7	34.914	N	139.121	E	10 G			0.4	7	NEAR S. COAST OF HONSHU, JAPAN. Felt (II JMA) at Aj and (I JMA) at Mishima.
	01	11	34	08.3	47.585	N	115.614	W	10 G			0.5	76	MONTANA. ML 3.6 (NEIS), 4.1 (BUT). Felt (IV) at Sal and Trout Creek, Montana. Also felt (IV) at Cataldo Mullan, Idaho. Felt (III) at Haugan, Montana and Bu Calder, Osburn, Pinehurst, Saint Maries and Wallace Idaho. Also felt at Thompson Falls, Montana.
	01	12	04	48.2%	40.289	N	29.694	E	10 G			0.4	6	TURKEY
	01	12	14	03.2?	6.16	S	130.48	E	118 ?	4.1		1.2	7	BANDA SEA
	01	12	50	03.6%	45.322	N	3.881	E	10 G			1.2	10	FRANCE. ML 2.7 (LDG).
	01	13	31	27.5?	9.23	S	124.42	E	33 H	3.9		1.5	7	TIMOR
	01	15	22	27.7*	21.828	N	94.966	E	120 *	4.2		1.1	11	BURMA
	01	16	03	09.9?	42.69	S	85.75	W	10 G	4.8		0.7	13	WEST CHILE RISE
	01	16	12	36.9	34.918	N	139.157	E	10 G			0.2	7	NEAR S. COAST OF HONSHU, JAPAN. Felt (II JMA) at Aj

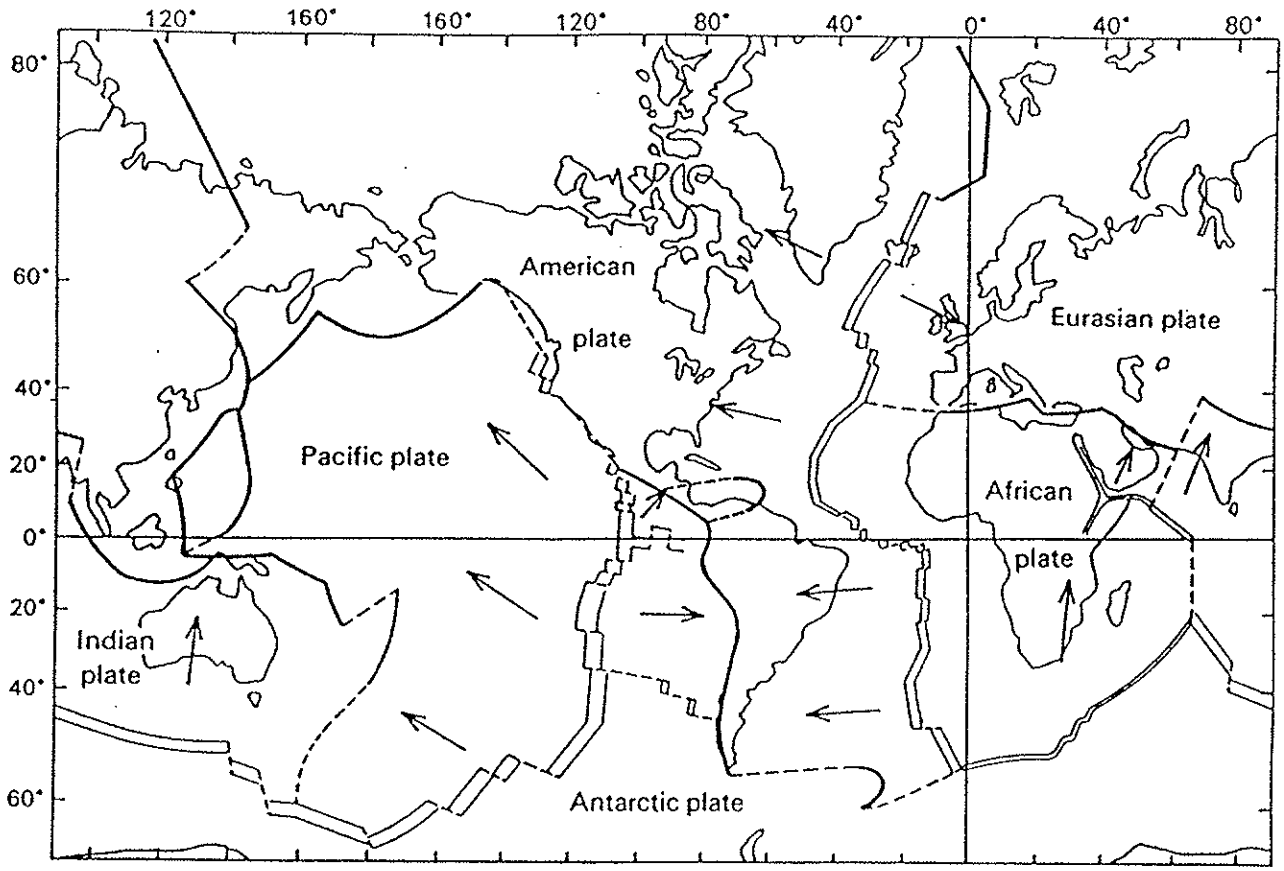

Figure 2.1 The Six Major Tectonic Plates and Their Approximate Linear Velocity Vectors (adapted from Park, 1983).

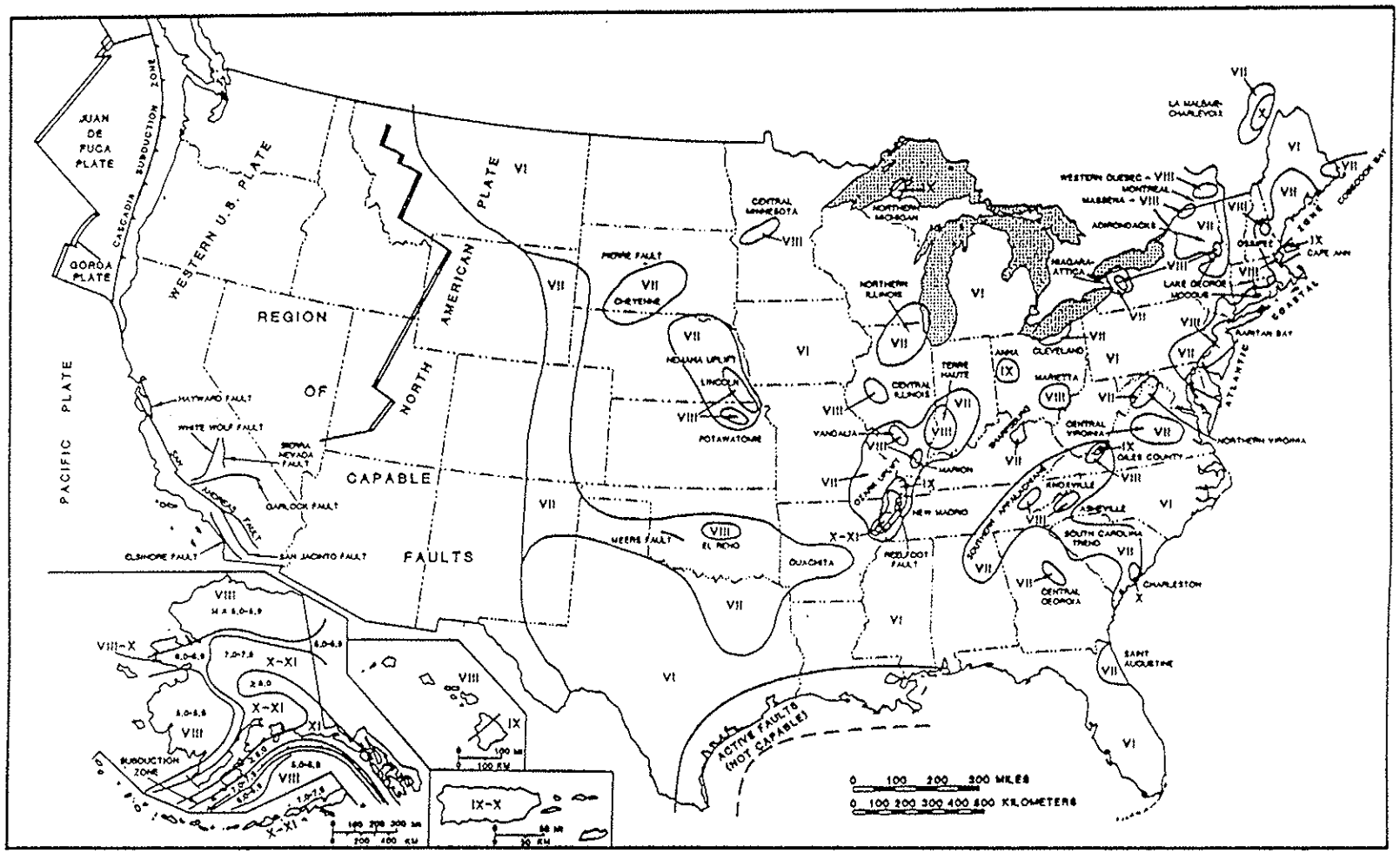

Figure 2.2 Seismic Source Areas in the United States (Krinitzsky et al., 1993).

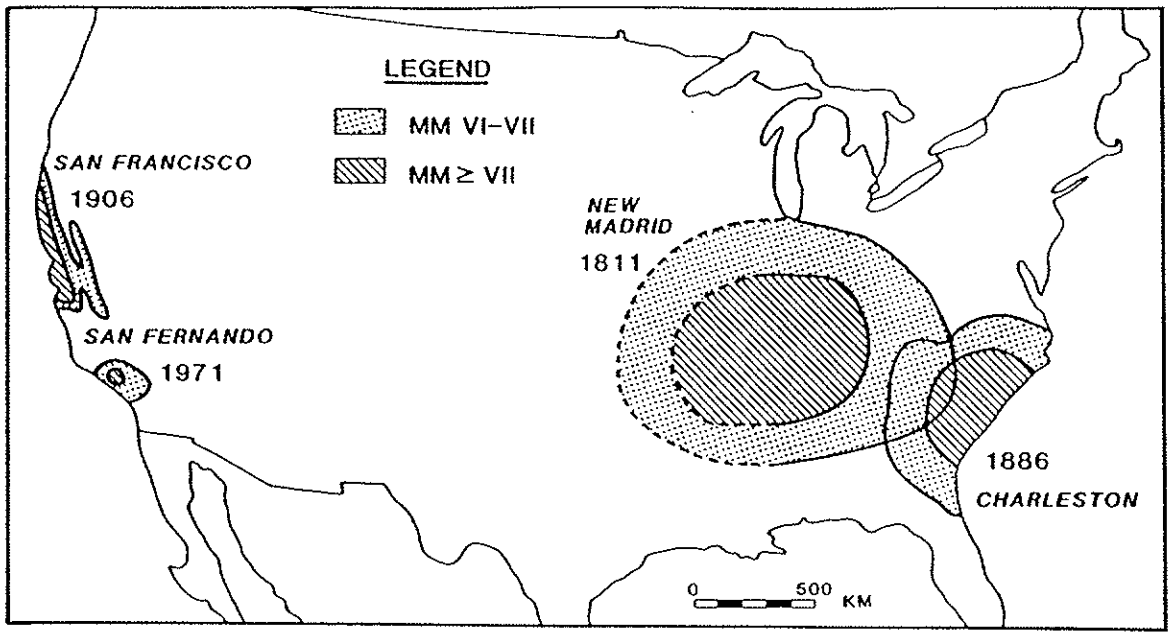

Figure 2.3 Isoseismal Contours for Intra-Plate vs. Edge-Plate Events of Similar Magnitude (Nuttli, 1974).

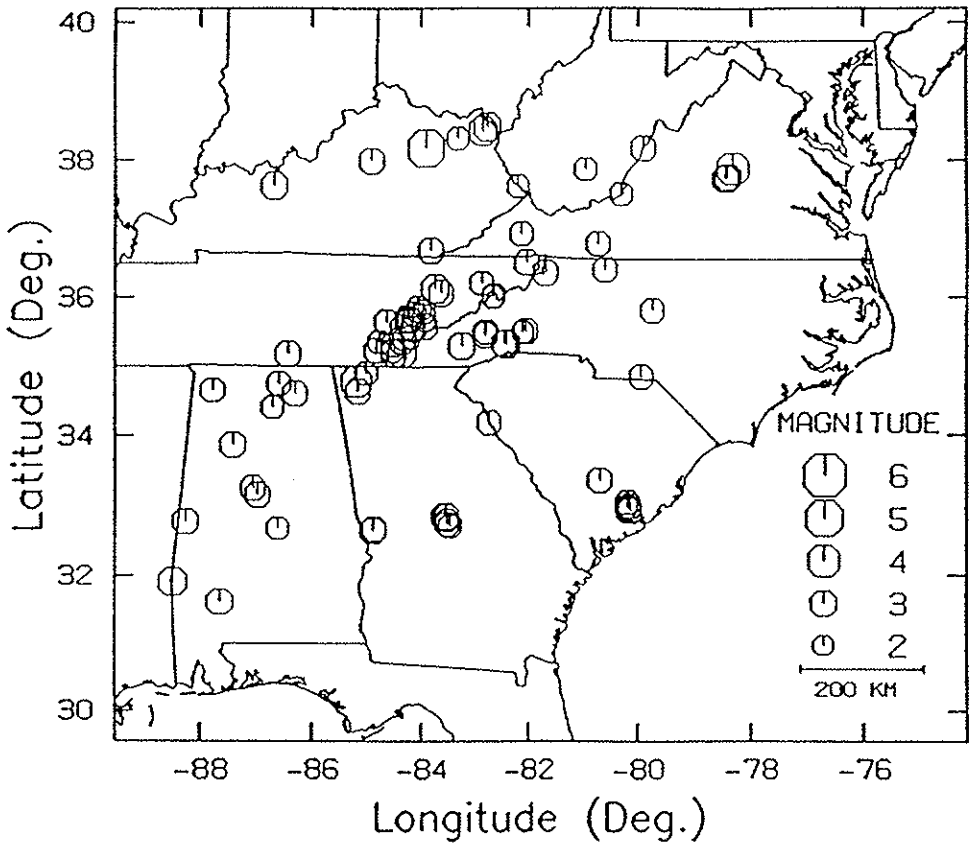

Figure 2.4 Epicenters for Earthquakes M $\geq$ 2.5 in the Southeastern United States (July 1977 - December 1984) (Sibol et al., 1984).

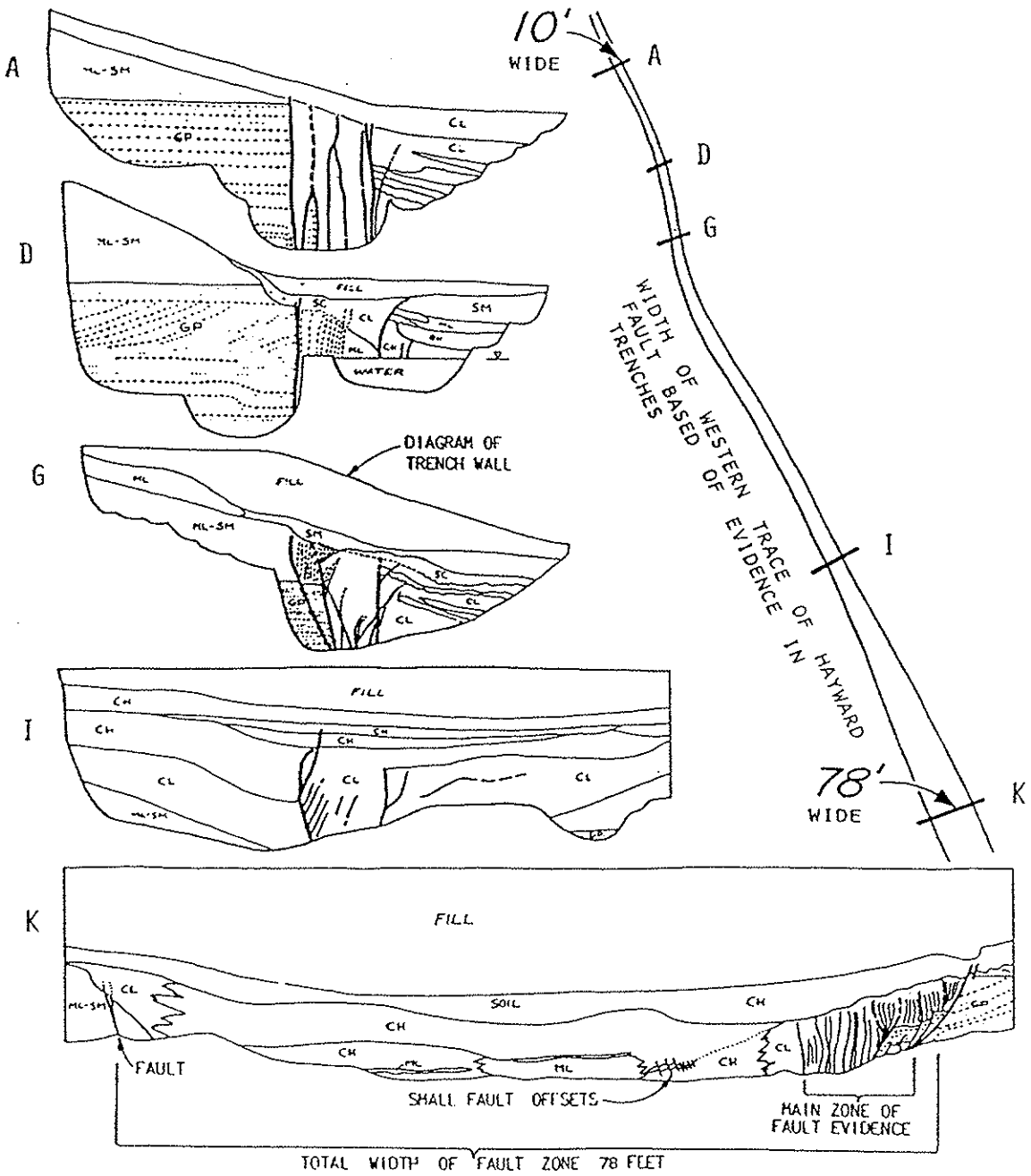

Figure 2.5 Characteristics of Hayward Fault as Exposed in Five Trenches at Fremont Site (Cluff et al., 1972).

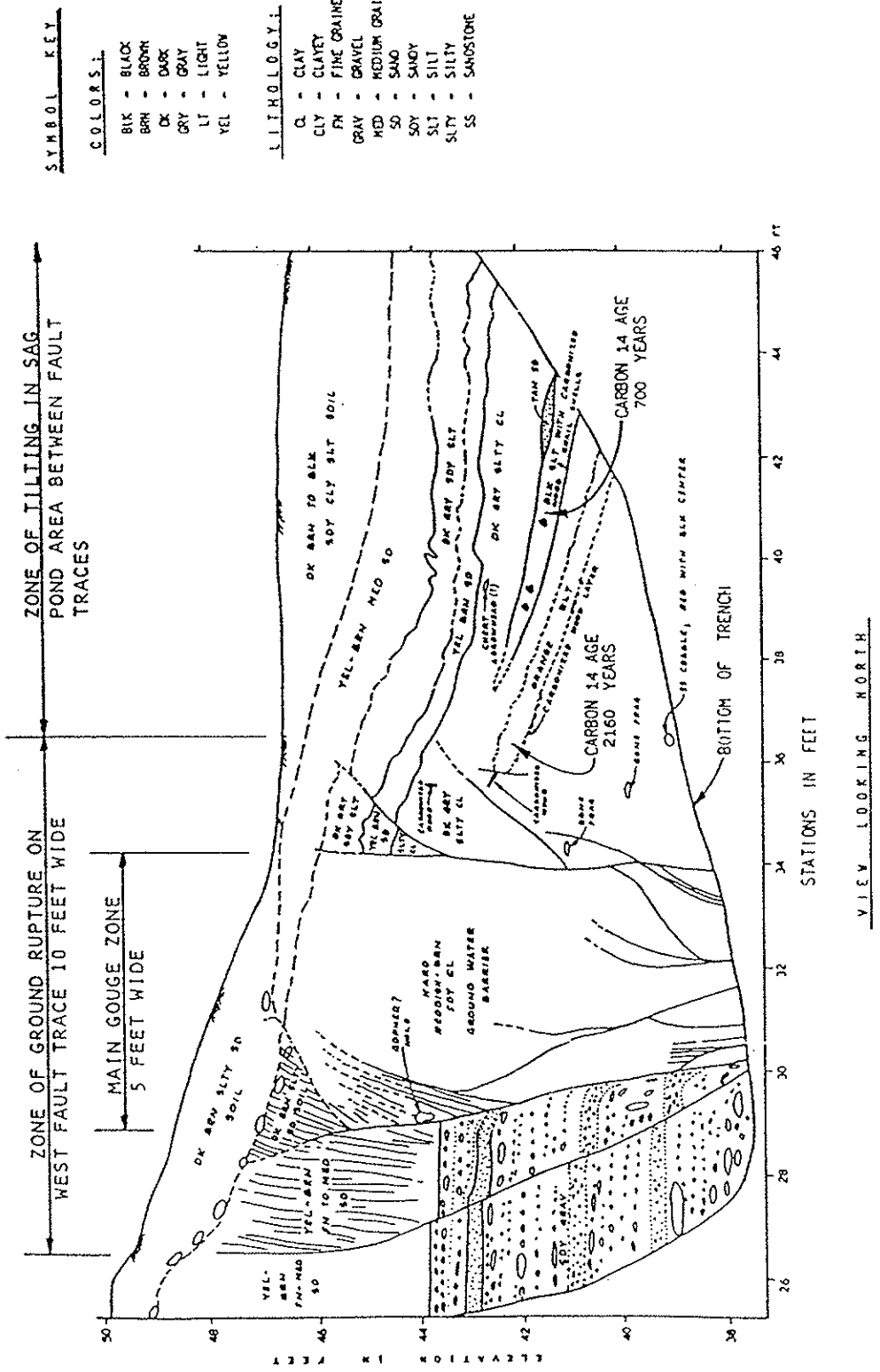

Figure 2.6 Detail of West Fault Trace Exposed in Trench "G" at Fremont Site (see Fig. 2.5) (Cluff et al., 1972).

SECTION 3

258.14 SEISMIC IMPACT ZONES: USGS PROBABILISTIC BEDROCK ACCELERATION

The maximum (peak) horizontal acceleration at the site of a proposed landfill is obtained from either the United States Geological Survey (USGS) seismic 250-year interval map (USGS, 1982; 1991), a regional equivalent, or from a site-specific seismic hazard study. The USGS map presents the estimated peak ground acceleration for a hypothetical bedrock outcrop at a project site. If bedrock is not present at or near the ground surface, the peak acceleration from the USGS map may need to be modified to account for local site conditions. Furthermore, liquefaction and seismic deformation analyses may require that the design engineer associate an earthquake magnitude with the peak ground acceleration. The USGS map was previously shown on Figure 1.1 in a reduced size format. The original map generated by USGS is sufficiently large that individual counties within the states are shown for ease in locating a particular landfill site. Selection of a peak horizontal ground acceleration from this map is a straight forward process. However, association of a magnitude with this peak acceleration requires interpretation and judgement.

This section of the guidance document provides background on the methodology used to generate the USGS seismic probability map and discusses interpretation of the acceleration value obtained from the map in order to obtain site-specific seismicity parameters for design.

3.1 Development of Probabilistic Model

Development of the USGS seismic probability model is predicated on the ability to (1) define source zones within and adjacent to the United States, (2) define seismic recurrence relationships for the seismic source zones within the United States, and (3) relate the impact of a seismic event in one seismic source zone to the ground motion experienced in surrounding zones. The basic methodology for performing such a probabilistic seismic hazard analysis is presented by Cornell (1968). The general strategy used in developing the USGS seismic probabilistic acceleration map is shown on Figure 3.1. This section provides a *simplified* description of the significant assumptions and methodologies used in preparing the seismic probability map. A more detailed discussion can be found in USGS (1982) and in the references provided therein.

Seismic recurrence relationships can be developed using three types of spatial source mechanisms: a point source, a line source, and an area source. Point and area sources are often

combined into a single type of source. Line sources are typically used to describe known active seismic faults. Point and area source mechanisms are used to handle intra-plate seismic events and regional seismicity for which an active fault cannot be defined. Mixed fault and point or area sources are used to superimpose random regional seismicity on top of known fault sources (see Figure 3.1a). Fault related source models are well suited for the Pacific coastal states that have a significant number of located and known seismically active faults that have experienced significant recent fault displacements. A variety of empirical relationships have been developed that relate the fault rupture length, fault rupture area, fault displacement, and the geologic slip rate of the fault to the magnitude of the earthquake that the fault rupture will generate (Bonilla et al., 1984; Hanks and Kanamori, 1979; Wesnousky, 1986; Woodward-Clyde Consultants; 1979; Wyss, 1979).

To develop the USGS (1982, 1991) maps, the contiguous United States was divided into 118 seismic source zones. The source zones were developed on the basis of regional geology, historic seismicity, known faults, and tectonic setting. The seismic source zones used in preparing the USGS seismic recurrence map are shown on Figure 3.2 (USGS, 1982).

A recurrence vs. earthquake magnitude relationship was developed for each of the USGS seismic source zones using historical records of regional seismicity and fault specific seismic events. The recurrence relationship was expressed in the form of the commonly used Gutenberg-Richter recurrence relationship:

$$Log\ N = a - bM \tag{3.1}$$

where a and b are empirical constants, and N is the number of earthquakes exceeding magnitude (M) per unit time (see Figure 3.1b).

A variety of different measures of earthquake magnitude exist (e.g., local (Richter) magnitude, surface wave magnitude, body wave magnitude, moment magnitude). These measures relate the energy released by the earthquake to some characteristic of the earthquake that is proportional to the released energy. The difference between and relationship among the various measures of earthquake magnitude are discussed by Idriss (1985), Heaton et al. (1986), and Boore and Joyner (1994). Unless otherwise specified, the magnitude measure used in this guidance document is local magnitude for $M < 6.0$ and body wave magnitude for $M \geq 6.0$.

The Gutenberg-Richter recurrence relationship is typically truncated at the maximum magnitude considered credible for an earthquake within a particular seismic zone. Table 3.1 presents the Gutenberg-Richter recurrence parameters, including the maximum magnitude, assigned to the 118 seismic source zones in the United States by the USGS to develop its probabilistic seismic hazard maps (USGS, 1982).

For smaller magnitude events ($M < 5.0$) in the western United States, the rate of occurrence is typically based upon instrumentally recorded seismicity. For larger events ($M > 5.0$) in the western United States, information on historical seismic activity is combined with information on the regional geologic slip rate from paleoseismic studies and satellite geodesy. Typically, regional seismicity cannot be entirely accounted for by known faults. The difference between the regional seismicity and the fault-specific seismicity is assigned to the seismic zone encompassing a fault as non fault-specific random seismicity.

For regions east of the Rocky Mountains, the recurrence relationship for larger magnitude seismic events ($M > 4.0$) must be based on regional seismicity, regional geologic structure, and historical seismic events in all areas of similar structure and seismicity. Recurrence intervals for lesser events in the eastern and central United States can still be based on the significant number of earthquakes detected and recorded by regional seismological networks.

The influence of the various seismic source zones on the seismic hazard at a specific site is evaluated using empirical acceleration vs. distance attenuation relationships developed as a function of earthquake magnitude (see Figure 3.1.b). The acceleration-distance-magnitude attenuation relationship appears to be highly regional, with earthquakes in the western states believed to have a much faster acceleration decay than earthquakes in the midwest and eastern states (Nuttli, 1981). The low rate of attenuation for east coast events results in the seismic hazard in large portions of the southeast being dominated by the accelerations resulting from the New Madrid seismic zone, source of three major earthquakes of 1811-1812, and the Charleston seismic zone, source of the Charleston earthquake of 1888 (see Figure 2.3).

The acceleration recurrence relationship for a given site is calculated as the sum of the acceleration contributions from the magnitude recurrence and acceleration-distance attenuation relationships from the source zone the site is in and all adjoining seismic source zones. In this manner, the cumulative probability of acceleration, F(a), is calculated for every point within each seismic source zone (see Figure 3.1.c).

Given the cumulative probability of ground acceleration, F(a), within a seismic source zone, the expected number of times a particular amplitude of ground motion is likely to occur in a given period of years at a site within the seismic source zone can be calculated, and the maximum amplitude of ground motion in a given number of years corresponding to any level of probability can be obtained. The probability, $F_{Max,t(a)}$, of not exceeding some acceleration amplitude, a, during a particular exposure time, t, is given by:

$$F_{Max,t(a)} = e^{-\phi[1-F(a)]} \tag{3.2}$$

where ϕ is the mean rate of occurrence of earthquakes used to generate F(a). The USGS maps present contours of peak ground acceleration with a probability of not being exceeded of 90 percent (a probability of being exceeded of 10 percent) in exposure periods of 50 and 250 years developed using this approach. The contoured values correspond to peak ground accelerations with expected average recurrence intervals (return periods) of 475 and 2,400 years, respectively.

An acceleration value from the USGS maps for any particular site is composed of contributions from a family of earthquakes of different magnitudes and distances. Figure 3.5 (Moriwaki et al., 1994) shows the distribution of magnitudes and distances from a hypothetical probabilistic seismic hazard analysis for a 10 percent probability of exceedance (90 percent probability of not being exceeded) over a 50 year exposure period (this corresponds to a 475 year return period). Selection of a representative magnitude from this data might be based upon either a 90 percentile criterion or the mean (expected) value at the discretion of the design engineer and regulatory agency.

The information on the distribution of magnitudes is generally not available for USGS or other regional seismic hazard studies, and most common seismic hazard programs must be modified to yield this data. As an alternative, the maximum magnitude assigned to the seismic source zones which contribute to the seismic hazard (the zone the site is in plus all adjacent zones) may be conservatively taken as the representative magnitude. Maximum magnitudes are presented in Table 3.1 for the USGS source zones shown in Figure 3.2, and Figure 3.3 presents maximum magnitudes for much of the central United States from a more recent study (Johnston and Nava, 1994).

3.2 Interpretation of Peak Bedrock Velocities and Accelerations

The attenuation relationships used to establish the USGS seismic probability maps are based on ground motions recorded at bedrock sites. Bedrock is commonly defined in engineering practice as material having a shear wave velocity greater than 2,500 feet per second (750 meters per second). This is referred to as lithified earth within Subtitle D. Lithified earth is defined in Subtitle D as all rock, including all naturally occurring and naturally formed aggregates or masses of minerals or small particles of older rock that formed by induration of loose sediments. Lithified earth does not include man-made materials such as fill, concrete and asphalt, or unconsolidated earth materials, soil, or regolith (saprolites) lying at or near the ground surface.

It is important to realize that the accelerations presented on the USGS maps are not the peak ground surface accelerations unless bedrock is exposed at the ground surface. Section 4.1 of this guidance document reviews methods for calculating the peak ground surface acceleration based on the site specific subgrade profile that exists above the top of lithified earth (rock) and the peak bedrock acceleration from the USGS map.

The peak acceleration is only one characteristic of the earthquake ground motion at a site. The damage potential of seismically-induced ground motions also depends upon the duration of the motion, the frequency content of the motion, and the intensity of the motion at times other than when the peak acceleration occurs. Acceleration, velocity, and displacement time-histories recorded at the top of the OII landfill in Los Angeles during the 17 January 1994 Northridge earthquake (Hushmand Associates, 1994) are shown on Figure 3.4. Note that the peak acceleration occurs only once during the record and that motions approaching the peak acceleration exist for only a small fraction of a second. Use of this peak acceleration for traditional geotechnical stability analyses is very conservative in most cases. Section 6.2 of this guidance document discusses the reduction of this peak ground surface acceleration to an equivalent pseudo-static acceleration for use in slope stability analyses.

3.3 References

Algermissen, S.T., Perkins, D.M. Thenhaus, P.C., Hanson, S.L., and Bender, B.L. (1982), "Probabilistic Estimates of Maximum Acceleration and Velocity in Rock in the Contiguous United States," U.S. Geological Survey Open-File Report 82-1033, 99 p.

Bonilla, M.G., Mark R.K., and Lienkaemper, J.J. (1984), "Statistical Relations Among Earthquake Magnitude, Surface Rupture Length and Surface Fault Displacement, *Journal of Geophysical Research*, Vol. 74, No. 6, pp. 2379-2411.

Boore, D.M., and Joyner, W.B. (1994), "Prediction of Ground Motion in North America," Proc. of the Seminar on New Developments in Earthquake Ground Motion Estimation and Implication for Engineering Design Practice, Applied Technology Council Publication No. ATC 35-1, Redwood City, California, pp. 6-1 - 6-41.

Cornell, C.A. (1968), "Engineering Seismic Risk Analysis," *Seismological Society of America Bulletin*, V. 58, pp. 1583-1606.

Hanks, T.C., and Kanamori, H. (1979), "A Moment Magnitude Scale," *Journal of Geophysical Research*, Vol. 84, No. B5, pp. 2348-2350.

Heaton, T.J., Tajima, F., and Mori, A.W. (1986), "Estimating Ground Motions Using Recorded Accelerograms" *Surveys in Geophysics*, Vol. 8, pp. 25-83.

Hushmand Associates (1994), "Landfill Response to Seismic Events," Report prepared for the USEPA Region IX, Hushmand Associates, Laguna Niguel, California.

Idriss, I.M. (1985), "Evaluating Seismic Risk in Engineering Practice," Proc. *Eleventh International Conference on Soil Mechanics and Foundation Engineering*, San Francisco, California, Vol. 1, pp. 255-320.

Johnston, A.C., and Nava, S.J. (1994), "Seismic Hazard Assessment in the Central United States," Proc. *Seminar on New Developments in Earthquake Ground Motion Estimation and Implications for Engineering Design Practice*, Applied Technology Council, ATC35-1, Redwood City, California, pp. 2-1 - 2-12.

Moriwaki, Y., Tan, P. and Somerville, P. (1994); "Some Recent Site-Specific Ground Motion Evaluations - Southern California Examples and Selected Issues," Proc. *Seminar on New Developments in Earthquake Ground Motion Estimation and Implications for Engineering Design Practice*, Applied Technology Council ATC35-1, Redwood City, California, pp. 14-1 - 14-25.

Nuttli, O.W. (1981), "Similarities and Differences Between Western and Eastern United States Earthquakes, and their Consequences for Earthquake Engineering," Earthquakes and Earthquake Engineering: The Eastern United States, Vol. 1, Assessing the Hazard - Evaluating the Risk, J.E. Beavers, Ed., Ann Arbor Science Publishers, Inc., Ann Arbor, Michigan, pp. 25-51.

USGS (1982), "Probabilistic Estimates of Maximum Acceleration and Velocity in Rock in the Contiguous United States, United State Geological Survey, Open-File Report 82-1033.

Wesnousky, S.G. (1986), "Earthquakes, Quaternary Faults and Seismic Hazard in California," *Journal of Geophysical Research*, Vol. 91, No. B12, pp. 12587-12631.

Woodward-Clyde Consultants (1979), "Evaluation of Maximum Earthquake and Site Ground Motion Parameters Associated with the Offshore Zone of Faulting, San Onofre Nuclear Generating Station," Report prepared for Southern California Edison Company, 241 p.

Wyss, M. (1979), "Estimating Maximum Expectable Magnitude of Earthquakes from Fault Dimensions," *Geology* Vol. 7, pp. 336-340.

Table 3.1: Parameters for Seismic Source Zones (USGS, 1982).

Zone No.*	No. of Modified Mercalli Maximum Intensity V's per year	b	Maximum Magnitude M**
p001	0.11010	-0.40	7.3
p002	0.43510	-0.40	7.3
p003	0.12440	-0.54	7.3
p004	0.34840	-0.62	7.3
p005	0.12390	-0.62	7.3
p006	0.02831	-0.62	7.3
p008	0.01642	-0.42	7.3
p009	0.20850	-0.28	7.9
p010	0.45200	-0.28	7.9
p011	0.96370	-0.28	7.9
p012	0.37090	-0.28	7.9
p013	0.69020	-0.28	7.9
p014	0.10940	-0.42	7.3
p015	0.34480	-0.42	7.3
p016	0.04926	-0.42	7.3
p017	0.87860	-0.28	7.9
p018	0.18810	-0.54	7.3
p019	0.04090	-0.54	7.3
c001	0.62770	-0.42	7.3
c002	0.15700	-0.42	7.3
c003	0.31960	-0.42	7.3
c004	0.31960	-0.42	7.3
c005	0.04843	-0.42	6.1
c006	0.15700	-0.42	7.3
c007	0.15700	-0.42	7.3
c008	0.04740	-0.42	6.1
c009	0.04843	-0.42	6.1
c010	0.18190	-0.42	6.1
c011	0.77010	-0.42	7.3
c012	0.19050	-0.42	7.3
c013	0.35840	-0.42	7.3
c014	0.91990	-0.66	7.9
c015	1.49200	-0.45	7.9
c016	0.22560	-0.51	7.9
c017	0.02760	-0.48	7.3
c018	1.09200	-0.49	7.3
c019	0.31980	-0.42	6.7
c020	0.19280	-0.42	6.1
c021	0.10880	-0.42	6.1
c022	0.02422	-0.42	6.1
c023	0.11650	-0.37	7.9
c024	1.97000	-0.43	8.5
c025	0.05085	-0.55	7.3
c026	0.09145	-0.55	7.3

Table 3.1: (continued)

Zone No.*	No. of Modified Mercalli Maximum Intensity V's per year	b	Maximum Magnitude M**
c027	0.03437	-0.37	7.3
c028	0.13010	-0.37	7.3
c029	0.02350	-0.37	7.3
c030	0.03630	-0.42	6.7
c031	0.47580	-0.51	6.7
c032	0.55190	-0.45	7.9
c033	0.23070	-0.37	7.9
c034	0.67120	-0.51	7.9
c035	0.02325	-0.60	7.3
c036	0.35220	-0.59	6.7
c037	0.81950	-0.51	6.1
c038	0.82680	-0.54	7.9
c039	0.35810	-0.45	7.9
c040	0.15820	-0.42	6.1
c041	0.08448	-0.37	7.9
001	0.22700	-0.73	7.3
002	0.03600	-0.73	7.3
003	0.08800	-0.73	6.1
004	0.22700	-0.54	7.3
005	0.09100	-0.73	7.3
006	0.13500	-0.73	7.3
007	0.41900	-0.73	7.3
008	0.21100	-0.73	6.1
009	0.19400	-0.54	6.1
010	0.20800	-0.54	7.3
011	0.55100	-0.64	7.3
012	0.34900	-0.64	7.3
013	0.05500	-0.64	7.3
014	0.49000	-0.73	7.3
015	0.01800	-0.73	6.7
016	0.14600	-0.73	6.1
017	0.69300	-0.59	7.3
018	0.26100	-0.54	7.3
019	0.11717	-0.54	7.3
020	1.84900	-0.64	7.3
022	0.19600	-0.64	6.1
023	0.15350	-0.54	7.3
024	0.27400	-0.64	7.3
025	0.16800	-0.64	6.1
026	0.47700	-0.64	6.1
027	0.11100	-0.64	5.5
029	1.31900	-0.64	7.3
030	0.58800	-0.64	7.3
031	1.82685	-0.54	7.3

Table 3.1: (continued)

Zone No.*	No. of Modified Mercalli Maximum Intensity V's per year	b	Maximum Magnitude M**
032	0.48114	-0.54	6.1
033	0.08557	-0.54	6.1
034	0.62380	-0.54	7.3
035	0.20070	-0.54	7.3
036	0.01800	-0.58	6.1
037	0.05100	-0.58	7.3
038	0.80600	-0.58	7.3
039	0.12000	-0.58	7.3
040	0.29100	-0.58	7.3
041	0.24400	-0.73	7.3
042	0.01800	-0.73	6.1
043	0.04600	-0.73	7.3
044	0.11300	-0.73	6.1
045	0.45600	-0.73	6.1
046	0.01274	-0.73	6.1
047	0.00427	-0.73	6.1
048	0.00329	-0.73	6.1
049	0.01663	-0.73	6.1
050	0.17000	-0.73	6.1
051	0.01706	-0.73	6.1
052	0.19000	-0.58	7.3
053	0.03600	-0.58	7.3
054	0.01800	-0.58	6.1
055	0.67300	-0.58	7.3
056	0.17700	-0.58	6.1
057	0.66200	-0.58	7.3
058	0.19800	-0.58	7.3
059	0.19200	-0.58	6.1
060	0.03600	-0.58	6.1
061	0.08900	-0.58	7.3
062	0.03600	-0.58	6.1
063	0.12900	-0.58	6.1
064	0.34400	-0.58	7.3
065	0.15200	-0.58	6.1
066	0.01800	-0.73	6.1
067	0.07715	-0.46	6.1
068	0.02894	-0.46	6.1
069	0.00588	-0.46	6.1
070	0.03552	-0.46	6.1
071	0.01176	-0.46	6.1
072	0.02026	-0.46	6.1
073	0.02353	-0.46	6.1
074	0.00270	-0.46	6.1
075	0.06510	-0.46	6.1

Table 3.1: (continued)

Zone No.*	No. of Modified Mercalli Maximum Intensity V's per year	b	Maximum Magnitude M**
076	0.14742	-0.46	6.1
077	0.03469	-0.46	6.1
078	0.04389	-0.46	6.1
079	0.03082	-0.46	6.1
080	0.02987	-0.46	6.1
081	0.02044	-0.46	6.1
082	0.03552	-0.46	6.1
083	0.00996	-0.46	6.1
084	0.04117	-0.46	6.1
085	0.03802	-0.46	6.1
086	0.04626	-0.46	6.1
087	0.29865	-0.46	8.5
088	0.09703	-0.46	6.1
089	0.15689	-0.46	6.1
090	0.06103	-0.46	6.1
091	0.00644	-0.46	6.1
092	0.02661	-0.46	6.1
093	0.02680	-0.46	6.1
094	0.10835	-0.46	6.1
095	0.05901	-0.46	6.1
096	0.02675	-0.46	6.1
097	0.01156	-0.46	6.1
098	0.01215	-0.46	6.1
099	0.24830	-0.50	7.3
100	0.42290	-0.50	7.3
101	0.18720	-0.50	7.3
102	0.09532	-0.50	7.3
103	0.33150	-0.50	7.3
104	0.05544	-0.50	7.3
106	0.01952	-0.50	6.7
107	0.19100	-0.50	7.3
108	0.29390	-0.50	6.7
109	0.10650	-0.50	7.9
110	0.30220	-0.50	7.9
111	0.32430	-0.50	7.9
112	0.01532	-0.50	6.7
113	0.07432	-0.50	6.7
114	0.00754	-0.50	6.7
115	0.05834	-0.50	7.3
116	0.06783	-0.50	6.7
117	0.03950	-0.50	7.3
118	0.01334	-0.50	7.3

*The zones are shown in Figure 3.2
**See text for definition of M

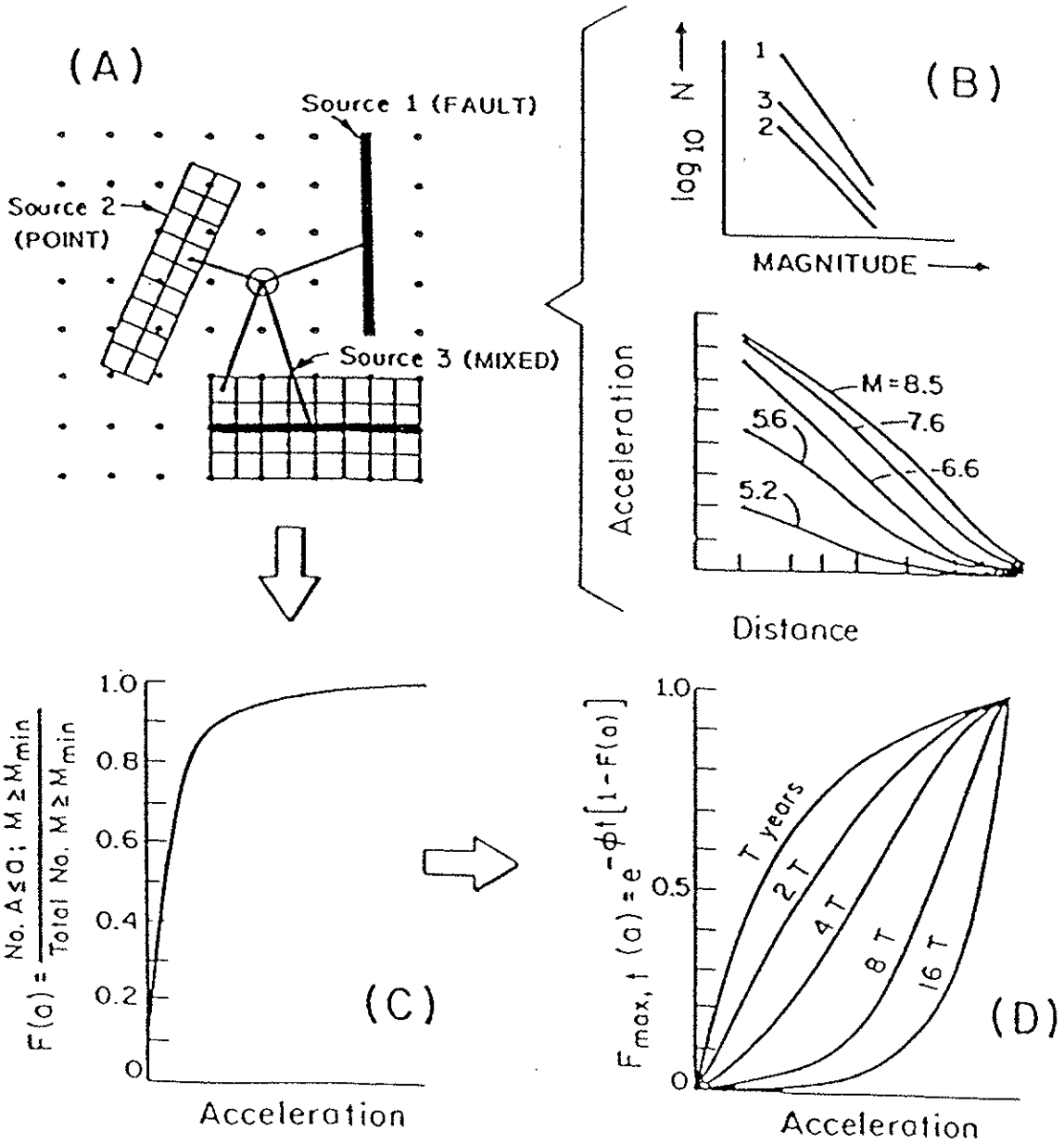

Figure 3.1 Basic Elements of the USGS Probabilistic Hazard Calculations: (a) Typical Source Areas and Grid of Points at Which the Hazard is to be Computed; (b) Statistical Analysis of Seismicity Data and Typical Attenuation Curves; (c) Cumulative Conditional Probability Distribution of Acceleration; (d) The Extreme Probability, $F_{max,t}$ (a) for Various Accelerations and Exposure Times (T) (USGS, 1982).

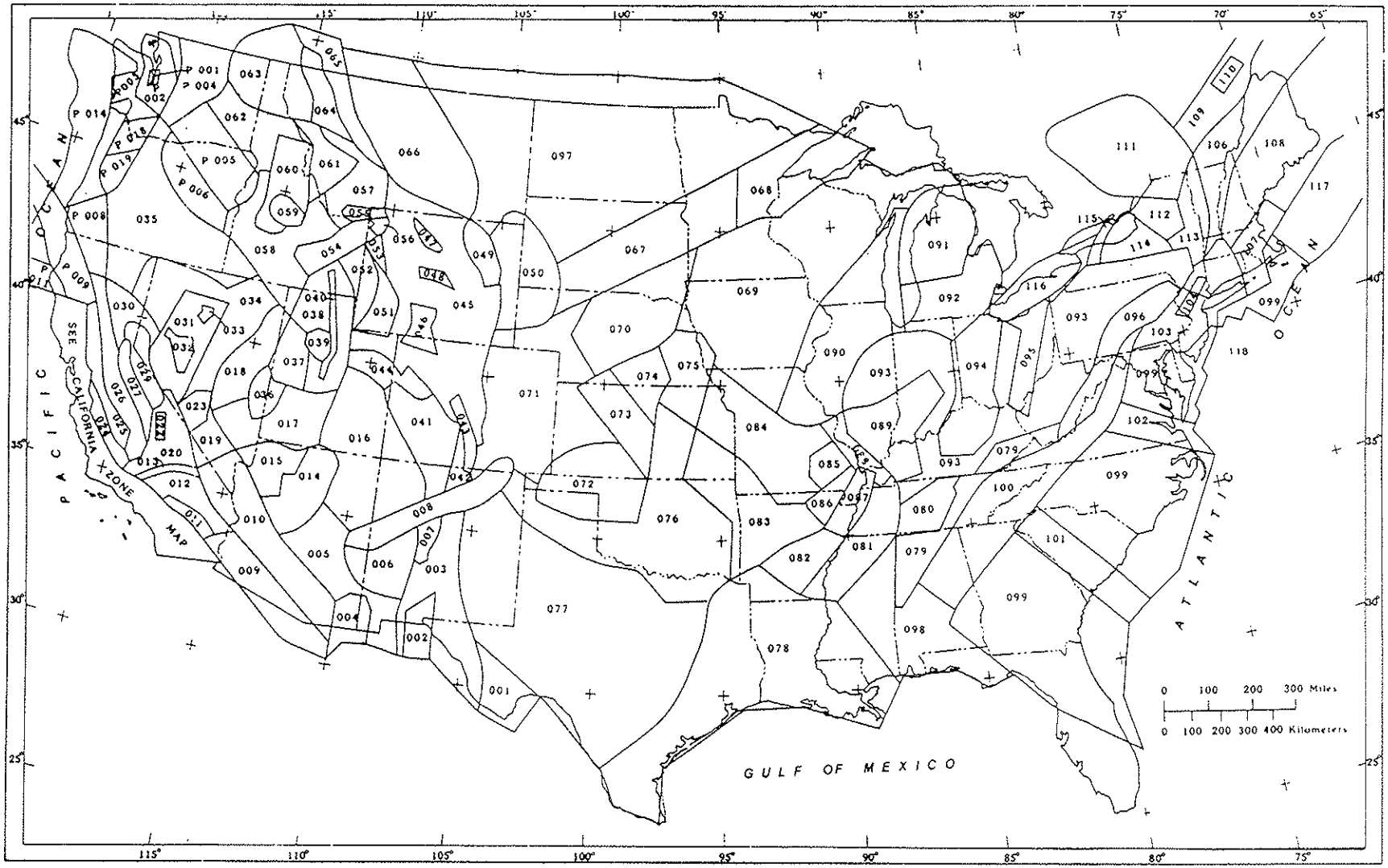

Figure 3.2 Seismic Source Zones in the Contiguous United States (USGS, 1982).

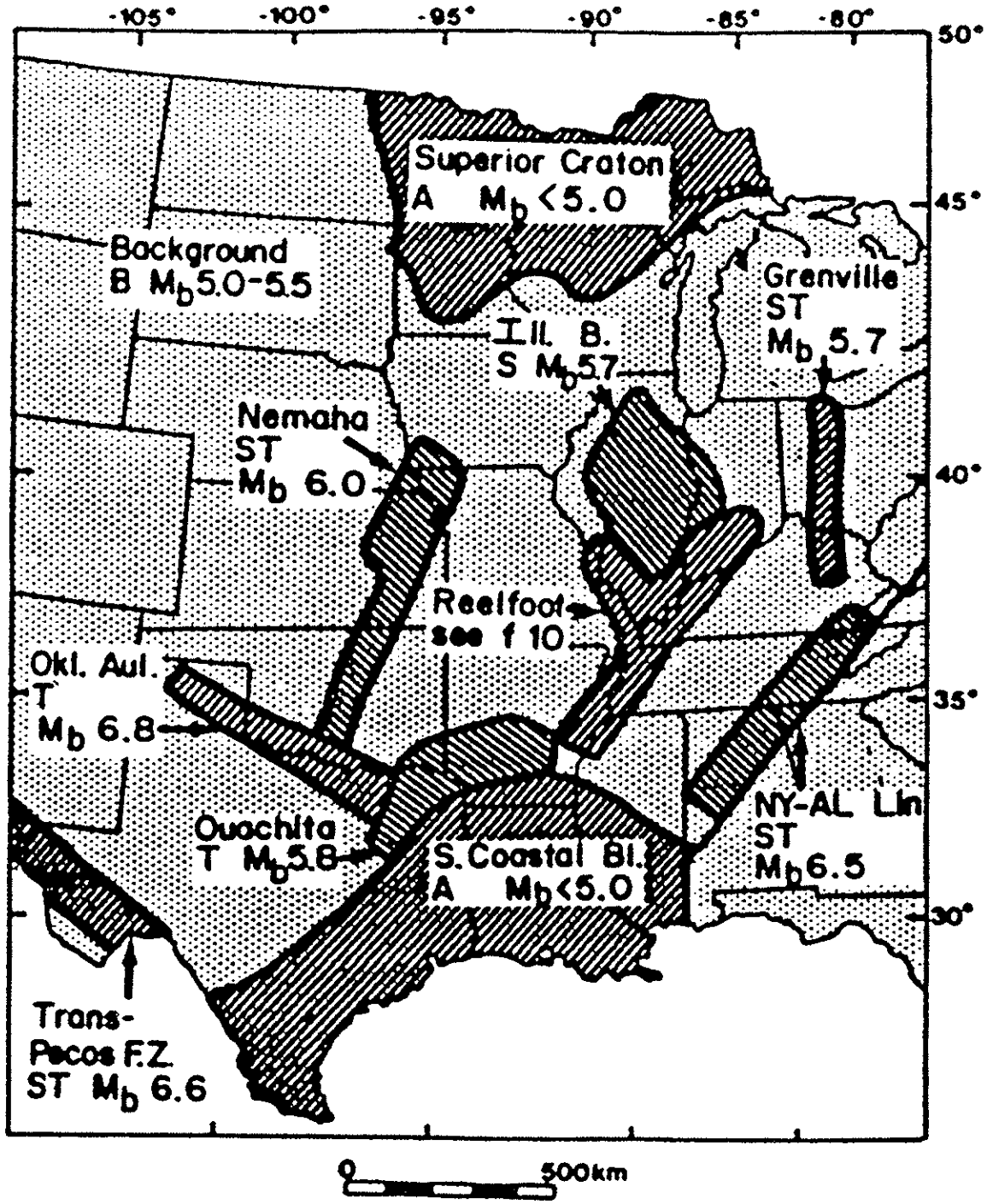

Figure 3.3 Seismic Source Zones in the Central United States (Johnston and Nava, 1994).

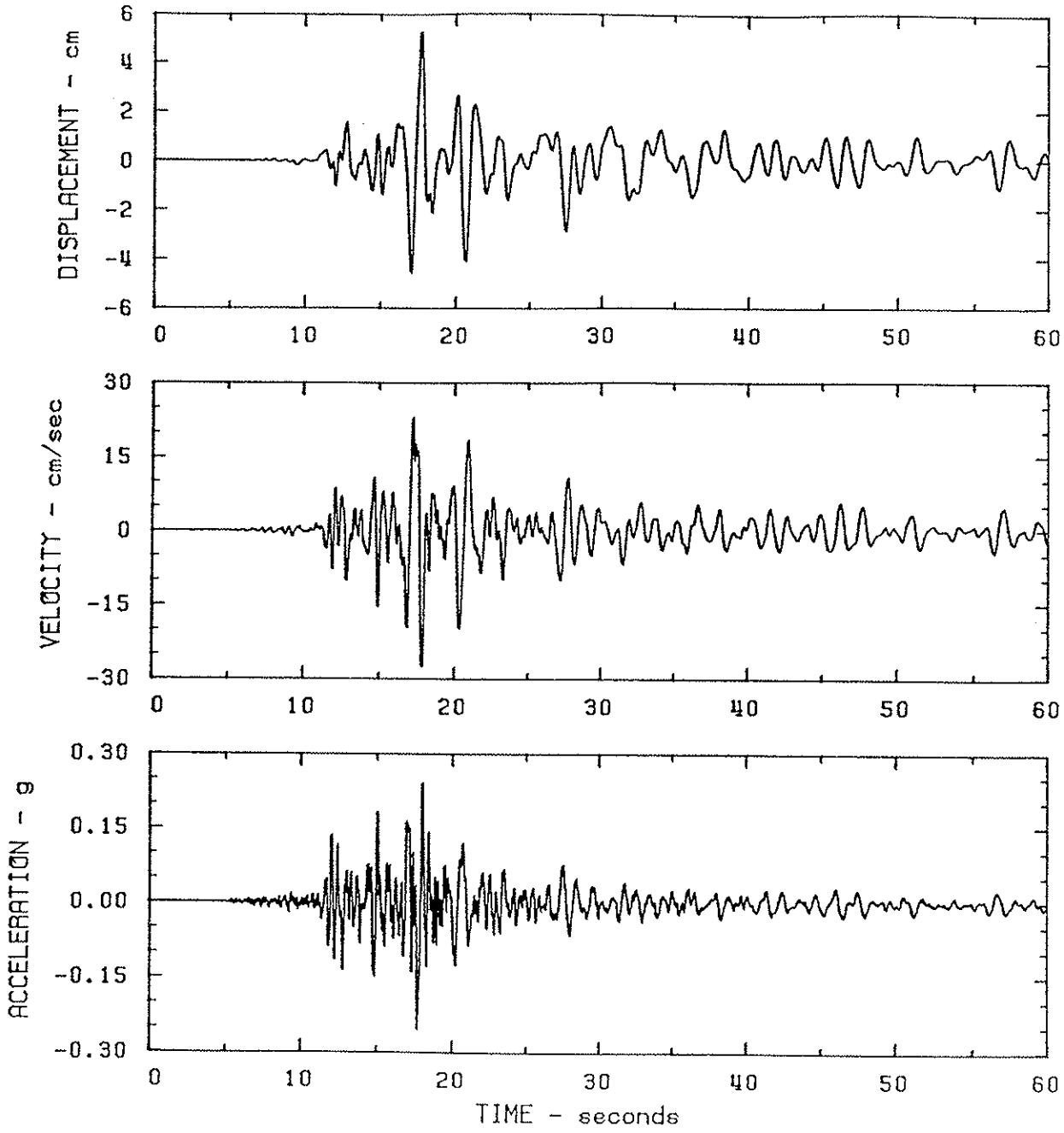

Figure 3.4 Time-Dependant Fluctuations in Seismic Ground Response Parameters (17 January 1994 Northridge, California Earthquake, OII Site, Longitudinal Component) (Hushmand Associates, 1994).

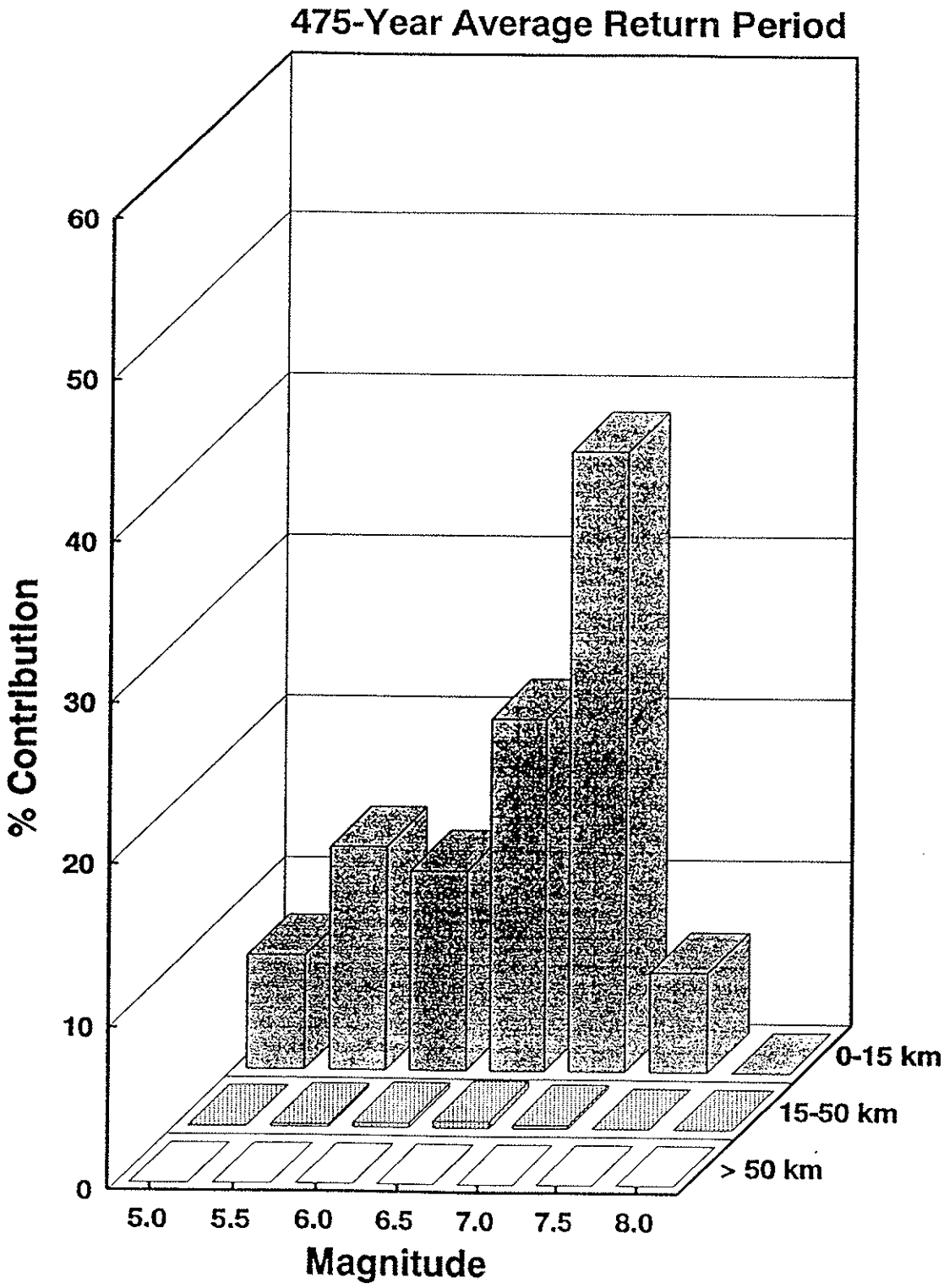

Figure 3.5 Contribution of Various Magnitudes and Distances to the Seismic Hazard (Moriwaki et al., 1994).

SECTION 4

258.14 SEISMIC IMPACT ZONES: SITE SPECIFIC SEISMIC DESIGN GROUND MOTION

The USGS map discussed in the previous section provides values for the peak ground acceleration of a hypothesized bedrock outcrop at a MSW landfill site. This section of the guidance document discusses methods for calculation of: (1) a peak acceleration in the free field at the ground surface at the project site that reflects the soil stratigraphy and (2) a peak acceleration at the top of the landfill that reflects the properties of the waste. These accelerations are used in later sections of this guidance document in evaluation of the seismic response of the landfill waste mass, the seismic performance of the liner and cover systems, and subgrade liquefaction potential.

Qualitative reports of the influence of local soil conditions on the intensity of shaking and on the damage induced by earthquake ground motions date back to at least the 1906 San Francisco earthquake (Wood, 1908). Reports of localization of areas of major damage within the same city and of preferential damage to buildings of a certain height within the same local area from the Mexico City earthquake of 1957, the Skopje, Macedonia earthquake of 1963, and the Caracas, Venezuela earthquake of 1967 focused the attention of the engineering community on local soil effects.

Back-analysis by Seed (1975) of accelerograms from the magnitude M 5.7 San Francisco earthquake of 22 March 1957, presented in Figure 4.1, demonstrate the influence of local soil conditions on site response. Peak accelerations and the frequency contents of ground motions measured at six sites approximately the same distance from the earthquake source were dependent on the soil profile beneath each specific site.

Figure 4.1 shows peak acceleration, the acceleration and velocity response spectra, and soil stratigraphy data at the six San Francisco sites from the 1957 earthquake. A response spectrum present the maximum response of a damped single degree-of-freedom (SDOF) linear elastic system to the accelerogram recorded at a site. The maximum response of the SDOF system is calculated for a range of system natural frequencies to plot the response spectrum. Response spectra are typically calculated for several levels of system damping, as shown on Figure 4.2. Acceleration data generated in response spectra analysis is commonly plotted on the tripartite plot shown on Figure 4.3. In addition to peak acceleration, the tripartite presentation also

provides approximate values of peak velocity and peak displacement for the response of the SDOF.

At the sites shown in Figure 4.1, the local soil deposits attenuated the peak ground acceleration by a factor of approximately two compared to the bedrock sites. However, the acceleration response spectra clearly show amplification of spectral accelerations at longer periods (periods greater than 0.25 sec). If the bedrock motions had greater energy at these longer periods, a characteristic of larger magnitude events and of events from a more distant source, or if the natural period of the local soil deposits more closely matched the predominant period of the bedrock motions, amplification of the peak acceleration could have occurred at the soil sites.

Amplification of long period bedrock motions by local soil deposits is now accepted as an important phenomenon that can exert a significant influence on the damage potential of earthquake ground motions. Significant structural damage has been attributed to amplification of both peak acceleration and spectral acceleration by local soil conditions. Amplification of peak acceleration occurs when the resonant frequency of the soil deposit is close to the predominant frequencies of the bedrock earthquake motions (the frequencies associated with the peaks of the acceleration response spectra). The resonant frequencies, f_n, of a soil layer (deposit) of thickness H can be estimated as a function of the average shear wave velocity of the layer, V_s, using the following equation:

$$f_n = \frac{V_s\,(2n - 1)}{4H} \quad n = (1,2,3...) \tag{4.1}$$

where f_1 is the resonant frequency for the first mode of vibration, f_2 is the resonant frequency for the second mode of vibration, f_3 is the resonant frequency for the third mode of vibration, and so on. At most soil sites, amplification of seismic motions is most important for the first (predominant) mode of vibration and rapidly decreases in significance with increasing mode number.

Spectral amplification may occur at soil sites in any earthquake at frequencies around the resonant frequency of the soil deposit. Spectral amplification causes damage when the resonant frequency of the soil deposit matches the resonant frequency of the structure. Some of the most significant damage in recent earthquakes (e.g., building damage in Mexico City in the 1985 earthquake and damage to freeway structures in the Loma Prieta earthquake of 1989) has occurred in situations where the predominant frequencies of the bedrock motions and the

resonant frequencies of both the local soil deposit and the overlying structure all fell within the same range.

Observations of ground motions generated in recent earthquakes at the OII landfill, a solid waste landfill in Los Angeles composed of both industrial and municipal wastes, have demonstrated that amplification of both spectral acceleration and peak acceleration can occur at the top of solid waste landfills. Anderson et al. (1992) report spectral amplification of greater than 10 at OII for low amplitude (less than 0.1 g) ground motions from small magnitude (less than M 5.0) earthquakes. Hushmand Associates (1994) report a peak horizontal acceleration amplification factor of 3.0 at OII during the M 7.4 Landers earthquake in 1992.

Considering the landfill facility as an engineered structure built upon a local soil deposit, there are clearly two different sources of local site effects that must be considered in a seismic impact analysis. First, the influence of the local soil conditions on the bedrock motions must be evaluated to determine the free field ground surface motions at the project site. Second, the influence of the landfill on the free field ground surface motions must be evaluated. While it is convenient conceptually to separate these two effects, in practice they may be inter-dependent and a coupled analysis of the interaction between the response of the foundation soil and the response of the landfill may be warranted.

This section of the guidance document presents simplified and detailed methods for evaluating both the free field ground response and the response of the landfill mass. The free field ground motions are used to evaluate the liquefaction potential of the foundation. The response analysis of the landfill mass provides input for seismic performance analyses of the landfill liner and cover systems.

4.1 General Methodology

The influence of local soil conditions on seismic ground motions is usually addressed using one-dimensional site response analyses. Conventional one-dimensional site response analyses are based upon the assumption of a horizontal shear wave propagating vertically upwards through horizontal soil layers of infinite lateral extent. The influence of vertical motions, compression waves, and laterally non-uniform soil conditions are typically not accounted for in a one-dimensional site response analysis. Similarly, geotechnical engineering analyses of liquefaction potential and seismic stability consider only the horizontal component of the seismic motions. This reliance solely on the horizontal component is consistent with common design and code practices.

The most common analytical method used for one-dimensional site response analyses is the equivalent linear method, wherein a layered vertical soil column is treated as a linear visco-elastic material characterized by an elastic modulus and a viscous damping ratio. To account for the non-linear, strain-dependent behavior of soil, the equivalent linear modulus and damping ratio are evaluated from the modulus and damping measured in uniform cyclic loading at the "representative" shear strain. Based on comparison of observed seismic site response with site response predicted using equivalent linear analysis, the representative shear strain is usually taken as 65 percent of the maximum shear strain calculated in the site response analysis. Because the maximum shear strain is not known prior to the start of an analysis, equivalent linear response analyses are performed in an iterative manner. The maximum shear strain from one run is used to evaluate the equivalent modulus and damping for the next run and continuing to convergence.

Input to one-dimensional equivalent linear site response analyses typically includes the shear wave velocity and mass density or small-strain shear modulus for each soil layer, curves relating the representative shear strain to a modulus reduction factor and the fraction of critical damping for each soil type (modulus reduction and damping curves), the representative shear strain factor (the fraction of the maximum shear strain assumed to correspond to the representative shear strain) and an input acceleration-time history. Other input parameters include the density and shear wave velocity of the underlying bedrock. The acceleration-time history may be input as the motion at a hypothetical bedrock outcrop or at the bedrock-soil interface at the base of the soil column. Results of the analysis provide shear stress- and acceleration-time histories for each layer within the soil profile.

An alternative to the equivalent linear method of site response analysis is truly non-linear site response analysis (Lee and Finn, 1978; Matasović and Vucetic, 1993). In a truly non-linear analysis, the actual hysteretic stress-strain behavior of each element of soil (or waste) is calculated in the time domain. Equivalent linear analysis are typically performed in the frequency domain, employing the principal of superposition to calculate the time history of ground motions. Non-linear site response analyses require a description of the hysteretic stress strain behavior of the soil (or waste), the mass density profile of the material, and an input acceleration time history. Truly non-linear site response analyses hold the promise of a more accurate representation of the seismic behavior of soil deposits and solid waste landfills. However, at the present time, truly non-linear site response analyses are still primarily a research tool and have yet to be widely employed in engineering practice.

4.1.1 Simplified Analysis

Whereas structural analyses typically require information on the spectral content of ground motions, and thus require a complete time history to characterize the design motion, geotechnical analyses frequently only require knowledge of either the peak ground acceleration or the peak ground acceleration and the earthquake magnitude. Several investigators have related the peak ground acceleration from a hypothetical bedrock outcrop, such as presented on the USGS maps, to the peak ground acceleration at a specific site as a function of the local soil conditions based upon the results of one-dimensional site response analysis and observations of ground motions during earthquakes. The top plot on Figure 4.4 shows an early relationship developed by Seed and Idriss (1982) for a variety of local soil conditions. This plot was developed using SHAKE, a computer program for equivalent linear one-dimensional site response analyses developed at the University of California, Berkeley (Schnabel et al., 1972).

Experience from recent earthquakes has shown that the curves in the top plot of Figure 4.4 can significantly under-predict site amplification effects in many situations. The plot on the bottom of Figure 4.4 shows a recent curve developed by Idriss (1990) for soft soil sites. This plot was developed from both SHAKE analysis and from field observations of soft soil site response in two recent earthquakes.

Observations of the response of the OII landfill in recent earthquakes (Hushmand Associates, 1994) and the results of truly non-linear one-dimensional seismic response analyses of landfills (Kavazanjian and Matasović, 1994) indicate that the Idriss (1990) soft soil-site amplification curve may also provide an appropriate representation of the potential for peak acceleration amplification at solid waste landfills. Data obtained at the OII landfill during four recent earthquakes is plotted in Figure 4.5 along with the soft soil site field data and recommended curve from Idriss (1990). Also plotted on this figure are the results of non-linear analyses of landfill seismic response performed by Kavazanjian and Matasović (1994) using waste parameters backfigured from strong motion records obtained at the OII landfill in the 17 January 1994 M 6.7 Northridge earthquake (peak acceleration at the landfill crest equal to 0.24 g).

Some of the non-linear landfill response analyses results plotted on Figure 4.5 at 0.3 g and 0.5 g bedrock acceleration fall significantly above the Idriss (1990) curve. However, the results that fall above the Idriss curve are from low amplitude (less than 0.1 g) accelerograms recorded at large distances from the earthquake source (greater than 50 kilometers) that were scaled up to large accelerations representative of near field conditions. Therefore, the large amplification factors computed for these cases may not be representative of the amplification potential from

real earthquakes. On this basis, Kavazanjian and Matasović (1994) concluded that the Idriss (1990) soft soil amplification curve provides a reasonable representation of the peak acceleration amplification potential at the top of solid waste landfills.

The soft soil site curve developed by Idriss and presented in Figure 4.5 may therefore be used in a three-step simplified procedure developed by GeoSyntec (1994) to perform a simplified site response analyses for the purpose of adjusting the peak acceleration from the USGS map for the influence of local soil conditions (to obtain the free field peak acceleration at a project site) and for the influence of the landfill (to obtain the peak acceleration at the crest of the landfill). The three-step procedure is as follows:

Step 1: *Classify the Site.* Classify the site as special study, soft, medium stiff, stiff, or rock on the basis of the average shear wave velocity for the top 30 meters (100 feet) of soil and the following table (Borcherdt, 1994):

CLASSIFICATION	AVERAGE SHEAR WAVE VELOCITY	
Special Study	Less than 100 m/s	($\leq$ 330 ft/s)
Soft	100 to 200 m/s	(330 to 660 ft/s)
Medium Stiff	200 to 375 m/s	(600 to 1,230 ft/s)
Stiff	375 to 700 m/s	(1,230 to 2,300 ft/s)
Rock	Greater than 700 m/s	($\geq$ 2,300 ft/s)

Note that special study soils also include liquefiable soils, quick and highly sensitive clays, peats, highly organic clays, very high plasticity clays (PI > 75%), and soft soil deposits more than 37 meters (120 feet) thick.

Step 2: *Estimate the Free field Acceleration.* Estimate the potential amplification of the bedrock motions by the local soil deposit based upon the soil profile classification. For soft soils, use the curve in Figure 4.5 recommended by Idriss (1990) to estimate the free field peak ground acceleration from the peak bedrock acceleration. For medium stiff soils, use an acceleration equal to the average of the rock site acceleration and the soft soil site acceleration from Idriss' curve in Figure 4.5 for peak bedrock accelerations less than or equal to 0.4 g. For medium stiff soils when the peak bedrock acceleration exceeds 0.4 g and for stiff sites for all acceleration levels, assume the free field peak ground acceleration at the site is equal to the peak bedrock acceleration. For Special Study soil sites,

Figure 4.5 should not be used. Instead, site specific seismic response analyses such as those described in the next section of this guidance document should be conducted.

Step 3: *Estimate the Peak Acceleration at the Top of the Landfill.* Estimate the potential amplification of the peak acceleration of the landfill mass using the soft soil site amplification curve in Figure 4.5. The free field ground acceleration developed in Step 2 is used in place of the peak bedrock acceleration on the abscissa of Figure 4.5, and the acceleration at the top of the landfill is obtained from the ordinate using the Idriss (1990) empirical curve for soft soil sites.

The three-step procedure presented above is a simplified, decoupled analysis that ignores interaction between the waste mass and the ground. Non-linear analyses of the coupled response of landfills and foundation soils indicates that this simplified, decoupled analysis will yield a conservative upper bound estimate of the combined amplification potential of a landfill and its foundation (GeoSyntec, 1994).

The peak acceleration at the top of the landfill estimated in Step 3 may be used in seismic performance analyses of the landfill cover and surface water drainage systems and in evaluation of other facilities constructed on top of the landfill (e.g., flare station or storage tanks). The acceleration calculated in Step 3 is not, however, the appropriate peak acceleration for use in seismic stability and deformation potential calculations of the waste mass. For seismic stability and deformation potential evaluations of the waste mass, the average acceleration of the assumed failure mass, and not the acceleration at the top of the landfill, is the relevant response quantity, as the average acceleration is directly proportional to the seismically-induced inertia forces and to the seismic shear stresses induced at the base of the failure mass (Repetto et al., 1993).

Makdisi and Seed (1978) developed a "typical" curve relating the ratio of peak average acceleration to peak ground acceleration to the depth of the failure surface for earth dams. Kavazanjian and Matasović (1994) have demonstrated that the Makdisi and Seed (1978) earth dams curve provides a reasonable representation of the profile of average acceleration versus depth in solid waste landfills. Figure 4.6 (Kavazanjian and Matasović, 1994) compares nine different solid waste landfill non-linear seismic response analyses to the representative profile developed by Makdisi and Seed. Based upon a maximum average acceleration ratio at the base of the landfill of 0.45, as indicated by Figure 4.6, and upon a maximum amplification factor of 2.0 from Figure 4.5 for a peak bedrock acceleration of 0.1 g or greater, Kavazanjian and Matasović (1994) concluded that the free field peak ground acceleration calculated for the

landfill site in Step 2 provides a conservative estimate of the peak average acceleration at the base of the landfill for use in analyses of base liner stability and seismic deformation potential.

4.1.2 One-Dimensional Site Response Analysis

For Special Study soil sites, for major projects, and when an analysis more accurate than the simplified one presented in the previous section is desired, a one-dimensional seismic site response analysis can be performed. The site response analysis can be performed for the foundation soils only, for the waste mass only, or for the coupled response of the foundation soil and waste mass, depending on the needs and desires of the design engineer.

The computer program, SHAKE, originally developed by Seed and his co-workers (Schnabel et al., 1972) and recently updated by Idriss and Sun (1992) is perhaps the most commonly used computer program for one-dimensional equivalent linear seismic site response analysis. Basic input to SHAKE includes the soil profile, soil properties, and the input time history. Soil properties include the maximum (small strain) shear wave velocity or shear modulus and unit weight for each soil layer plus curves relating the reduction in modulus and damping ratio to shear strain for each soil type.

Modulus reduction and damping curves can be specified by the user based upon laboratory testing or upon recommendations from previous investigations. Laboratory data on soil modulus and damping at small strains (shear strains less than 10^{-4}%) can be obtained from resonant column tests. At larger strains, cyclic simple shear, cyclic triaxial, and cyclic torsional shear tests can be used. American Society for Testing and Materials (ASTM) standards exists for resonant column testing (ASTM D-3999) and cyclic triaxial testing (ASTM D-4015). Small strain modulus can also be determined from field measurements of shear wave velocity. Shear wave velocity can be measured in the field using geophysical methods such as down-hole and cross-hole velocity testing, seismic refraction, and spectral analyses of surface waves. Field measurements are generally considered more reliable than laboratory measurements of shear wave velocity or small strain modulus. Field techniques for measurement of the dynamic modulus at large strains and of the damping ratio are not currently available. Shear wave velocity is related to small strain shear modulus, G_{max}, by the equation:

$$G_{max} = \rho \cdot V_s^2 \qquad (4.2)$$

As an alternative to laboratory or field measurement of soil properties, dynamic moduli and damping for soils may be estimated as a function of soil type based upon recommendations for typical values from previous investigations. One set of practical recommendations for estimating modulus and damping of typical soils are summarized in Figure 4.7 and Table 4.1 Figure 4.7 presents typical modulus reduction and damping curves as a function of the plasticity index of the soil, PI, from Vucetic and Dobry (1991). These curves are for all soil types for a broad range of overconsolidation ratios. Table 4.1 presents coefficients and exponents for evaluating the small strain shear modulus for different soil types using the Standard Penetration Test blow count, N, and the following equation from Imai and Tonouchi (1982):

$$G_{max} = c(N)^a \tag{4.3}$$

where N is in blows per foot of penetration and c and a are coefficients from Table 4.1. Equation 4.3 was developed using Japanese data. Therefore, a blowcount corresponding to hammer efficiency of 60 percent, N_{60}, as used in U.S. practice (described in Section 5.3), needs to be converted to Japanese standards by multiplying N_{60} by 0.833 before input to Equation 4.3:

$$N = 0.833(N_{60}) \tag{4.4}$$

Unit weight, shear modulus, and damping values are also required for MSW if the MSW is included in the response analysis. Measurement of the dynamic properties of MSW in the laboratory is considered neither practical nor reliable due to the difficulties inherent to sampling and testing MSW. Back calculation of MSW properties from field observations is generally considered to be the most reliable means of evaluating these properties at this time (Kavazanjian et al., 1994b). Evaluation of the density of MSW from reported field measurements is discussed in Section 6.1.

At present, the shear wave velocity of MSW has been measured in-situ at a limited number of locations. Cross-hole shear wave velocity measurements at the Puente Hills MSW Landfill in southern California reported by Earth Technology (1988) varied from 213 m/s (700 ft/s) at the ground surface to 278 m/s (920 ft/s) at a depth of approximately 14 meters (45 feet). Sharma et al. (1990) report an average shear wave velocity of 198 m/s (455 ft/s) for MSW at depths between 0 and 15 meters (0 and 50 feet) at a landfill in Richmond, California from downhole shear wave velocity measurements. Singh and Murphy (1990) cite an investigation by others

at the Redwood Landfill in the San Francisco Bay area where an average shear wave velocity of 91 m/s (300 ft/s) was reported for the refuse. Shear wave velocities backfigured using assumed values of Poisson's ratio and waste density from Young's Modulus values developed by Carey et al. (1993) from cross-hole shear wave velocity measurements vary from 185 m/s (610 ft/s) near the surface to 478 m/s (1,580 ft/s) at a depth of 30 meters (100 feet) at the Brookhaven landfill on Long Island in New York (actual shear wave velocity measurements were not reported). Measurements at 8 MSW landfills in southern California made using Spectral Analysis of Surface Waves (SASW) were reported by Kavazanjian et al. (1994a). Shear wave velocities varied from 78 to 170 m/s (260 to 560 ft/s) near the ground surface, and from 150 to 300 m/s (500 to 990 ft/s) at a depth of 20 meters (66 feet). Shear wave velocity was reported to increase steadily with depth in the waste at all 8 sites.

Hushmand Associates (1994) report that seismic refraction surveys performed by others at the OII landfill yielded a shear wave velocity of between 200 to 240 meters per second (660 to 800 feet per second). Hushmand Associates (1994) also report that measurements of micro tremors from small earthquakes and of ambient vibrations at a strong motion instrumentation station located over an estimated 75 meters (250 feet) of waste at the OII site indicate a predominant period of between 0.8 and 1.2 seconds (corresponding to a predominant frequency of between 1.25 and 0.83 cycles per second) for the waste mass. Using Equation 4.1, this corresponds to an average shear wave velocity of between 240 and 360 meters per second (800 and 1200 feet per second) for the assumed 75 meter (250 foot) waste column. While the OII landfill is composed of mixed industrial and municipal waste, the portion of the landfill at which the strong motion station is located is believed to be composed primarily of MSW (personnel communication, Professor R.B. Seed, U.C. Berkeley, to Dr. Edward Kavazanjian, Jr., GeoSyntec Consultants).

Based upon the data cited above, Kavazanjian et al. (1994b) developed a "representative" shear wave velocity profile for MSW landfills. Figure 4.8 (Kavazanjian et al., 1994b) presents a composite plot of the available MSW shear wave velocity data along with the shear wave velocity profile developed by these investigators for use in the absence of site-specific data. In developing this shear wave velocity profile, the seismic refraction data from the OII site was assumed to represent the average velocity over the top 30 meters (100 feet) of waste and the data derived from cross-hole measurements was considered unreliable due to the potential for "short-circuiting" of the wave travel path by layers of daily and intermediate cover soils.

Modulus reduction and damping curves for MSW have never been measured in the laboratory. Prior to the 17 January 1994 Northridge earthquake, no data was available to back-calculate MSW modulus and damping from the observed seismic response of landfills. In the absence of special measurements, most investigators based the modulus reduction and damping curves for MSW upon those of clay and peat soils (Earth Technology, 1988; Singh and Murphy, 1990; Sharma and Goyal, 1991; and Repetto et al., 1993). Figure 4.9 presents recommendations from Earth Technology (1988) for modulus reduction and damping curves for MSW. These curves are reported to be based upon modulus reduction curves for peat and damping curves for clay. Figure 4.10 presents recommendations for modulus reduction and damping in MSW from Singh and Murphy (1990). The "recommended" curves are described by Singh and Murphy as the "average" of typical modulus reduction and damping curves for peat and clay that are used in engineering practice.

The strong motion recordings captured at the OII landfill in the M 6.7 Northridge earthquake represent the first (and currently the only) direct measurement of the seismic response of a solid waste landfill. In the Northridge event, the peak ground acceleration at the monitoring station on the rock outcrop adjacent to the landfill was 0.25 g, while the peak ground acceleration at the top of the landfill was 0.24 g (Hushmand Associates , 1994). Time histories of acceleration, velocity, and displacement recorded at the top of the landfill for one horizontal component of motion were previously presented in Figure 3.4.

Kavazanjian and Matasović (1994) developed the MSW modulus reduction and damping curves shown in Figure 4.11 from the observed response of the OII landfill in the Northridge event. Using the representative shear wave velocity profile shown in Figure 4.8 and the "typical" unit weight profile developed by Kavazanjian et al. (1994b), presented subsequently in Figure 6.3 of this document, Kavazanjian and Matasović (1994) back-calculated parameters describing the cyclic behavior of MSW for a non-linear site response model from the observed landfill response. Then, these investigators used the non-linear model to predict the response of MSW to uniform cyclic loading and compute the modulus reduction and damping curves for MSW shown in Figure 4.11.

The modulus reduction and damping curves for MSW shown in Figure 4.11 were used by Kavazanjian and Matasović (1994) in the program SHAKE to perform an equivalent linear response analysis of the response of the OII landfill in the Northridge earthquake. By trial and error, a representative shear strain factor of 0.8 (representative shear strain equal to 0.8 times the maximum cyclic shear strain) was found to give the best agreement between observed and predicted behavior.

Figure 4.12 compares the OII landfill response observed in the Northridge earthquake to the response predicted by Kavazanjian and Matasović (1994) using SHAKE, the modulus reduction and damping curves in Figure 4.11, and a representative shear strain factor of 0.8. This figure also shows landfill response predicted by Kavazanjian et al. (1994b) using SHAKE and various combinations of modulus reduction and damping curves for peat and clay along with the best fit representative shear strain factor. Based upon this comparison, Kavazanjian et al. (1994b) suggested that the modulus reduction and damping curves shown in Figure 4.11 be used in equivalent linear seismic response analysis of MSW landfills until additional information on the cyclic response of MSW becomes available.

4.1.3 Two- and Three-Dimensional Site Response Analysis

Computer programs are available for equivalent linear and truly non-linear two- and three-dimensional seismic site response analyses. However, such programs are not commonly used in engineering practice. The programs for two- and three-dimensional site response analyses are not particularly "user-friendly". Furthermore, experience with two-dimensional site response analyses of earth dams has shown that one-dimensional site response analyses of vertical columns within the embankment typically yield accelerations and stresses within ten percent of the results of the more sophisticated two- and three-dimensional analyses (Vrymoed and Calzascia, 1978). Two- and three-dimensional effects may logically be expected to be even less significant with respect to the seismic response of landfills compared to earth dams, as landfills tend to be massive structures with broad decks. Considering the level of uncertainty associated with input motions and material properties, two- and tree-dimensional seismic response analyses do not appear to be warranted for most landfill projects at this time.

Once the soil profile and material properties have been specified, the only remaining input is the input earthquake motion. Selection of representative time histories for the input motion is discussed in Section 4.2.

4.2 Selection of Earthquake Time History

Earthquake time histories may be required for input to SHAKE seismic response analyses or, if a simplified seismic response analysis is employed, for input to the seismic deformation analyses described in Section 6. Time histories can be developed either by selecting a representative time history from the catalog of acceleration time histories recorded in previous earthquakes or by synthesizing an artificial accelerogram. Selection of a representative time history from the catalog of available strong motion records and scaling it to the appropriate peak

acceleration is, in general, a preferable approach to use of a synthetic time history. However, due to limitations in the catalog of available records, it is not always possible to find a representative time history from the catalog of available records, particularly for the eastern and central United States.

In selecting a representative time history from the catalog of available records, an attempt should be made to match as many of the relevant characteristics of the design earthquake as possible. Important characteristics that should be considered in selecting a time history from the catalog include:

- earthquake magnitude;
- source mechanism (e.g., strike-slip, normal, or reverse faulting);
- focal depth;
- site to source distance;
- site geology; and
- peak ground acceleration.

These factors are ranked in a general order of decreasing importance. However, the relative importance may vary from case to case. For instance, if a bedrock record is chosen for use in a SHAKE analysis of the influence of local soil conditions, site geology will not be particularly important in selection of the input bedrock time history. However, if a soil site record scale to a peak ground acceleration that already includes consideration of the potential for amplification of motions by local soil conditions is to be used in the response analysis, site geology can be a critical factor in selection of an appropriate time history.

Scaling of the peak acceleration of a record by a factor of more than 2 is not recommended, as the frequency characteristics of ground motions can be directly and indirectly related to the amplitude of the motion. Leeds (1992) and Naeim and Anderson (1993) present summaries of available strong motion records and their characteristics.

Due to uncertainties in the selection of a representative earthquake time history, response analyses should never be performed using only a single time history. The use of a suite of at least three time histories is recommended for purposes of evaluating seismic site response. For earthquakes in the western United States, it should be possible to find 3 representative time histories that satisfy the above criteria. However, at the present time, there are only two bedrock strong motion records available from earthquakes of magnitude M 5.0 or greater in the central and eastern North America:

- the Les Eboutements record with a peak horizontal acceleration of 0.23 g from the 1988 Saguenay, Quebec earthquake of magnitude M 6.0; and

- the Loggie Lodge record with a peak horizontal acceleration of 0.4 g from the 1981 Mirimichi, New Brunswick earthquake of magnitude M 5.0.

Therefore, for analysis of sites east of the Rocky Mountains, at least one record from a western United States site, an international recording site, or a synthetic accelerogram may be required to compile a suite of three records for analysis. For the new Madrid seismic zone, where neither the Mirimichi nor Saguenay record is of appropriate magnitude, all three records must be from either the western United States, an international site, or synthetically generated.

One of the primary differences anticipated between earthquakes in the eastern and central United States and those in the western United States is frequency content (Nuttli, 1981; Atkinson, 1987). There may also be a difference in duration due to the different rates of acceleration attenuation. For liquefaction analyses which depend only on peak acceleration, use of a western United States earthquake record of appropriate magnitude and intensity for analysis of a site in the eastern or central United States should be acceptable. However, for analysis of seismic deformation potential at an eastern or central United States site, the appropriateness of using a western United States earthquake record is uncertain. The greater energy at lower frequencies in typical western U.S. records could result in a conservative estimate of deformation potential at an eastern or central United States site. On the other hand, the potential for a longer duration on the east coast compared to the west coast for an earthquake of the same magnitude and distance could have the opposite effect.

Due to the difference in the anticipated depths of the causative faults, when using a western United States record to analyze a site in the eastern United States precedence should be given to matching hypocentral distance over peak acceleration. Hypocentral distance is the distance from the site to the center of energy release for the earthquake. Hypocentral distance includes the effect of the depth of the earthquake in the distance measure.

Computer programs are available to generate a synthetic seismic accelerogram to meet peak acceleration, duration, and frequency content requirements (Gasparin and Vanmarcke, 1976; Ruiz and Penzien, 1969; Silva and Lee, 1987). Synthetic earthquake accelerograms for many regions of the country are currently being compiled by Dr. Klaus Jacob at the Lamont-Doherty Observatory of Columbia University under the auspices of the National Center for Earthquake Engineering Research (see Table 2.2). However, at the time of preparation of this guidance

document this compilation was not yet available. The generation of synthetic acceleration time-histories is not generally within the technical expertise of civil engineering firms and should not be undertaken without expert consultation. For this reason, generation of synthetic earthquake acceleration time-histories is beyond the scope of this manual. However, appropriate synthetic accelerograms may be available to the engineer from previous studies and may be used if they are shown to be appropriate for the site.

4.3 References

Anderson, D.G., Hushmand, B., and Martin, G.R. (1992), "Seismic Response of Landfill Slopes, " Proc. *Stability and Performance of Slopes and Embankments - II*, Vol. 2, ASCE Geotechnical Special Publication No. 31, Berkeley, California, pp. 973-989.

Atkinson, G.M. (1987), "Implications of Eastern Ground Motion Characteristics for Seismic Hazard Assessment in Eastern North America," Proc. *Symposium on Seismic Hazards, Ground Motions, Soil-Liquefaction and Engineering Practice in Eastern North America*, Tuxedo, New York, NCEER Technical Report No. NCEER-87-0025.

Borcherdt, R.D. (1994) "New Developments in Estimating Site Effects on Ground Motion," Proc. *Seminar on New Developments in Earthquake Ground Motion Estimation and Implications for Engineering Design Practice*, Applied Technology Council, ATC35-1, Redwood City, California, pp. 2-1 - 2-12.

Carey, P.J., Koragappa, N. and Gurda, J.J. (1993) "A Case Study of the Brookhaven Landfill - Long Island, New York," Proc. *Waste Tech '93*, Marina del Rey, California, 15 p.

Earth Technology (1988), "In-Place Stability of Landfill Slopes, Puente Hills Landfill, Los Angeles, California," Report No. 88-614-1, The Earth Technology Corporation, Long Beach, California.

Gasparin, D.A. and Vanmarcke, E.H. (1976) "SIMQKE - A Program for Artificial Motion Generation," Department of Civil Engineering, Massachusetts Institute of Technology, Massachusetts.

GeoSyntec (1994), "Non-Linear Seismic Response Analysis of Solid Waste Landfills," Internal Research Report, GeoSyntec Consultants, Huntington Beach, California.

Hushmand Associates (1994), "Landfill Response to Seismic Events," Report prepared for the USEPA Region IX, Hushmand Associates, Laguna Niguel, California.

Idriss, I.M. (1990), "Response of Soft Soil Sites During Earthquakes," Proc. *Symposium to Honor Professor H.B. Seed*, Berkeley, California.

Idriss, I.M. and Sun, J.I. (1992) "User's Manual for SHAKE91," Center for Geotechnical Modeling, Department of Civil and Environmental Engineering, University of California, Davis, California, 13 p. (plus Appendices).

Imai, T. and Tonouchi, K. (1982), "Correlation of N Value with S-Wave Velocity," Proc. *2nd European Symposium on Penetration Testing*, Amsterdam, The Netherlands, pp. 67-72.

Kavazanjian, E., Jr., and Matasović, N. (1994), "Seismic Analysis of Solid Waste Landfills," paper accepted for publication at *Geoenvironment 2000*, ASCE Specialty Conference, New Orleans, Louisiana, 22-24 February 1995.

Kavazanjian, E., Jr., Snow, M.S., Matasović, N., Poran, C., and Satoh, T. (1994a), "Non-Intrusive Rayleigh Wave Investigations at Solid Waste Landfills." Proc. *1st International Congress on Environmental Geotechnics*, Edmonton, Alberta, pp. 707-712.

Kavazanjian, E., Jr., Matasović, N., Bonaparte, R., and Schmertmann, G.R. (1994b), "Evaluation of MSW Properties for Seismic Analysis," paper accepted for publication at *Geoenvironment 2000*, ASCE Specialty Conference, New Orleans, Louisiana, 22-24 February 1995.

Lee, M.K.W., and Finn, W.D.L. (1978), "DESRA-2, Dynamic Effective Stress Response Analysis of Soil Deposits with Energy Transmitting Boundary Including Assessment of Liquefaction Potential," *Soil Mechanics Series No. 36*, Department of Civil Engineering, University of British Columbia, Vancouver, Canada, 60 p.

Leeds, D.L. (1992) "State-of-the-Art for Assessing Earthquake Hazards in the United States: Report 28, Recommended Accelerograms for Earthquake Ground Motions," Misc. Paper S-73-1, Geotechnical Laboratory, U.S Army Waterways Experiment Station, Vicksburg, Mississippi, 171 p. (plus Appendices).

Matasović, N. and Vucetic, M. (1993), "Cyclic Characterization of Liquefiable Sands," *Journal of Geotechnical Engineering*, ASCE, Vol. 119, No. 11, pp. 1805-1822.

Naeim, F. and Anderson, J.C. (1993), "Classification and Evaluation of Earthquake Records for Design," Report No. CE 93-08, Department of Civil Engineering, University of Southern California, Los Angeles, 288 p.

Nuttli, O.W. (1981), "Similarities and Differences Between Western and Eastern United States Earthquakes, and their Consequences for Earthquake Engineering," Earthquakes and Earthquake Engineering: The Eastern United States, Vol. 1, Assessing the Hazard - Evaluating the Risk, J.E. Beavers, Ed., Ann Arbor Science Publishers, Inc., Ann Arbor, Michigan, pp. 25-51.

Repetto, P.C., Bray, J.D., Byrne, R.J. and Augello, A.J., (1993), "Applicability of Wave Propagation Methods to the Seismic Analysis of Landfills," Proc. *Waste Tech '93*, Marina Del Rey, California, pp. 1.50-1.74.

Ruiz, J. and Penzien, J., (1969) "PSEQGN - Artificial Generation of Earthquake Accelerograms," Report No. EERC 69-3, Earthquake Engineering Research Center, University of California, Berkeley, California.

Schnabel, P.B., Lysmer, J. and Seed, H.B. (1972) "SHAKE: A Computer Program for Earthquake Response Analysis of Horizontally Layered Sites." Report No. EERC 72-12, Earthquake Engineering Research Center, University of California, Berkeley, California.

Seed, H.B. (1975) "Earthquake Effects on Soil-Foundation Systems," *In Foundation Engineering Handbook*, H.F. Winterkorn and H.Y. Fang Eds., Van Nostrand Reinhold, New York, pp. 700-732.

Seed, H.B. and Idriss, I.M., (1982), "Ground Motions and Soil Liquefaction During Earthquakes," *Monograph No. 5*, Earthquake Engineering Research Institute, Berkeley, California, 134 p.

Sharma, H.D., Dukes, M.T., and Olsen, D.M., (1990), "Field Measurements of Dynamic Moduli and Poisson's Ratio of Refuse and Underlying Soils at a Landfill Site," *In Geotechnics of Waste Fill - Theory and Practice*, ASTM STP 1070, pp. 57-70.

Sharma, H.D. and Goyal, H.K. (1991), "Performance of a Hazardous Waste and Sanitary Landfill Subjected to Loma Prieta Earthquake," Proc. *2nd International Conference on Recent Advances in Geotechnical Earthquake Engineering and Soil Dynamics*, St. Louis, Missouri, pp. 1717-1725.

Silva, W.D. and Lee, K. (1987) "State-of-the-Art for Assessing Earthquake Hazards in the United States: Report 24, WES RASCAL Code for Synthesizing Earthquake Ground Motions," Misc. Paper S-73-1, Geotechnical Laboratory, U.S. Army Waterways Experiment Station, Vicksburg, Mississippi.

Singh, S. and Murphy, B.J., (1990), "Evaluation of the Stability of Sanitary Landfills," *In Geotechnics of Waste Fills - Theory and Practice*, ASTM STP 1070, pp. 240-258.

Vrymoed, J.L. and Calzascia, E.R. (1978), "Simplified Determination of Dynamic Stresses in Earth Dams," Proc. *Earthquake Engineering and Soil Dynamics*, ASCE, Pasadena, California, pp. 991-1006.

Vucetic, M. and Dobry, R. (1991) "Effect of Soil Plasticity on Cyclic Response." *Journal of the Geotechnical Engineering*, ASCE, Vol. 117, No. 1, 89-107.

Wood, H.O. (1908), "Distribution of Apparent Intensity in San Francisco," in *The California Earthquake of April 18*, 1906," Report of the State Earthquake Investigation Commission, Carnegie Institution of Washington, D.C., pp. 220-245.

TABLE 4.1: PARAMETERS FOR THE EMPIRICAL RELATIONSHIP TO ESTIMATE G_{max} (After Imai and Tonouchi, 1982)

SOIL TYPE	c (kg/cm^2)	a (-)
Peat	53.7	1.08
Clay	176.0	0.607
Sand	125.0	0.611
Gravel	82.5	0.767

Notes: (1) G_{max} = Small strain shear modulus; $G_{max} = c(N)^a$; G_{max} in kg/cm^2.
(2) N = (uncorrected) SPT blowcount according to Japanese standards. Multiply N_{60} from U.S. practice by 0.833 to estimate a comparable blow count.
(3) Correlation applies only for soils of alluvial origin. For soils of other origin, the original reference should be consulted.

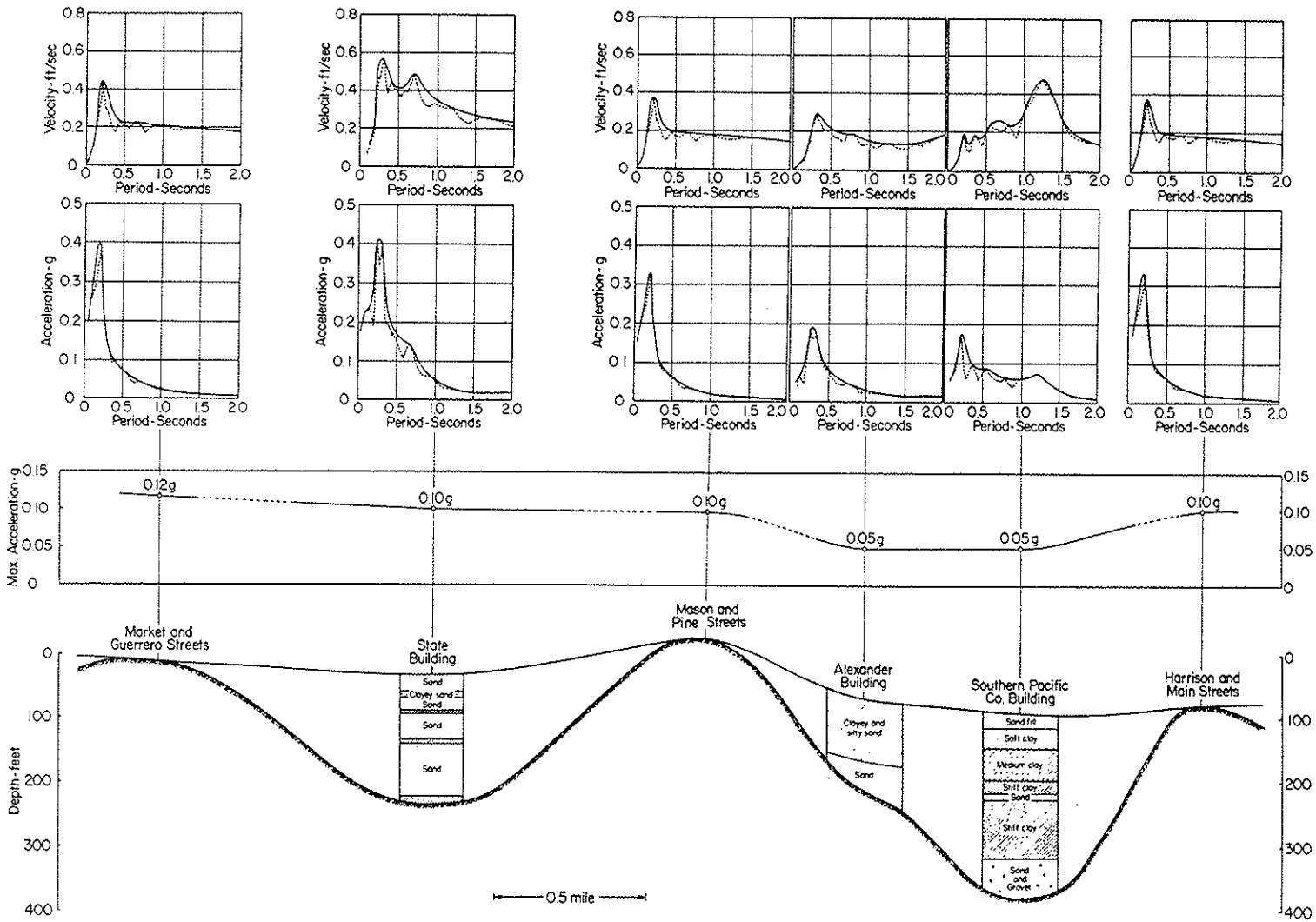

Figure 4.1 Soil Conditions and Characteristics of Recorded Ground Motions, San Francisco M 5.7 Earthquake of 22 March 1957 (Seed, 1975).

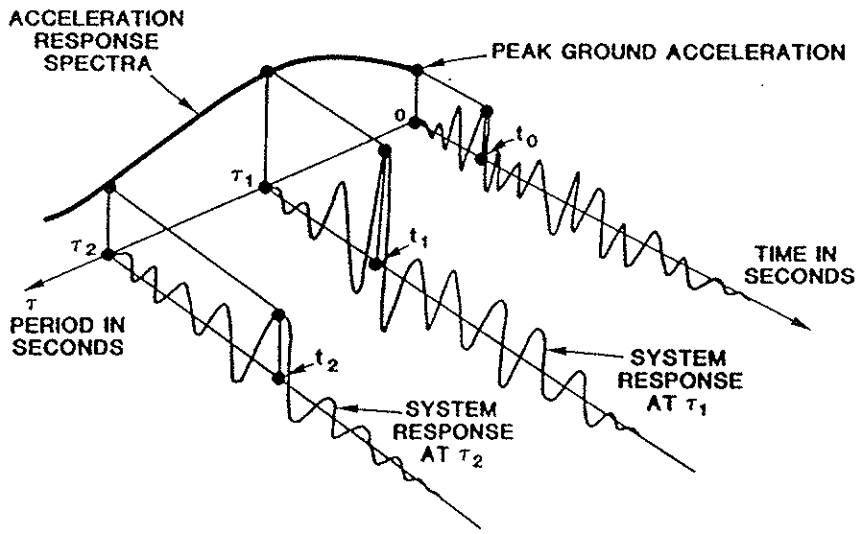

Figure 4.2 Development of Acceleration Response Spectrum for Damped Single Degree of Freedom System.

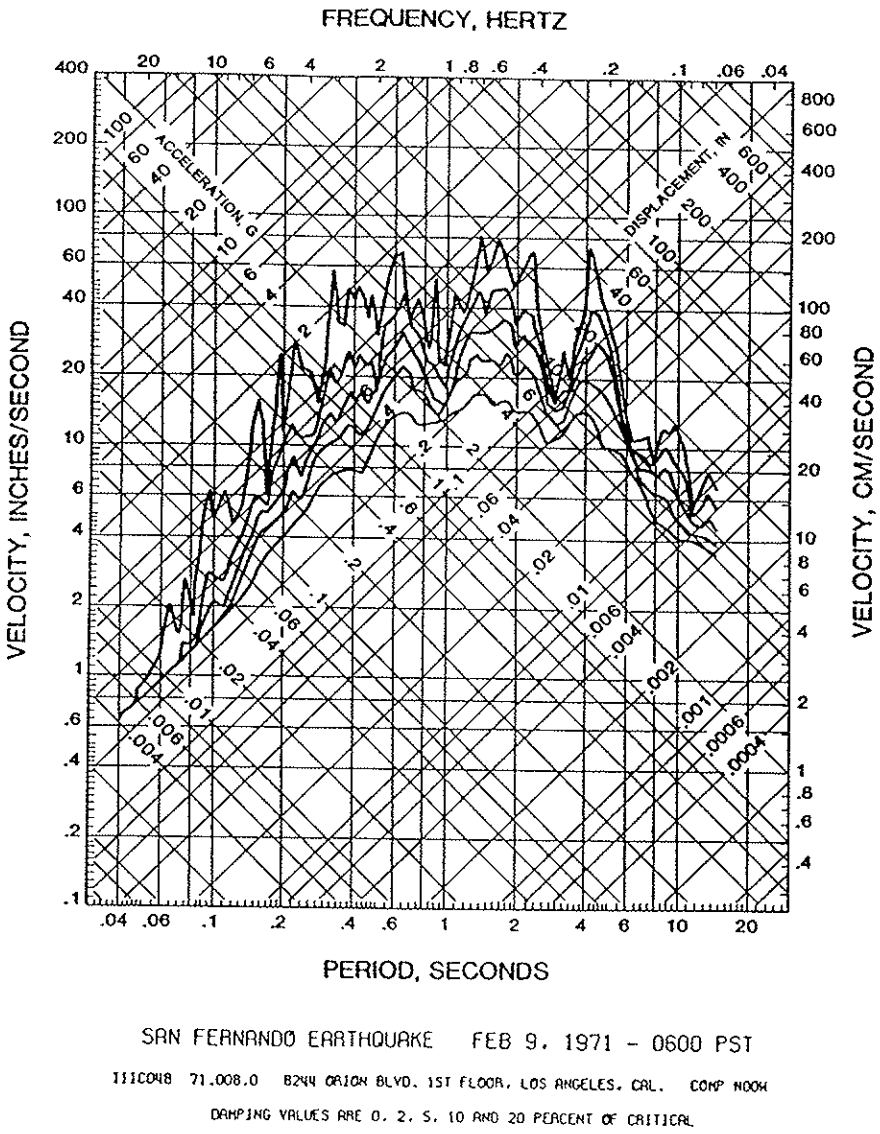

Figure 4.3 Tripartite Representation of Response Spectra.

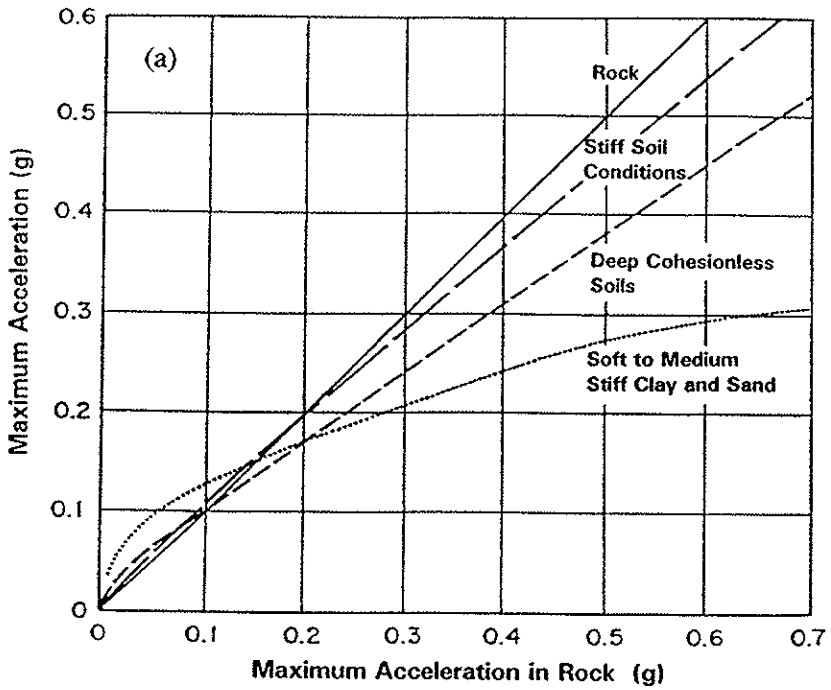

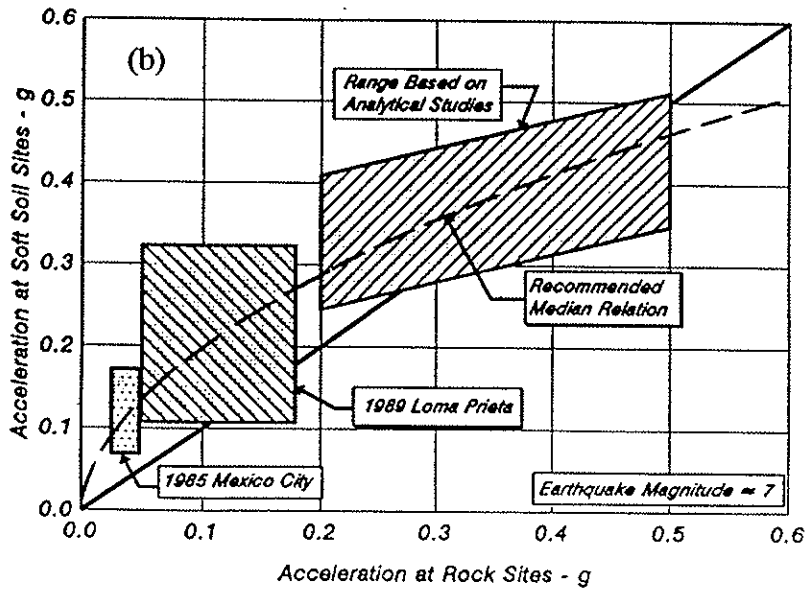

Figure 4.4 Relationship Between Maximum Acceleration on Rock and Other Local Site Conditions: (a) Seed and Idriss (1982); (b) Idriss (1990).

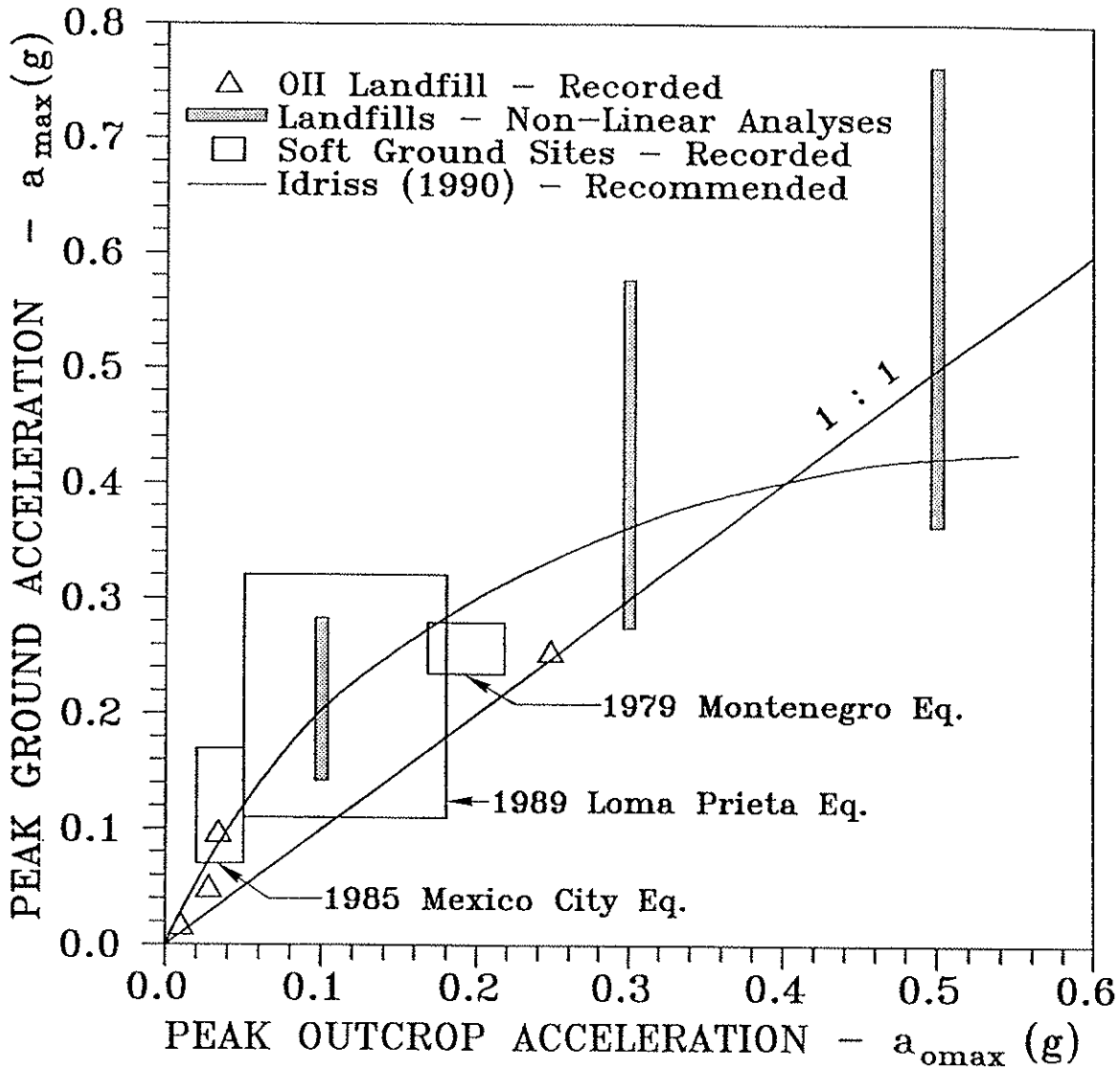

Figure 4.5 Observed Variations of Peak Horizontal Accelerations on Soft Soil and MSW Sites in Comparison to Rock Sites (Kavazanjian and Matasović, 1994).

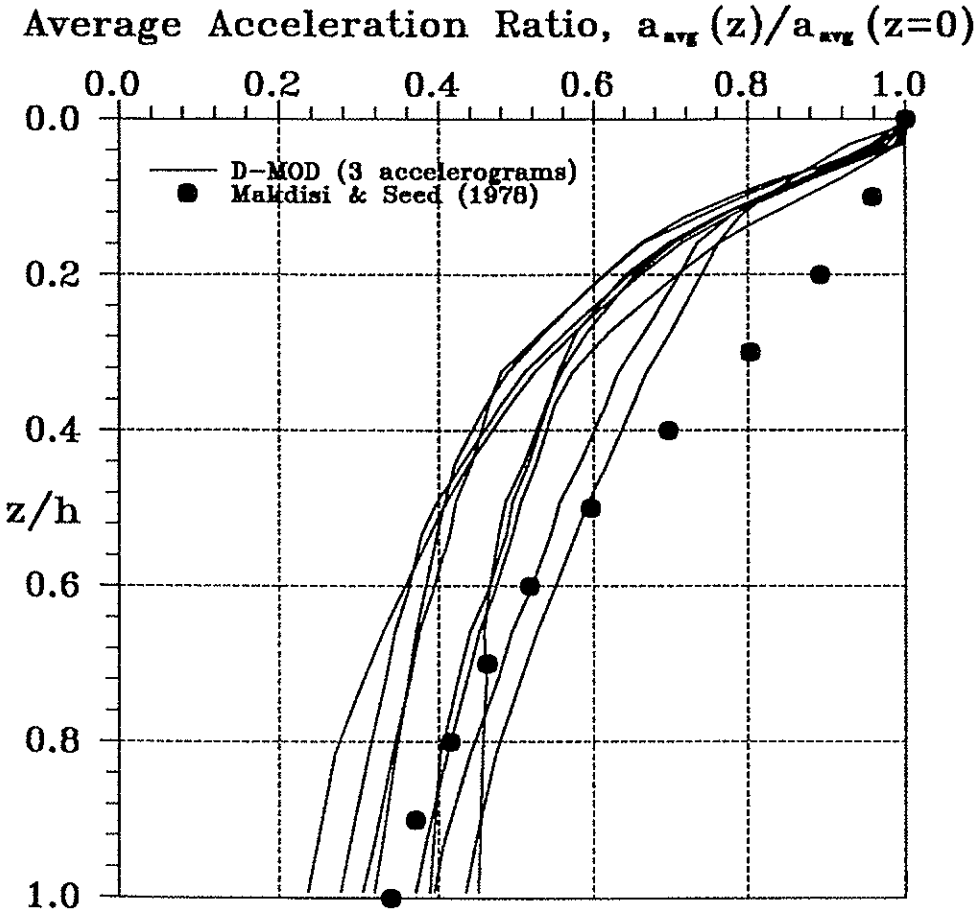

Figure 4.6 Variation of Maximum Average Acceleration Ratio with Depth of Sliding Mass (Kavazanjian and Matasović, 1994).

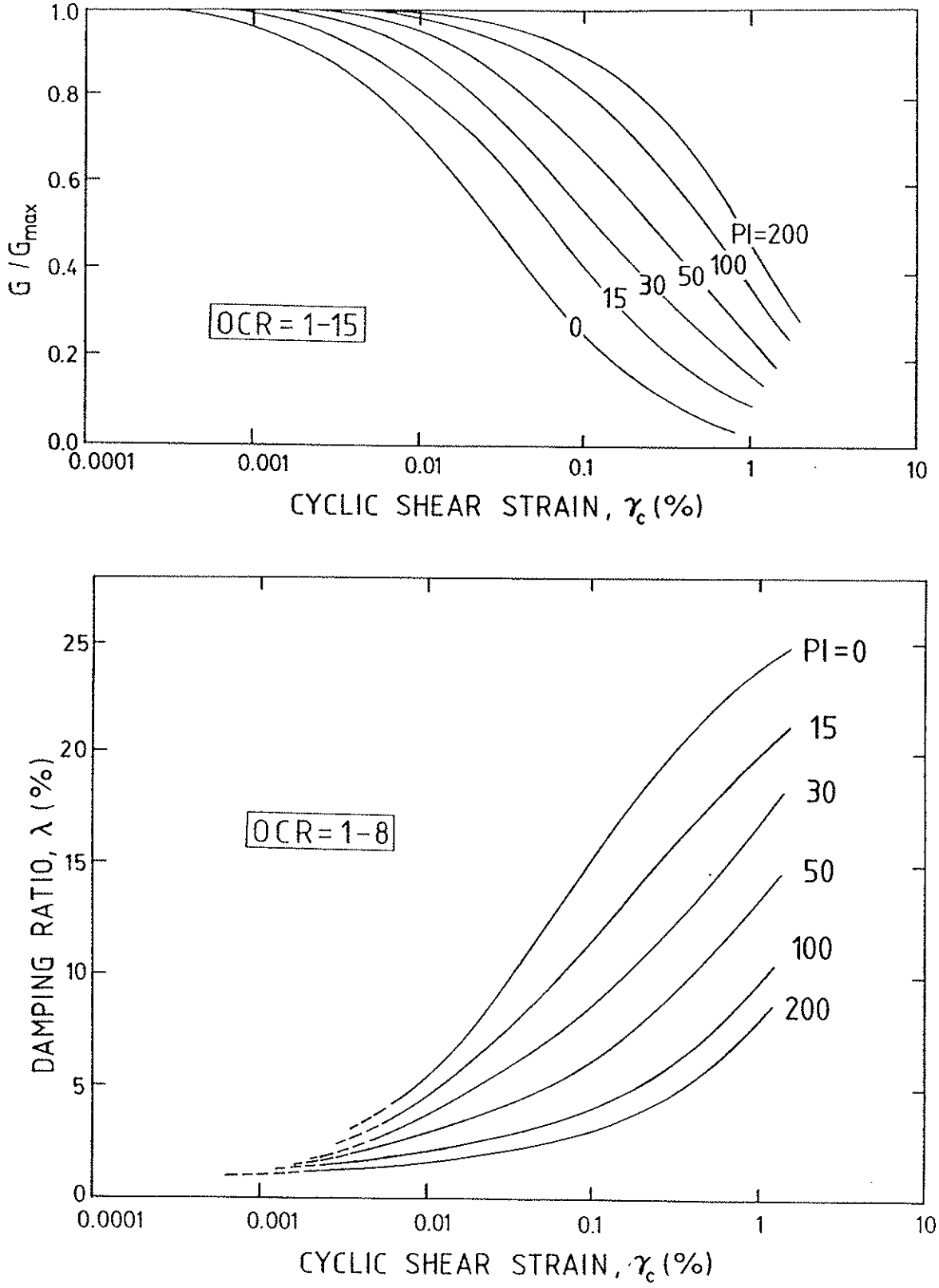

Figure 4.7 Modulus Reduction and Damping Curves for Soils of Different Plasticity Index (PI) (Vucetic and Dobry, 1991).

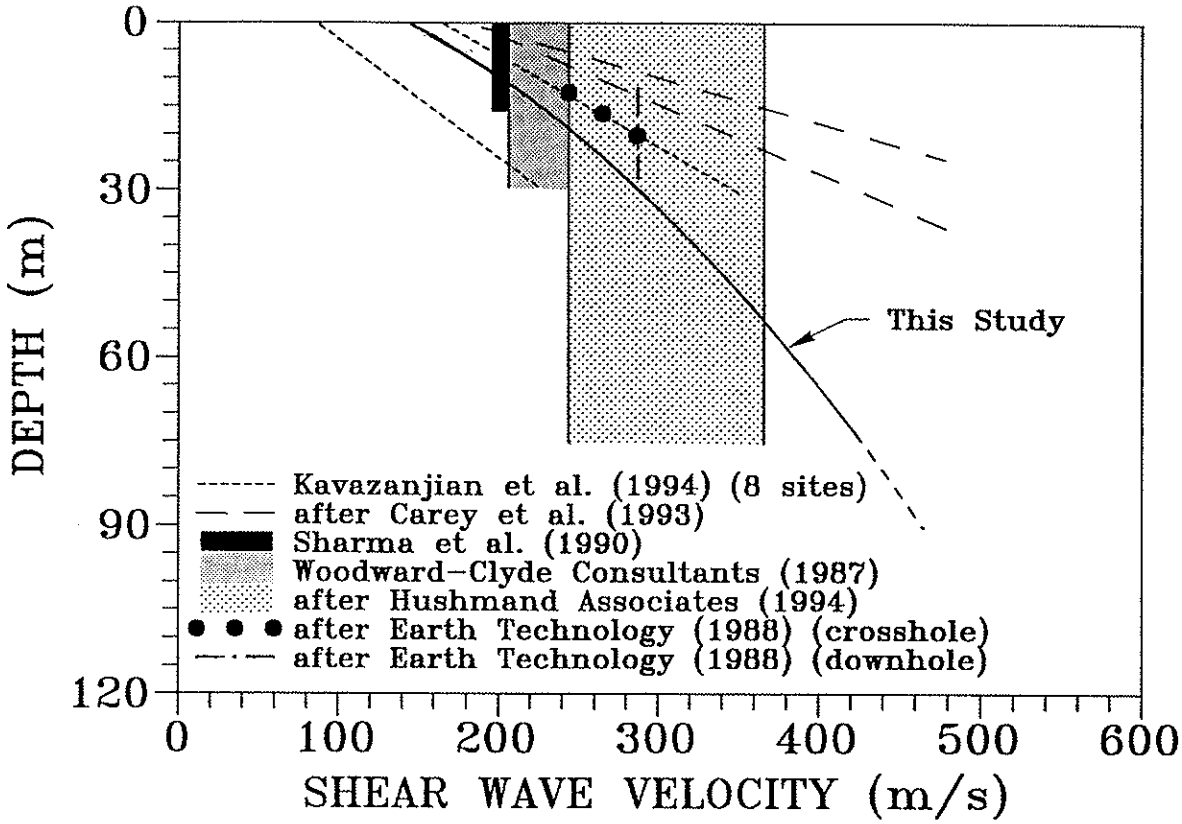

Figure 4.8 Shear Wave Velocity of MSW (Kavazanjian et al., 1994b).

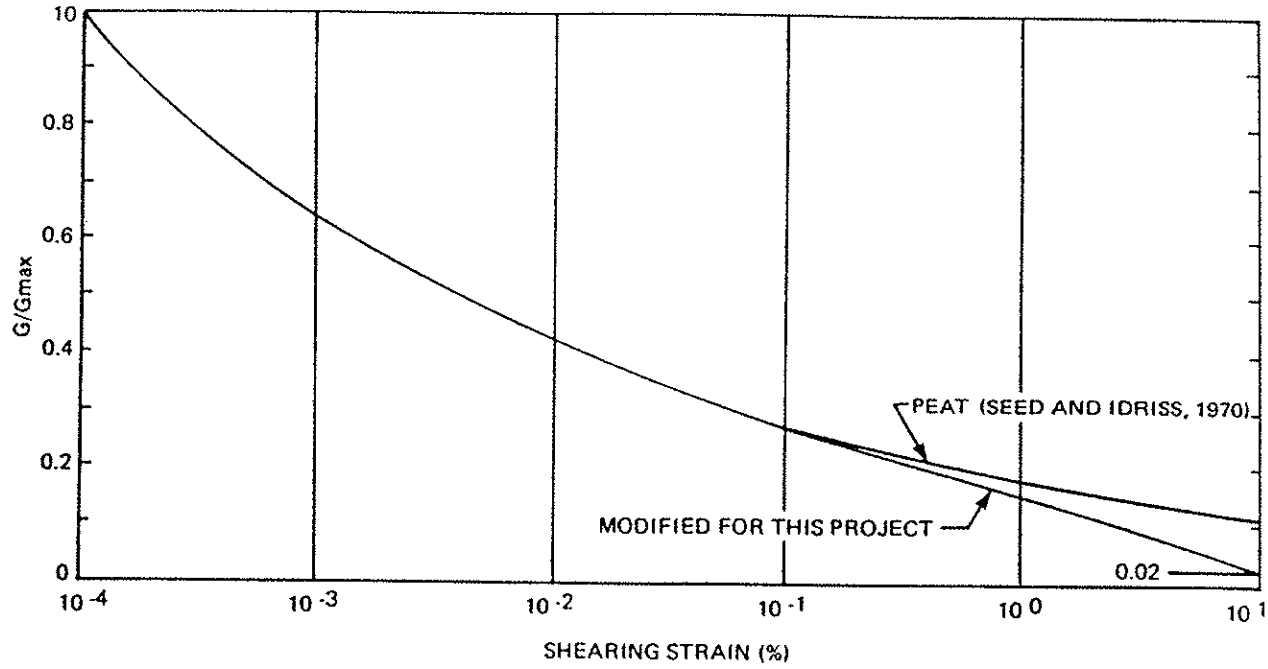

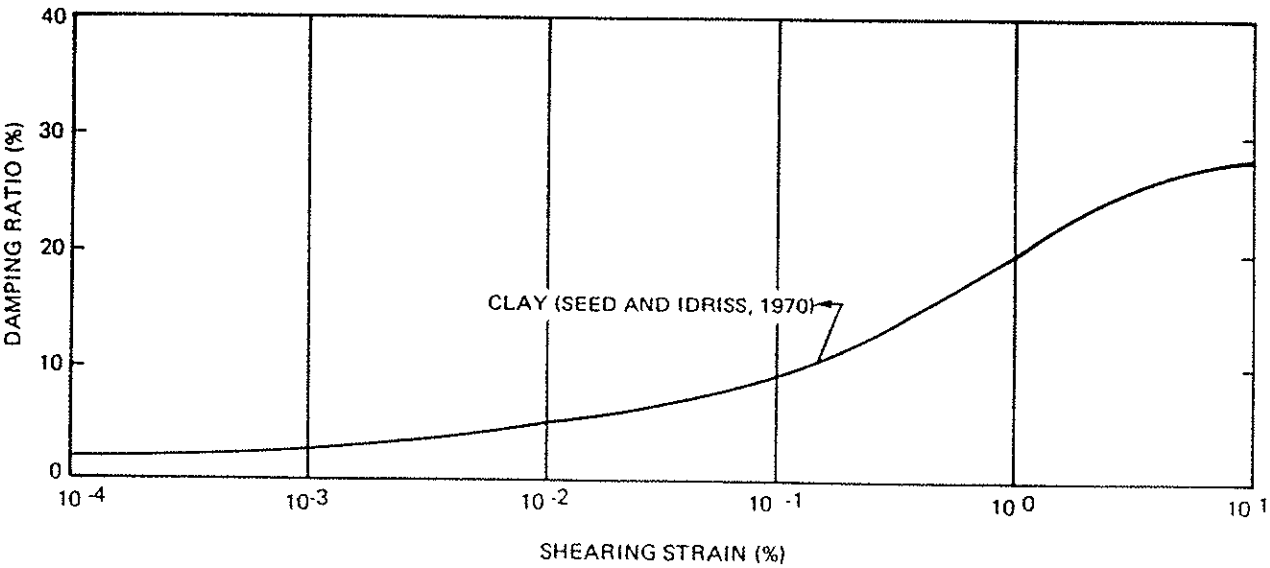

Figure 4.9 Modulus Reduction and Damping Curves for MSW (Earth Technology, 1988).

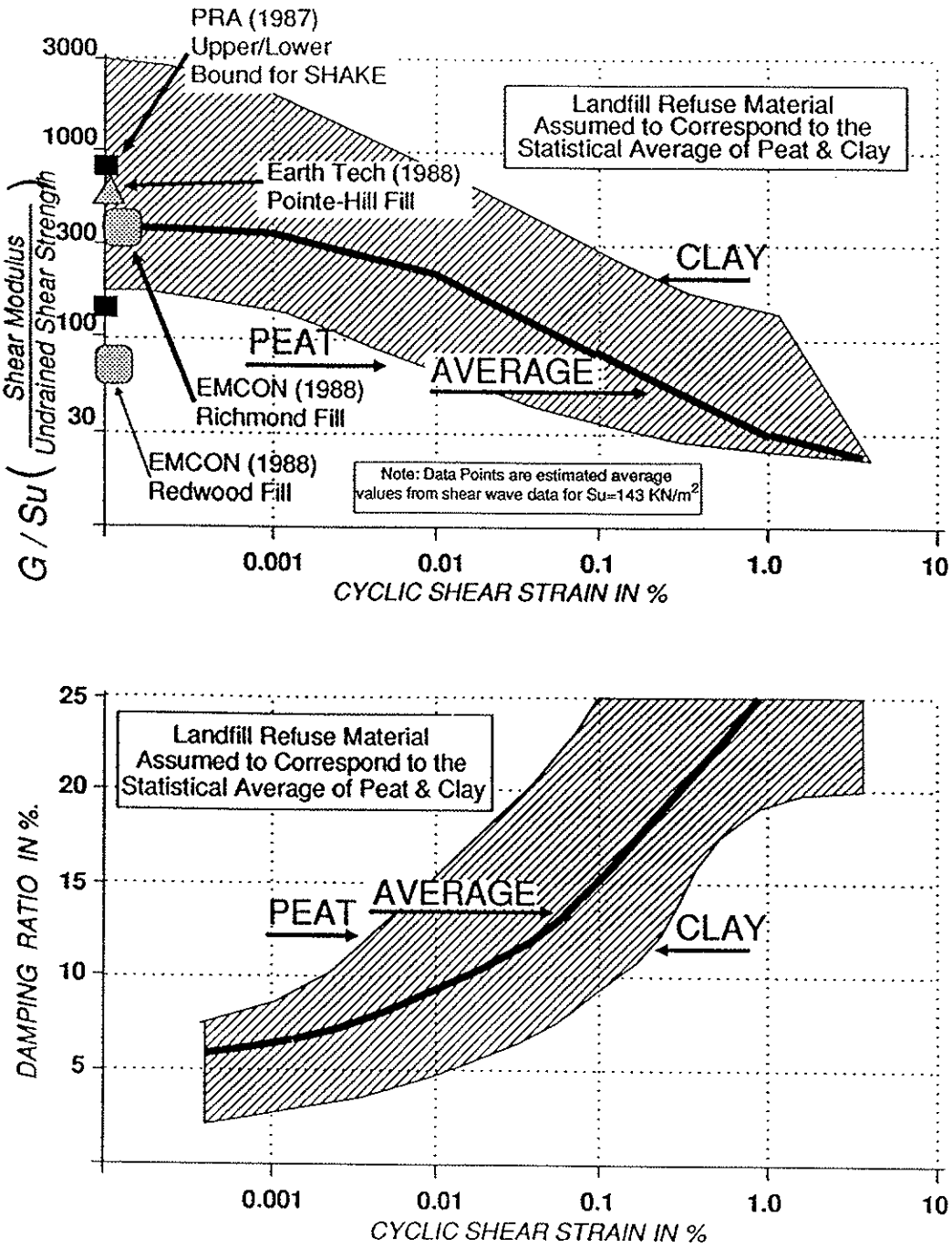

Figure 4.10 Modulus Reduction and Damping Curves for MSW (Singh and Murphy, 1990).

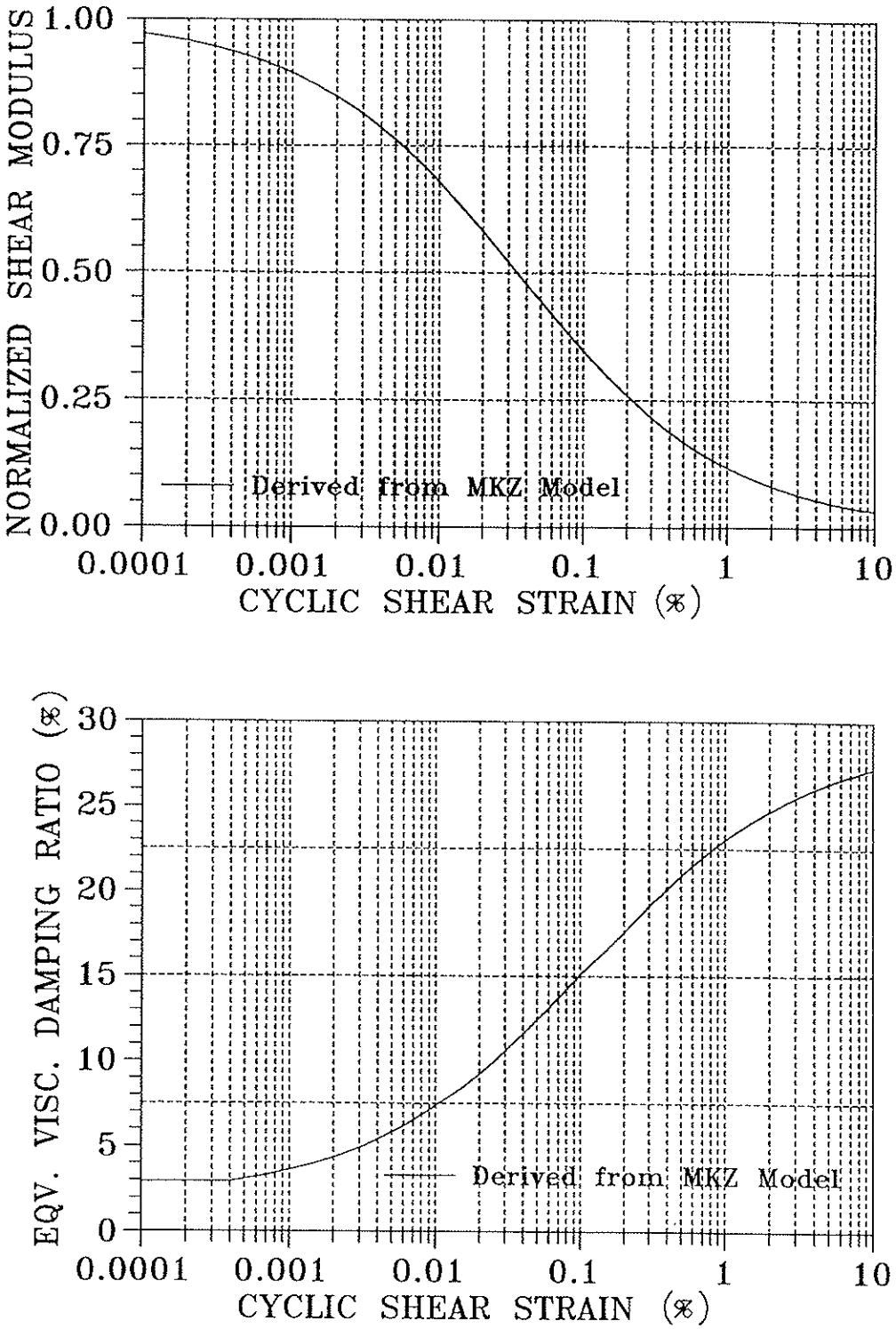

Figure 4.11 Modulus Reduction and Damping Curves for MSW (Kavazanjian and Matasović, 1994).

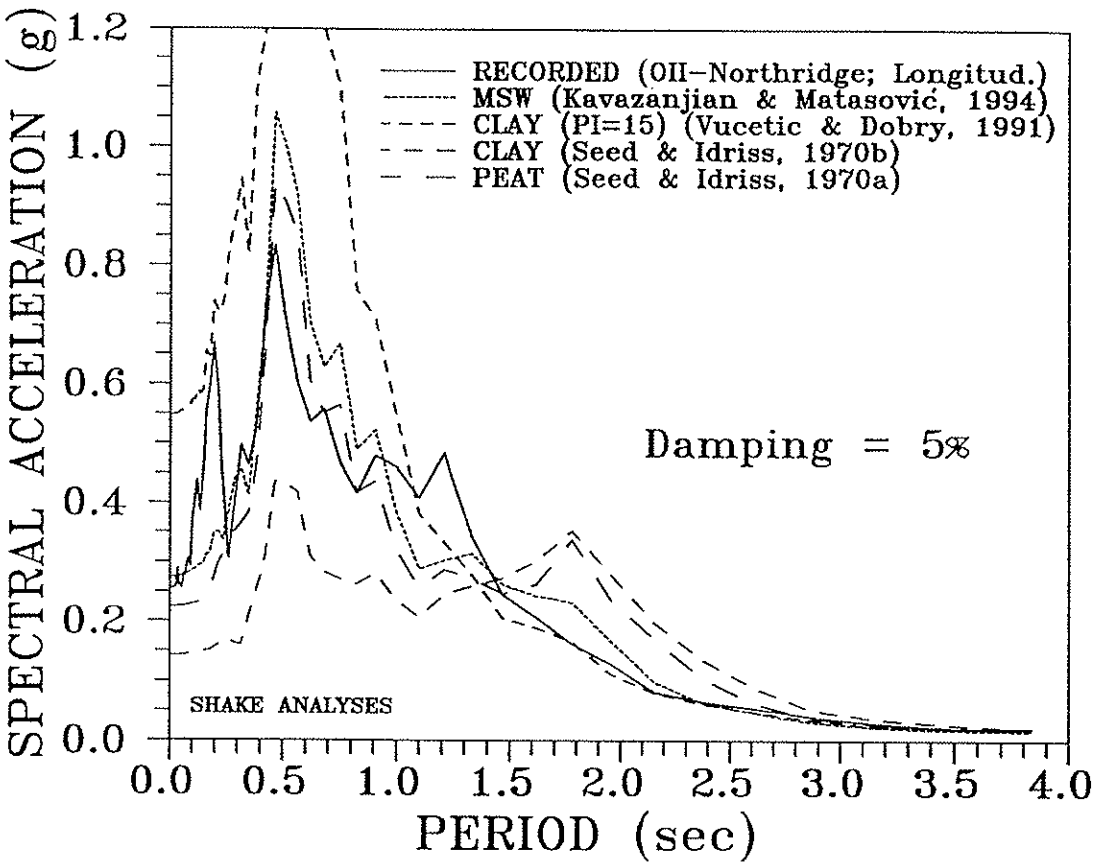

Figure 4.12 Comparison of OII Landfill Response to Results of Equivalent Linear Analysis (Kavazanjian et al., 1994b).

SECTION 5
258.14 SEISMIC IMPACT ZONES: LIQUEFACTION ANALYSIS

During strong earthquake shaking, loose, saturated soil deposits may experience a sudden loss of strength and stiffness, sometimes resulting in large, permanent displacements of the ground. This phenomenon is called soil liquefaction. Liquefaction beneath and in the vicinity of a municipal solid waste landfill facility (MSWLF) can have severe consequences with respect to the integrity of the landfill containment system. Localized bearing capacity failures, lateral spreading, and excessive settlements resulting from liquefaction may damage landfill liner and cover systems. Liquefaction-associated lateral spreading and flow failures can also affect the global stability of the landfill. Therefore, a liquefaction potential assessment is a key element in the seismic design of landfills.

This Section outlines the current state-of-the practice for evaluation of the potential for soil liquefaction and the consequences of soil liquefaction (should it occur) as it applies to the seismic design of a MSWLF. Initial screening criteria to determine whether or not a liquefaction analysis is needed are presented in Section 5.1. The simplified procedure for liquefaction potential assessment commonly used in engineering practice is presented in Section 5.2. Methods for performing a liquefaction impact assessment are presented in Section 5.3. Methods for mitigation of liquefaction potential and the consequences of liquefaction are discussed in Section 5.4. Advanced methods for liquefaction potential assessments, including one- and two-dimensional fully-coupled effective stress site response analyses, are also discussed in Section 5.4.

5.1 Initial Screening

The first step in any liquefaction evaluation is to assess whether the potential for liquefaction exists at a site. A variety of screening techniques exists to distinguish sites that are clearly safe with respect to liquefaction from those sites that require more detailed study (e.g., Dobry et al., 1980). The following five screening criteria are most commonly used to make this assessment:

- *Geologic age and origin.* Liquefaction potential decreases with increasing age of a soil deposit. Pre-Holocene age soil deposits generally do not liquefy. Table 5.1 presents the liquefaction susceptibility of soil deposits as a function of age and origin (Youd and Perkins, 1978).

- *Fines content and plasticity index.* Liquefaction potential decreases with increasing fines content and increasing plasticity index, PI. Data presented in Figure 5.1 (Ishihara et al., 1989) show grain size distribution curves of soils known to have liquefied in the past. This data serves as a rough guide for liquefaction potential assessment of cohesionless soils. Soils having less than 15 percent (by weight) finer than 0.005 mm, a liquid limit below 35 percent, and an in-situ water content less than 0.9 times the liquid limit generally do not liquefy (Seed and Idriss, 1982).

- *Saturation.* Although partially saturated soils have been reported to liquefy, full saturation is generally deemed to be a necessary condition for soil liquefaction. In many locations, the water table is subject to seasonal oscillation. In general, it is prudent that the highest anticipated seasonal water table elevation be considered for initial screening.

- *Depth below ground surface.* While failures due to liquefaction of end-bearing piles resting on sand layers up to 100 ft (30 m) below the ground surface have been reported, liquefaction is generally not likely to occur more than 50 ft (15 m) below the ground surface.

- *Soil Penetration Resistance.* According to the data presented in Seed and Idriss (1985), liquefaction has not been observed in soil deposits having normalized Standard Penetration Test (SPT) blowcount, $(N_1)_{60}$ larger than 22. Marcuson, et al. (1990) suggest a normalized SPT value of 30 as the threshold value above which liquefaction will not occur. However, Chinese experience, as quoted in Seed et al. (1983), suggests that in extreme conditions liquefaction is possible in soils having normalized SPT blowcounts as high as 40. Shibata and Teparaska (1988), based on a large number of observations, conclude that no liquefaction is possible if normalized Cone Penetration Test (CPT) cone resistance, q_c, is larger than 157 tsf (15 MPa). This CPT resistance corresponds to normalized blow counts between 30 and 60, depending on the grain size of the soil (see Figure 5.2).

If three or more of the above criteria indicate that liquefaction is not likely, the potential for liquefaction may be dismissed. If, however, based on the above initial screening criteria, the potential for liquefaction at the site of a planned landfill (new construction or lateral expansion) cannot be dismissed, more rigorous analysis of liquefaction potential is needed.

Liquefaction susceptibility maps, derived on the basis of the some (or all) of the above listed criteria, are available for many major urban areas in seismic zones (e.g., Kavazanjian et al., 1985; Tinsley et al., 1985; Hadj-Hamou and Elton, 1988; Hwang and Lee, 1992). However, as most new MSWLF's are sited outside of major urban areas, these maps may not be available for many landfill sites.

There have been several attempts to establish threshold criteria for values of seismic shaking that can induce liquefaction (e.g., minimum earthquake magnitude, minimum peak horizontal acceleration, maximum distance from causative fault). Most of these criteria have eventually been shown to be misleading, since even low intensity bedrock ground motions from distant earthquakes can be amplified by local soils to intensity levels strong enough to induce liquefaction, as observations of liquefaction in the 1985 Mexico City and 1989 Loma Prieta earthquakes demonstrate.

5.2 Liquefaction Potential Assessment

Due to the difficulties in obtaining undisturbed representative samples from most liquefiable soil deposits and to the difficulties and limitations of laboratory testing, the use of in-situ test results to evaluate liquefaction potential is generally the preferred method for liquefaction potential assessment among most practicing engineers. Liquefaction potential assessment procedures involving both the SPT and the CPT are widely used in practice (e.g., Seed and Idriss, 1982; Ishihara, 1985; Seed and De Alba, 1986; Shibata and Teparaska, 1988).

The most common procedure used in practice for liquefaction potential assessment, the *Simplified Procedure*, was originally developed by Seed and Idriss (1982). As used in engineering practice today, the Simplified Procedure has been progressively revised, extended and refined (Seed et al., 1983; Seed et al., 1985; Seed and De Alba, 1986; Liao and Whitman, 1986). The Simplified Procedure may be used with both CPT and SPT data. Recent summaries of the various revisions to the Simplified Procedure are provided by Marcuson et al., (1990) and by Seed and Harder (1990). Based on the recommendations from these two studies, the Simplified Procedure for evaluating liquefaction potential at the site of a MSWLF can be carried out using the following steps:

Step 1: From in-situ testing and laboratory index tests, develop a detailed understanding of site conditions: stratigraphy, layer geometry, material properties and their variability, and the areal extent of potential problem zones. Establish the most critical zones to be analyzed and develop simplified sections amenable to

analysis. The data should include location of the water table, either SPT blowcount, N, or tip resistance of a standard CPT cone, q_c, and mean grain size, D_{50}, the unit weight of the soil, and the percentage of fines (percent by weight passing the No. 200 sieve) for the materials involved in the liquefaction potential assessment.

Step 2: Evaluate the total vertical stress, σ_o, and vertical effective stress, σ_o', in the deposit at the time of exploration and for design. Design values should include the overburden stress due to the landfill. Outside of the waste footprint, the exploration and design values may be the same if the design ground water level is at the same elevation as the ground water was during sampling, or they may be different due to temporal fluctuations in the water table.

Step 3: Evaluate the stress reduction factor, r_d. The stress reduction factor is a soil flexibility factor defined as the ratio of the peak shear stress for the soil column, $(\tau_{max})_d$, to that of a rigid body, $(\tau_{max})_r$. There are several ways to determine r_d. For depths less than 40 ft (12 m), the average value from Figure 5.3 (Seed and Idriss, 1982) can be used. Alternatively, the following equation proposed by Iwasaki et al. (1978) can be used:

$$r_d = 1 - 0.015\ D \tag{5.1}$$

where D is depth in meters.

If results of a site response analyses (e.g., a SHAKE analysis) are available, r_d can be determined directly from results of such analysis, as:

$$r_d = \frac{(\tau_{max})_{@depth=D}}{(\sigma_o)_{@depth=D} \cdot (a_{max}/g)_{@surface}} \tag{5.2}$$

where a_{max} is the peak ground surface acceleration and g is the acceleration of gravity.

Use of the results of a site response analysis to evaluate r_d is considered to be generally more reliable than either of the two simplified approaches and is strongly recommended for sites that are marginal with respect to liquefaction potential (sites where the factor of safety for liquefaction is close to 1.0).

Step 4: Calculate the critical stress ratio induced by the design earthquake, CSR_{EQ}, as:

$$CSR_{EQ} = 0.65\ (a_{max}/g)\ r_d\ (\sigma_o/\sigma_o') \tag{5.3}$$

Step 5: Evaluate the *standardized* SPT blowcount, N_{60}. N_{60} is the standard penetration test blowcount for a hammer with an efficiency of 60 percent (60 percent of the nominal SPT energy is delivered to the rods). The "standardized" equipment corresponding to an efficiency of 60 percent is specified in Table 5.4. If nonstandard equipment is used, N_{60} is determined as:

$$N_{60} = N \cdot C_{60} \tag{5.4}$$

where C_{60} is the product of various correction factors. Correction factors recommended by various investigators for some common non-standard SPT configurations are provided in Table 5.3. Alternatively, if CPT data are used, N_{60} can be obtained from the chart relating N_{60} to q_c and D_{50} shown in Figure 5.2 (Seed and De Alba, 1986).

Step 6: Calculate the normalized standardized SPT blowcount, $(N_1)_{60}$. $(N_1)_{60}$ is the standardized blow count normalized to an effective overburden pressure of 1 tsf (2000 psf or 950 kPa) in order to eliminate the influence of confining pressure. The most commonly used way to normalize blowcount is via the correction factor, C_N, shown in Figure 5.4 (Seed et al., 1983). However, the closed-form expression proposed by Liao and Whitman (1986) may also be used:

$$C_N = (1/\sigma_o')^{1/2} \tag{5.5}$$

where σ_o' equals the vertical effective stress at the sampling point in tons/ft^2.

As illustrated in Figure 5.4, Equation 5.5, and the correction factor curves are valid only for depths greater than 3 m (10 ft). For depths of less than 3 m

(10 ft), Seed et al. (1983) suggested a correction factor of 0.75. The normalized standardized blowcount is calculated as:

$$(N_1)_{60} = N_{60} \cdot C_N \quad (D \geq 3\ m) \tag{5.6a}$$

$$(N_1)_{60} = 0.75 \cdot N_{60} \quad (D < 3\ m) \tag{5.6b}$$

Step 7: Evaluate the critical stress ratio (CSR) at which liquefaction is expected to occur during an earthquake of magnitude M 7.5 as a function of $(N_1)_{60}$. Use the chart developed by Seed et al. (1985), shown in Figure 5.5, to find CSR ($= \tau_{av}/\sigma_o'$).

Step 8: Calculate the *corrected* critical stress ratio resisting liquefaction, CSR_L. Corrections applied to the CSR calculated in Step 7 include: k_M, the correction factor for magnitudes other than 7.5; k_σ, the correction factor for stress levels larger than 1 tsf (2000 psf); and k_α, the correction factor for the driving static shear stress (this is a correction for non-level ground conditions). CSR_L is therefore calculated as:

$$CSR_L = CSR \cdot k_M \cdot k_\sigma \cdot k_\alpha \tag{5.7}$$

k_M can be determined from chart given in Figure 5.6, developed by interpolation through tabular data presented by Seed et al., (1983). k_σ can be determined from the chart presented in Figure 5.7 (Harder, 1988; Hynes, 1988). k_α depends on the relative density of the soil, D_r, and can be determined from Figure 5.8, originally proposed by Seed and modified by Harder, (1988), and Hynes (1988).

Step 9: Calculate the factor of safety against liquefaction, FS_L, as:

$$FS_L = CSR_L \ / \ CSR_{EQ} \tag{5.8}$$

There is no general agreement on the appropriate factor of safety against liquefaction (NRC, 1985). However, when the design ground motion is extreme or conservative, most geotechnical engineers are satisfied with a factor of safety, FS_L, greater than or equal to 1.0. It should be noted that the Simplified Procedure is aimed primarily at moderately strong ground motions

(0.2 g < a_{max} < 0.5 g). If the peak horizontal acceleration is larger than 0.5 g, more sophisticated, truly non-linear effective stress-based analytical approaches should be considered. Computer programs for non-linear evaluation of liquefaction potential described in the technical literature include DESRA-2 (Lee and Finn, 1978) and its derivative codes DESRAMOD (Vucetic, 1986) and D-MOD (Matasović, 1993), DYNAFLOW (Prevost, 1981), TARA-3 (Finn et al., 1986), LINOS (Bardet, 1987), and DYSAC2 (Muraletharan et. al., 1991).

An example of liquefaction analysis using the Simplified Procedure is presented in Appendix A.

5.3 Liquefaction Impact Assessment

For the soil layers for which the factor of safety against the liquefaction is unsatisfactory, a liquefaction impact analysis should be conducted. A liquefaction impact analysis may consist of the following steps:

Step 1: Calculate the magnitude and distribution of liquefaction induced settlement by multiplying the post-liquefaction volumetric strain, ε_v, by thickness of the liquefiable layer, H. ε_v can be estimated from chart presented in Figure 5.9 (Tokimatsu and Seed, 1987). An alternative chart has recently been proposed by Ishihara (Ishihara, 1993). However, application of Ishihara's chart requires translation of normalized SPT blowcount $(N_1)_{60}$ values determined in Section 5.1 to Japanese-standard N_1 values ($N_1 = 0.833\ (N_1)_{60}$; after Ishihara, 1993). The magnitude of seismic settlement should be calculated at each boring or CPT sounding location to evaluate the potential variability in seismic settlement across the site.

Step 2: Estimate the liquefaction-induced lateral displacement, Δ_L. The empirical equation proposed by Hamada et al. (1987) may be used to estimate Δ_L in meters:

$$\Delta_L = 0.75\ (H)^{1/2}\ (S)^{1/3} \qquad (5.9)$$

in which H is the thickness of the liquefied layer in meters and S is the ground slope in percent.

The Hamada et al. (1987) formula is mainly based on Japanese data on displacements of very loose sands for soil deposits having a slope, *S*, less than 10%. Therefore, Equation 5.9 should be assumed to provide only as a rough estimate of lateral displacement. Since the equation does not reflect the density, or $(N_1)_{60}$ value of the soil, or the depth of the liquefiable layer, it may provide a conservative estimate of lateral displacement for denser sands or for cases where the soil liquefies at depth. Note that estimate of lateral displacement by this equation predicts large liquefaction-induced lateral displacements in areas of essentially flat ground conditions.

Step 3: In areas of significant ground slope, or in situations when a deep failure surface may pass through waste and through underlying liquefied layers, a flow slide can occur following liquefaction. The potential for a flow slide to occur should be checked using conventional limit equilibrium approach for slope stability analyses (discussed in Section 6 of this document) together with residual shear strength in zones in which liquefaction may occur. Residual shear strength can be estimated from the penetration resistance values of the soil using the chart proposed by Seed et al. (1988) presented in Figure 5.10. Marcuson et al. (1990) present a step by step procedure for performing a post-liquefaction stability assessment using residual shear strengths.

The above liquefaction-associated deformation phenomena, if too great in magnitude, can adversely impact the integrity of the landfill containment structures. The question the engineer must answer is "What magnitude of deformation is excessive?" The magnitude of acceptable deformation should be determined by the design engineer on a case-by-case basis. Seed and Bonaparte (1992) report that calculated seismic deformations along the liner-waste interface on the order of 0.15 to 0.30 m (0.5 to 1.0 ft) are generally deemed to be acceptable in current practice in California. As cover deformations are readily observable and damage to the cover is repairable, larger deformations are typically considered acceptable along interfaces in the cover system than along liner system interfaces. At the current time, determination of allowable deformations remains a subject requiring considerable engineering judgement.

5.4 Liquefaction Mitigation

If the seismic impact analysis presented in Section 5.3 yields unacceptable deformations, consideration may be given to performing a more sophisticated liquefaction potential assessment and to liquefaction potential mitigation measures. Generally, the design engineer has the

following options: (1) proceed with a more advanced analysis technique; (2) design the facility to resist the anticipated deformations; (3) remediate the site to reduce the anticipated deformations to acceptable levels; or (4) choose an alternative site. These options may require additional subsurface investigation, advanced laboratory testing, more sophisticated numerical modeling, and, in rare cases, physical modeling. Discussion of these techniques is beyond the scope of this study.

Design to resist anticipated deformations could include the use of reinforced earth, structural walls, or buttress fills keyed into non-liquefiable strata to resist the effects of lateral spreading.

A variety of techniques exist to remediate potential liquefiable soils and mitigate the liquefaction hazard. Table 5.4 presents a summary of available methods for improvement of liquefiable soil foundation conditions (NRC, 1985). The cost of foundation improvement can vary over an order of magnitude, depending on site conditions (e.g., adjacent sensitive structures) and the nature and geometry of the liquefiable soils. Remediation costs can vary from as low as several thousand dollars per acre for dynamic compaction of shallow layers of clean sands in open areas to upwards of $100,000. per acre for deep layers of silty soils adjacent to sensitive structures.

5.5 References

Bardet, J.P. (1987), "LINOS, a Nonlinear Finite Element Program for Geomechanics and Geotechnical Engineering," *University of Southern California, Los Angeles.*

Dobry, R., Powell, D.J., Yokel, F.Y., and Ladd, R.S. (1980), "Liquefaction Potential of Saturated Sand - The Stiffness Method," Proc. *7th World Conference on Earthquake Engineering*, Istanbul, Turkey, Vol. 3, pp. 25-32.

Finn, W.D. Liam, Yogendrakumar, M., Yoshida, N. and Yoshida, H. (1986), "TARA-3: A Program to Compute the Response of 2-D Embankments and Soil-Structure Interaction Systems to Seismic Loadings, Department of Civil Engineering, University of British Columbia, Vancouver, Canada.

Hadj-Hamou, T., and Elton, D.J. (1988), "A Liquefaction Potential Map for Charleston, South Carolina," Report No. GT-88-1, Toluane University, New Orleans, Louisiana, 67 p.

Hamada, M. Towhata, I., Yasuda S., and Isoyama, R. (1987), "Study on Permanent Ground Displacements Induced by Seismic Liquefaction," *Computers and Geomechanics* 4, pp. 197-220.

Harder, L.F., Jr. (1988)*, "Use of Penetration Tests to Determine the Cyclic Loading Resistance of Gravelly Soils During Earthquake Shaking," Ph.D. Dissertation, University of California, Berkeley, California.

Hwang, H. and Lee, C.S. (1992), "Evaluation of Liquefaction Potential in Memphis Area, USA." Proc. *10th World Conference on Earthquake Engineering*, pp. 1457-1460.

Hynes, M.E. (1988)*, "Pore Pressure Generation Characteristics of Gravel Under Undrained Cyclic Loading," Ph.D. Dissertation, University of California, Berkeley, California.

Ishihara, K. (1985), "Stability on Natural Deposits During Earthquakes," Proc. *11th International Conference on Soil Mechanics and Foundation Engineering*, San Francisco, California, Vol. 1, pp. 321-376.

Ishihara, K., Kokusho, T., and Silver, M.L. (1989), "Recent Developments in Evaluating Liquefaction Characteristics of Local Soils," State-of-the-Art Report, Proc. *12th International Conference on Soil Mechanics and Foundation Engineering*, Rio de Janeiro, Brazil, Vol. 4, pp. 2719-2734.

Ishihara (1993), "Liquefaction and Flow Failure During Earthquakes," *Géotechnique* 43, No. 3, pp. 351-415.

Iwasaki, T., Tatsuoka, F., Tokida, K-I and Yasuda, S. (1978), "A Practical Method for Assessing Soil Liquefaction Potential Based on Case Studies at Various Sites in Japan," Proc. *2nd International Conference on Microzonation*, San Francisco, California, Vol. 2. pp. 885-896.

Kavazanjian, E. Jr., Roth, R.A., and Echezuria, H. (1985), "Liquefaction Potential Mapping for San Francisco," *Journal of Geotechnical Engineering*, ASCE, Vol. 111, No. 1, pp. 54-76.

Lee, M.K.W., and Finn, W.D.L. (1978), "DESRA-2, Dynamic Effective Stress Response Analysis of Soil Deposits with Energy Transmitting Boundary Including Assessment of Liquefaction Potential," *Soil Mechanics Series No. 36*, Department of Civil Engineering, University of British Columbia, Vancouver, Canada, 60 p.

* Available through University Microfilms International, (313) 761-4700 Ext. 3879, or (800) 521-0600 Ext. 3879

Liao, S.S.C. and Whitman, R.V. (1986), "Overburden Correction Factors for SPT in Sand," *Journal of Geotechnical Engineering*, ASCE, Vol. 112, No. 3, pp. 373-377.

Marcuson, W.F., III, Hynes, M.E. and Franklin, A.G. (1990), "Evaluation and Use of Residual Strength in Seismic Safety Analysis of Embankments," *Earthquake Spectra*, Vol. 6, No. 3, pp. 529-572.

Matasović, N. (1993)*, "Seismic Response of Composite Horizontally-Layered Soil Deposits." Ph.D. Dissertation, Civil and Environmental Engineering Department, University of California, Los Angeles, 452 p.

Muraleetharan, K.K., Mish, K.D., Yogachandran C., and Arulanandan, K., (1991), "User's Manual for DYSAC2: Dynamic Soil Analysis Code for 2-Dimensional Problems," Report, Department of Civil Engineering, University of California, Davis, California.

NRC (1985), "Liquefaction of Soils During Earthquakes." National Research Council, Committee on Earthquake Engineering, Washington, DC.

Prevost, J.H. (1981), "DYNAFLOW: A nonlinear transient finite element analysis program." Department of Civil Engineering and Operational Research, Princeton University, (Last update January 1994).

Riggs, C.O. (1986), "North American Standard Penetration Test Practice," In *Use of InSitu Tests in Geotechnical Engineering*, ASCE Geotechnical Special Publication No. 6, pp. 949-965.

Seed, H.B. and Idriss, I.M., (1982), "Ground Motions and Soil Liquefaction During Earthquakes," *Monograph No. 5*, Earthquake Engineering Research Institute, Berkeley, California, 134 p.

Seed, H.B., Idriss, I.M. and Arango, I. (1983), "Evaluation of Liquefaction Potential Using Field Performance Data," *Journal of Geotechnical Engineering*, ASCE, Vol. 109, No. 3, pp. 458-482.

Seed, H.B., Tokimatsu, K., Harder, L.F. and Chung, R.M. (1985), "Influence of SPT Procedures in Soil Liquefaction Resistance Evaluations," *Journal of Geotechnical Engineering*, ASCE, Vol. 111, No. 12, pp. 1425-1445.

* Available through University Microfilms International, (313) 761-4700 Ext. 3879, or (800) 521-0600 Ext. 3879

Seed, H.B. and De Alba, P. (1986), "Use of SPT and CPT Tests for Evaluating the Liquefaction Resistance of Sands." In *Use of In-Situ Tests in Geotechnical Engineering*, ASCE Geotechnical Special Publication No. 6, pp. 281-302.

Seed, H.B., Seed, R.B., Harder, L.F., Jr., and Jong, H.-L. (1988), "Re-Evaluation of the Slide in the Lower San Francisco Dam in the Earthquake of February 9, 1971." Report No. UCB/EERC-88/04, University of California, Berkeley, California.

Seed, R.B., and Harder, L.F., Jr. (1990), "SPT-Based Analysis of Cyclic Pore Pressure Generation and Undrained Residual Strength," Proc. *H.B. Seed Memorial Symposium*, Vol. 2, pp. 351-376.

Seed, R.B., and Bonaparte, R. (1992), "Seismic Analysis and Design of Lined Waste Fills: Current Practice," In *Proceedings of Stability and Performance of Slopes and Embankments - II*, Vol. 2, Berkeley, California, ASCE Geotechnical Special Publication No. 31, pp. 1521-1545.

Shibata, T., and Taparaska, W. (1988), "Evaluation of Liquefaction Potentials of Soils Using Cone Penetration Tests," *Soils and Foundations*, Vol. 28, No. 2, pp. 49-60.

Skempton, A.W. (1986), "Standard Penetration Test Procedures and the Effects in Sands of Overburden Pressure, Relative Density, Particle Size, Ageing and Overconsolidation," *Géotechnique*, Vol. 36, No. 3, pp. 425-447.

Tinsley, J.C., Youd, T.L., Perkins, D.M., and Chen, A.T.F. (1985), "Evaluating Liquefaction Potential," in J.I. Ziony, ed, Evaluating Earthquake Hazards in the Los Angeles Region, an Earth Science Perspective," *U.S. Geological Survey Professional Paper 1360*, pp. 263-315.

Tokimatsu, K. and Seed, H.B. (1987), "Evaluation of Settlements in Sands due to Earthquake Shaking," *Journal of Geotechnical Engineering*, ASCE, Vol. 113, No. 8, pp. 861-879.

Vucetic, M. (1986)*, "Pore Pressure Buildup and Liquefaction of Level Sandy Sites During Earthquakes," Ph.D. Thesis, Rensselaer Polytechnic Institute, Troy, New York, 616 p.

Youd, T.L., and Perkins, D.M. (1978), "Mapping Liquefaction-Induced Ground Failure Potential," *Journal of Geotechnical Engineering*, ASCE, Vol. 104, No. GT4, pp. 433-446.

* Available through University Microfilms International, (313) 761-4700 Ext. 3879, or (800) 521-0600 Ext. 3879

Table 5.1 Estimated Susceptibility of Sedimentary Deposits to Liquefaction During Strong Seismic Shaking (Youd and Perkins, 1978).

Type of deposit (1)	General distribution of cohesionless sediments in deposits (2)	Likelihood that Cohesionless Sediments, When Saturated, Would Be Susceptible to Liquefaction (by Age of Deposit)			
		<500 yr (3)	Holocene (4)	Pleistocene (5)	Pre-pleistocene (6)
(*a*) Continental Deposits					
River channel	Locally variable	Very high	High	Low	Very low
Flood plain	Locally variable	High	Moderate	Low	Very low
Alluvial fan and plain	Widespread	Moderate	Low	Low	Very low
Marine terraces and plains	Widespread	—	Low	Very low	Very low
Delta and fan-delta	Widespread	High	Moderate	Low	Very low
Lacustrine and playa	Variable	High	Moderate	Low	Very low
Colluvium	Variable	High	Moderate	Low	Very low
Talus	Widespread	Low	Low	Very low	Very low
Dunes	Widespread	High	Moderate	Low	Very low
Loess	Variable	High	High	High	Unknown
Glacial till	Variable	Low	Low	Very low	Very low
Tuff	Rare	Low	Low	Very low	Very low
Tephra	Widespread	High	High	?	?
Residual soils	Rare	Low	Low	Very low	Very low
Sebka	Locally variable	High	Moderate	Low	Very low
(*b*) Coastal Zone					
Delta	Widespread	Very high	High	Low	Very low
Esturine	Locally variable	High	Moderate	Low	Very low
Beach					
High wave energy	Widespread	Moderate	Low	Very low	Very low
Low wave energy	Widespread	High	Moderate	Low	Very low
Lagoonal	Locally variable	High	Moderate	Low	Very low
Fore shore	Locally variable	High	Moderate	Low	Very low
(*c*) Artificial					
Uncompacted fill	Variable	Very high	—	—	—
Compacted fill	Variable	Low	—	—	—

TABLE 5.2: RECOMMENDED "STANDARDIZED" SPT EQUIPMENT (After Seed et al., 1985, and Riggs, 1986)

Sampler:	Standard split-spoon sampler with: (a) O.D. = 2.00 in., and (b) I.D. = 1.38 in. (constant - i.e. no room for liners in the barrel)
Drill Rods:	A or AW for depths less than 50 ft; N or NW for greater depths
Hammer:	Standard (safety) hammer with: (a) weight = 140 lb; (b) drop = 30 in. (delivers 2,520 in.-lbs which is 60% of theoretical freefall)
Rope:	Two wraps of rope around the pulley
Borehole:	4 to 5-in. diameter rotary borehole with bentonite mud for borehole stability (hollow stem augers where SPT is taken through the stem)
Drill bit:	Upward deflection of drilling mud (tricone or baffled drag bit)
Blowcount Rate:	30 to 40 blows per minute
Penetration Resistance Count:	Measured over range of 6 to 18 in. of penetration into the ground.

Note: If the equipment meets the above specifications, $N = N_{60}$ and only a correction for overburden is needed.

TABLE 5.3: CORRECTION FACTORS FOR NONSTANDARD SPT PROCEDURE AND EQUIPMENT

CORRECTION FOR	CORRECTION FACTOR	REFERENCE
Nonstandard Hammer Type (DH = donnut hammer; ER = energy ratio)	C_{HT} = 0.75 for DH w/rope and pully C_{HT} = 1.33 for DH w/trip/auto & ER = 80	Seed et al. (1985)
Nonstandard Hammer Weight or height of fall (H = height of fall in inches; W = weight in lbs)	$C_{HW} = \frac{H \cdot W}{140 \, x \, 30}$	calculated per Seed et. al (1985)
Nonstandard Sampler Setup (standard samples with room for liners, but used without liners)	C_{SS} = 1.10 for loose sand C_{SS} = 1.20 for dense sand	Seed et al. (1985)
Nonstandard Sampler Setup (standard sampler with room for liners, and liners are used)	C_{SS} = 0.90 for loose sand C_{SS} = 0.80 for dense sand	Skempton (1986)
Change in Rod Length	C_{RL} = 0.75 for rod length 0-10 feet	Seed et al. (1983)
Nonstandard Borehole Diameter	C_{BD} = 1.05 for 6 in. diameter C_{BD} = 1.15 for 8 in. diameter	Skempton (1986)

Note: $C_{60} = C_{ST} \cdot C_{HW} \cdot C_{SS} \cdot C_{RL} \cdot C_{BD}$

Table 5.4 Improvement Techniques for Liquefiable Soil Foundation Conditions (NRC, 1985).

Method	Principle	Most Suitable Soil Conditions/Types	Maximum Effective Treatment Depth	Economic Size of Treated Area	Ideal Properties of Treated Material[a]	Applications[b]	Case[c]	Relative Costs[d]
			IN-SITU DEEP COMPACTION					
(1) Blasting	Shock waves and vibrations cause limited liquefaction, displacement, remolding, and settlement to higher density.	Saturated, clean sands; partly saturated sands and silts after flooding.	>40 m	Any size	Can obtain relative densities to 70–80%; may get variable density; time-dependent strength gain.	Induce liquefaction in controlled and limited stages and increase relative density to potentially nonliquefiable range.	2 3	Low ($2.00–$4.00/m³)
(2) Vibratory probe (a) Terraprobe (b) Vibrorods (c) Vibrowing	Densification by vibration; liquefaction-induced settlement and settlement in dry soil under overburden to produce a higher density.	Saturated or dry clean sand; sand.	20 m routinely (ineffective above 3–4 m depth); >30 m sometimes; Vibrowing, 40 m	>1,000 m²	Can obtain relative densities of 80% or more. Ineffective in some sands.	Induce liquefaction in controlled and limited stages and increase relative density to potentially nonliquefiable range. Has been shown effective in preventing liquefaction.	2 3	Moderate ($6.00–$13.00/m³)
(3) Vibrocompaction (a) Vibroflot (b) Vibro-Composer system (c) Soil Vibratory stabilizing	Densification by vibration and compaction of backfill material of sand or gravel.	Cohesionless soils with less than 20% fines.	>30 m	>1,000 m²	Can obtain high relative densities (over 85%), good uniformity.	Induce liquefaction in controlled and limited stages and increase relative densities to nonliquefiable condition. Is used extensively to prevent liquefaction. The dense column of backfill provides (a) vertical support, (b) drains to relieve pore water pressure, and (c) shear resistance in horizontal and inclined directions. Used to stabilize slopes and strengthen potential failure surfaces or slip circles.	1 2 Δ[e]	Low to moderate ($6.00–$9.00/m³)
(4) Compaction piles	Densification by displacement of pile volume and by vibration during driving, increase in lateral effective earth pressure.	Loose sandy soils; partly saturated clayey soils; loess.	>20 m	>1,000 m²	Can obtain high densities, good uniformity. Relative densities of more than 80%.	Useful in soils with fines. Increases relative densities to nonliquefiable range. Is used to prevent liquefaction. Provides shear resistance in horizontal and inclined directions. Useful to stabilize slopes and strengthen potential failure surfaces or slip circles.	1 2 3	Moderate to high
(5) Heavy tamping (dynamic compaction)	Repeated application of high-intensity impacts at surface.	Cohesionless soils best, other types can also be improved.	30 m (possibly deeper)	>3,300 m²	Can obtain high relative densities, reasonable uniformity. Relative densities of 80% or more.	Suitable for some soils with fines; usable above and below water. In cohesionless soils, induces liquefaction in controlled and limited stages and increases relative density to potentially nonliquefiable range. Is used to prevent liquefaction.	2 3	Low ($0.40–$6.00/m³)
(6) Displacement/compaction grout	Highly viscous grout acts as radial hydraulic jack when pumped in under high pressure.	All soils.	Unlimited	Small	Grout bulbs within compressed soil matrix. Soil mass as a whole is strengthened.	Increase in soil relative density and horizontal effective stress. Reduce liquefaction potential. Stabilize the ground against movement.	1 2 3	Low to moderate ($3.00–$15.00/m³)

[a] SP, SW, or SM soils that have average relative density equal to or greater than 85 percent and the minimum relative density not less than 80 percent are in general not susceptible to liquefaction (TM 5-818-1). D'Appolonia (1970) stated that for soil within the zone of influence and confinement of the structure foundation, the relative density should not be less than 70 percent. Therefore, a criteria may be used that relative density increase into the 70–90 percent range is in general considered to prevent liquefaction. These properties of treated materials and applications occur *only under ideal conditions* of soil, moisture, and method application. The methods and properties achieved are not applicable and will not occur in all soils.

[b] Applications and results of the improvement methods are dependent on: (a) soil profiles, types, and conditions, (b) site conditions, (c) earthquake loading, (d) structure type and condition, and (e) material and equipment availability. Combinations of the methods will most likely provide the best and most stable solution.

[c] Site conditions have been classified into three cases. Case 1 is for beneath structures, Case 2 is for the not-underwater free field adjacent to a structure, and Case 3 is for the underwater free field adjacent to a structure.

[d] The costs will vary depending on: (a) site working conditions, location, and environment, (b) the location, area, depth, and volume of soil involved, (c) soil type and properties, (d) materials (sand, gravel, admixtures, etc.), equipment, and skills available, and (e) environmental impact factors. The costs are average values based on: (a) verbal communication from companies providing the service, (b) current literature, and (c) literature reported costs updated for inflation.

[e] Δ means the method has potential use for Case 3 with special techniques required that would increase the cost.

Table 5.4: (continued)

Method	Principle	Most Suitable Soil Conditions/Types	Maximum Effective Treatment Depth	Economic Size of Treated Area	Ideal Properties of Treated Material[a]	Applications[b]	Case[c]	Relative Costs[d]
			COMPRESSION					
(7) Surcharge/buttress	The weight of a surcharge/buttress increases the liquefaction resistance by increasing the effective confining pressures in the foundation.	Can be placed on any soil surface.	—	>1,000 m²	Increase strength and reduce compressibility.	Increase the effective confining pressure in a liquefiable layer. Can be used in conjunction with vertical and horizontal drains to relieve pore water pressure. Reduce liquefaction potential. Useful to prevent movements of a structure and for slope stability.	2 3	Moderate if vertical drains used
			PORE WATER PRESSURE RELIEF					
(8) Drains (a) Gravel (b) Sand (c) Wick (d) Wells (for permanent dewatering)	Relief of excess pore water pressure to prevent liquefaction. (Wick drains have comparable permeability to sand drains.) Primarily gravel drains; sand/wick may supplement gravel drain or relieve existing excess pore water pressure. Permanent dewatering with pumps.	Sand, silt, clay.	Gravel and sand >30 m; depth limited by vibratory equipment; wick, >45 m	>1,500 m², any size for wick	Pore water pressure relief will prevent liquefaction.	Prevent liquefaction by gravel drains. Sand and gravel drains are installed vertically; however, wick drains can be installed at any angle. Dewatering will prevent liquefaction but not seismically induced settlements.	Gravel and sand 2 Δ[e] Wick 1 2 3	Sand and gravel 0.3 m dia. ($11.50–$21.50/m³); wick ($2.00–$4.00/m³); dewatering very expensive
			INJECTION AND GROUTING					
(9) Particulate grouting	Penetration grouting—fill soil pores with soil, cement, and/or clay.	Medium to coarse sand and gravel.	Unlimited	Small	Impervious, high strength with cement grout. Voids filled so they cannot collapse under cyclic loading.	Eliminate liquefaction danger. Slope stabilization. Could potentially be used to confine an area of liquefiable soil so that liquefied soil could not flow out of the area.	1 2 3	Lowest of grout methods ($3.00–$30.00/m³)
(10) Chemical grouting	Solutions of two or more chemicals react in soil pores to form a gel or a solid precipitate.	Medium silts and coarser	Unlimited	Small	Impervious, low to high strength. Voids filled so they cannot collapse under cyclic loading.	Eliminate liquefaction danger. Slope stabilization. Could potentially be used to confine an area of liquefiable soil so that liquefied soil could not flow out of the area. Good water shutoff.	1 2 3	High ($75.00–$250.00/m³)
(11) Pressure-injected lime	Penetration grouting—fill soil pores with lime.	Medium to coarse sand and gravel	Unlimited	Small	Impervious to some degree. No significant strength increase. Collapse of voids under cyclic loading reduced.	Reduce liquefaction potential.	1 2 3	Low ($10.00/m³)
(12) Electrokinetic injection	Stabilizing chemicals moved into and fills soil pores by electro-osmosis or colloids into pores by electro-phoresis.	Saturated sands, silts, silty clays.	Unknown	Small	Increased strength, reduced compressibility, voids filled so they cannot collapse under cyclic loading.	Reduce liquefaction potential.	1 2 3	Expensive
(13) Jet grouting	High-speed jets at depth excavate, inject, and mix a stabilizer with soil to form columns or panels.	Sands, silts, clays.	Unknown	Small	Solidified columns and walls.	Slope stabilization by providing shear resistance in horizontal and inclined directions, which strengthens potential failure surfaces or slip circles. A wall could be used to confine an area of liquefiable soil so that liquefied soil could not flow out of the area.	1 2 3	High $250.00–$650.00/m³

[a] SP, SW, or SM soils that have average relative density equal to or greater than 85 percent and the minimum relative density not less than 80 percent are in general not susceptible to liquefaction (TM 5-818-1). D'Appolonia (1970) stated that for soil within the zone of influence and confinement of the structure foundation, the relative density should not be less than 70 percent. Therefore, a criteria may be used that relative density increase into the 70–90 percent range is in general considered to prevent liquefaction. These properties of treated materials and applications occur *only under ideal conditions* of soil, moisture, and method application. The methods and properties achieved are not applicable and will not occur in all soils.

[b] Applications and results of the improvement methods are dependent on: (a) soil profiles, types, and conditions, (b) site conditions, (c) earthquake loading, (d) structure type and condition, and (e) material and equipment availability. Combinations of the methods will most likely provide the best and most stable solution.

[c] Site conditions have been classified into three cases. Case 1 is for beneath structures, Case 2 is for the not-underwater free field adjacent to a structure, and Case 3 is for the underwater free field adjacent to a structure.

[d] The costs will vary depending on: (a) site working conditions, location, and environment, (b) the location, area, depth, and volume of soil involved, (c) soil type and properties, (d) materials (sand, gravel, admixtures, etc.), equipment, and skills available, and (e) environmental impact factors. The costs are average values based on: (a) verbal communication from companies providing the service, (b) current literature, and (c) literature reported costs updated for inflation.

[e] Δ means the method has potential use for Case 3 with special techniques required that would increase the cost.

Table 5.4: (continued)

Method	Principle	Most Suitable Soil Conditions/Types	Maximum Effective Treatment Depth	Economic Size of Treated Area	Ideal Properties of Treated Material[a]	Applications[b]	Case[c]	Relative Costs[d]
			ADMIXTURE STABILIZATION					
(14) Mix-in-place piles and walls	Lime, cement, or asphalt introduced through rotating auger or special in-place mixer.	Sand, silts, clays, all soft or loose inorganic soils.	>20 m (60 m obtained in Japan)	Small	Solidified soil piles or walls of relatively high strength.	Slope stabilization by providing shear resistance in horizontal and inclined directions, which strengthens potential failure surfaces or slip circles. A wall could be used to confine an area of liquefiable soil so that liquefied soil could not flow out of the area.	1 2 3	High ($250.00–$650.00/m³)
			THERMAL STABILIZATION					
(15) In-situ vitrification	Melts soil in place to create an obsidian-like vitreous material.	All soils and rock.	>30 m	Unknown	Solidified soil piles or walls of high strength. Impervious; more durable than granite or marble; compressive strength, 9–11 ksi; splitting tensile strength, 1–2 ksi.	Slope stabilization by providing shear resistance in horizontal and inclined directions, which strengthens potential failure surfaces or slip circles. A wall could be used to confine an area of liquefiable soil so that liquefied soil could not flow out of the area.	1 2 3	Moderate ($53.00–$70.00/m³)
			SOIL REINFORCEMENT					
(16) Vibro-replacement stone and sand columns (a) Grouted (b) Not grouted	Hole jetted into fine-grained soil and backfilled with densely compacted gravel or sand hole formed in cohesionless soils by vibro techniques and compaction of backfilled gravel or sand. For grouted columns, voids filled with a grout.	Sands, silts, clays.	>30 m (limited by vibratory equipment)	>1500 m²; fine-grained soils, >1000 m²	Increased vertical and horizontal load carrying capacity. Density increase in cohesionless soils. Shorter drainage paths.	Provides (a) vertical support, (b) drains to relieve pore water pressure, and (c) shear resistance in horizontal and inclined directions. Used to stabilize slopes and strengthen potential failure surfaces or slip circles. For grouted columns, no drainage provided but increased shear resistance. In cohesionless soil, density increase reduces liquefaction potential	1 2 Δ[e]	Moderate ($11.00–$70.00/m³)
(17) Root piles, soil nailing	Small-diameter inclusions used to carry tension, shear, compression.	All soils.	Unknown	Unknown	Reinforced zone of soil behaves as a coherent mass.	Slope stability by providing shear resistance in horizontal and inclined directions to strengthen potential failure surfaces or slip circles. Both vertical and angled placement of the piles and nails.	1 2 3	Moderate to high

[a]SP, SW, or SM soils that have average relative density equal to or greater than 85 percent and the minimum relative density not less than 80 percent are in general not susceptible to liquefaction (TM 5-818-1). D'Appolonia (1970) stated that for soil within the zone of influence and confinement of the structure foundation, the relative density should not be less than 70 percent. Therefore, a criteria may be used that relative density increase into the 70–90 percent range is in general considered to prevent liquefaction. These properties of treated materials and applications occur *only under ideal conditions* of soil, moisture, and method application. The methods and properties achieved are not applicable and will not occur in all soils.

[b]Applications and results of the improvement methods are dependent on: (a) soil profiles, types, and conditions, (b) site conditions, (c) earthquake loading, (d) structure type and condition, and (e) material and equipment availability. Combinations of the methods will most likely provide the best and most stable solution.

[c]Site conditions have been classified into three cases. Case 1 is for beneath structures. Case 2 is for the not-underwater free field adjacent to a structure, and Case 3 is for the underwater free field adjacent to a structure.

[d]The costs will vary depending on: (a) site working conditions, location, and environment, (b) the location, area, depth, and volume of soil involved, (c) soil type and properties, (d) materials (sand, gravel, admixtures, etc.), equipment, and skills available, and (e) environmental impact factors. The costs are average values based on: (a) verbal communication from companies providing the service, (b) current literature, and (c) literature reported costs updated for inflation.

[e]Δ means the method has potential use for Case 3 with special techniques required that would increase the cost.

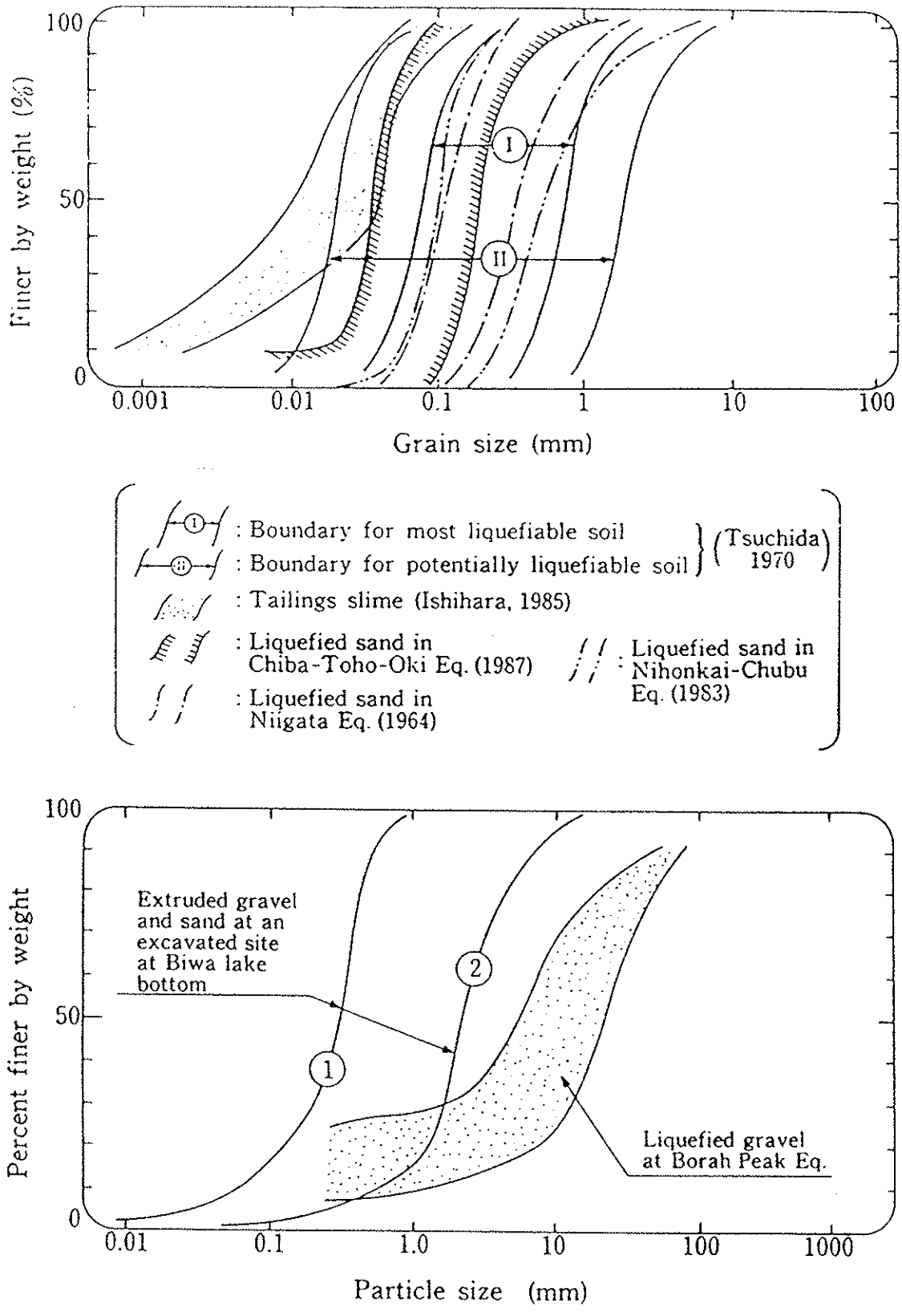

Figure 5.1 Grain Size Distribution Curves of Liquefied Soils (Ishihara et al., 1989).

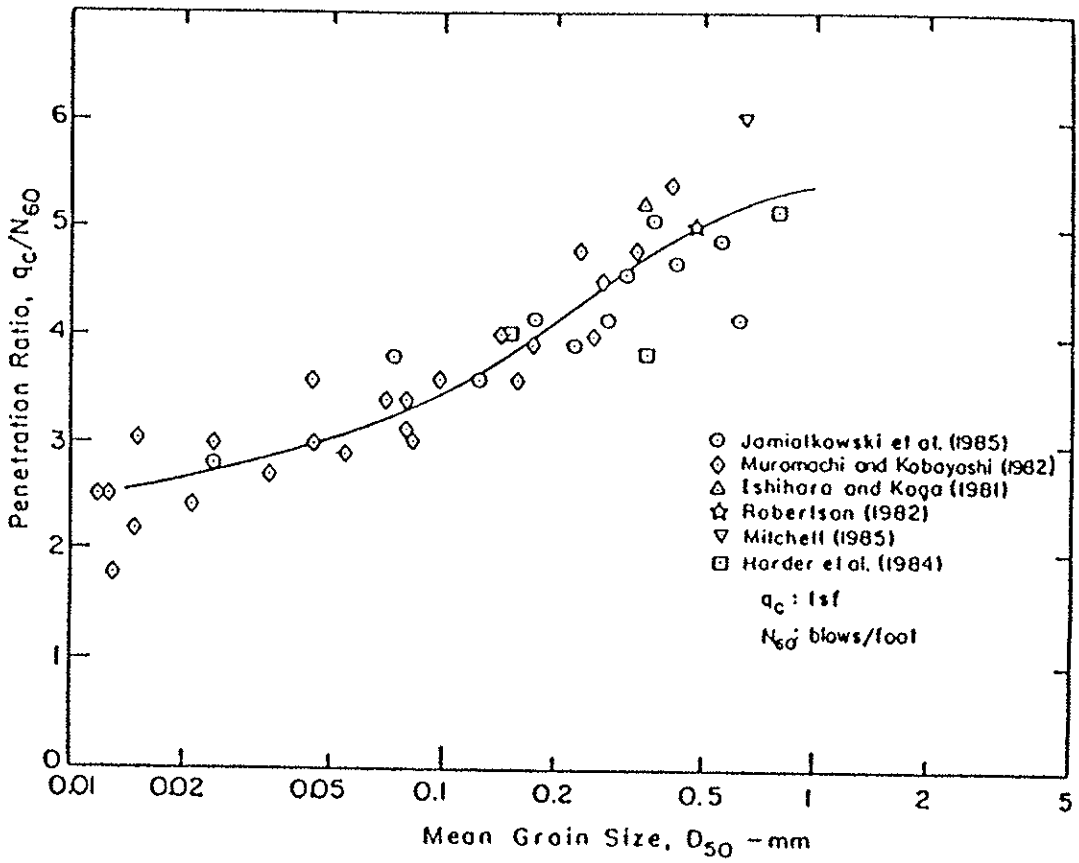

Figure 5.2 Variation of q_c/N_{60} Ratio with Mean Grain Size, D_{50} (Seed and De Alba, 1986).

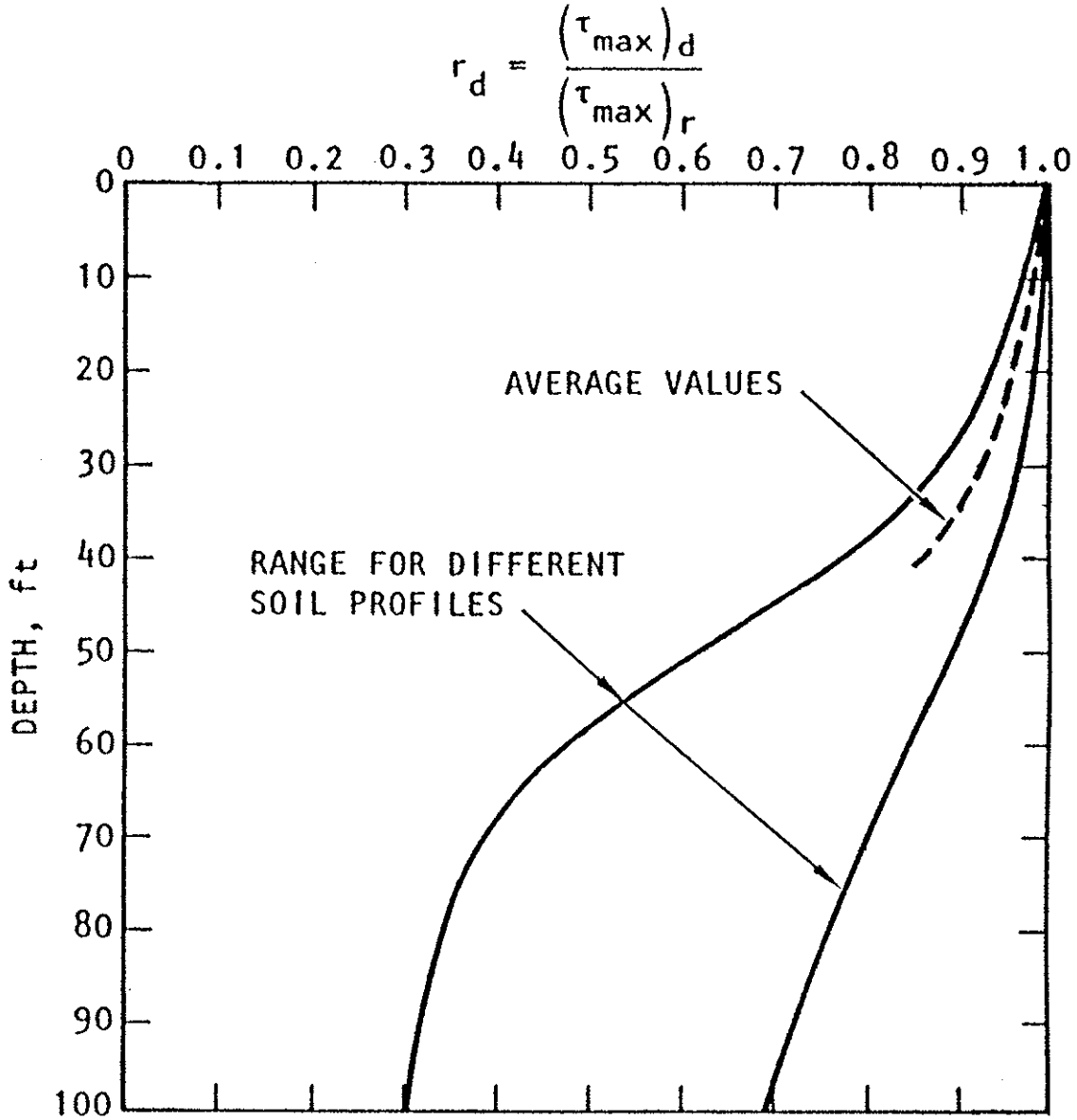

Figure 5.3 Stress Reduction Factor, r_d (Seed and Idriss, 1982).

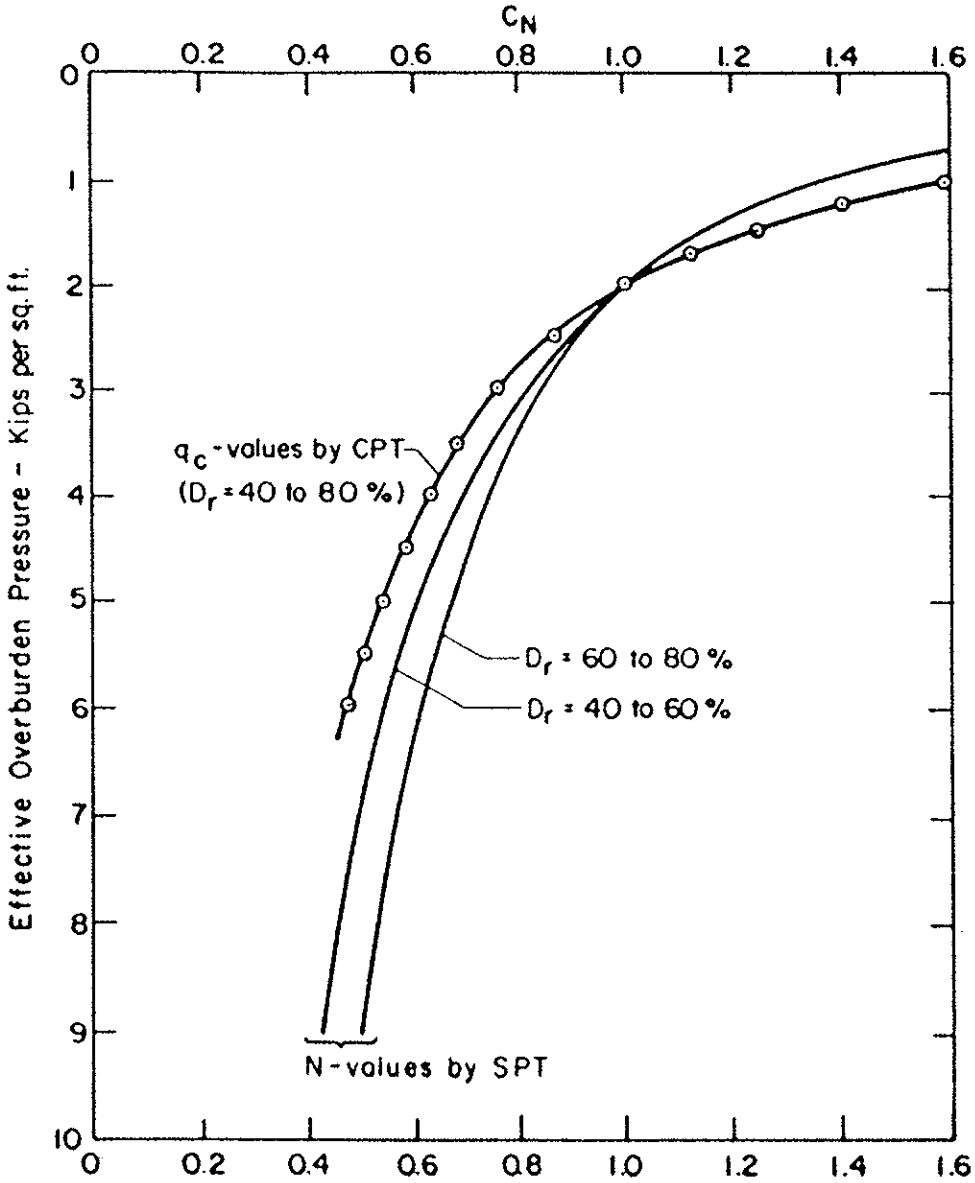

Figure 5.4 Correction Factor for the Effective Overburden Pressure, C_N (Seed et al., 1983).

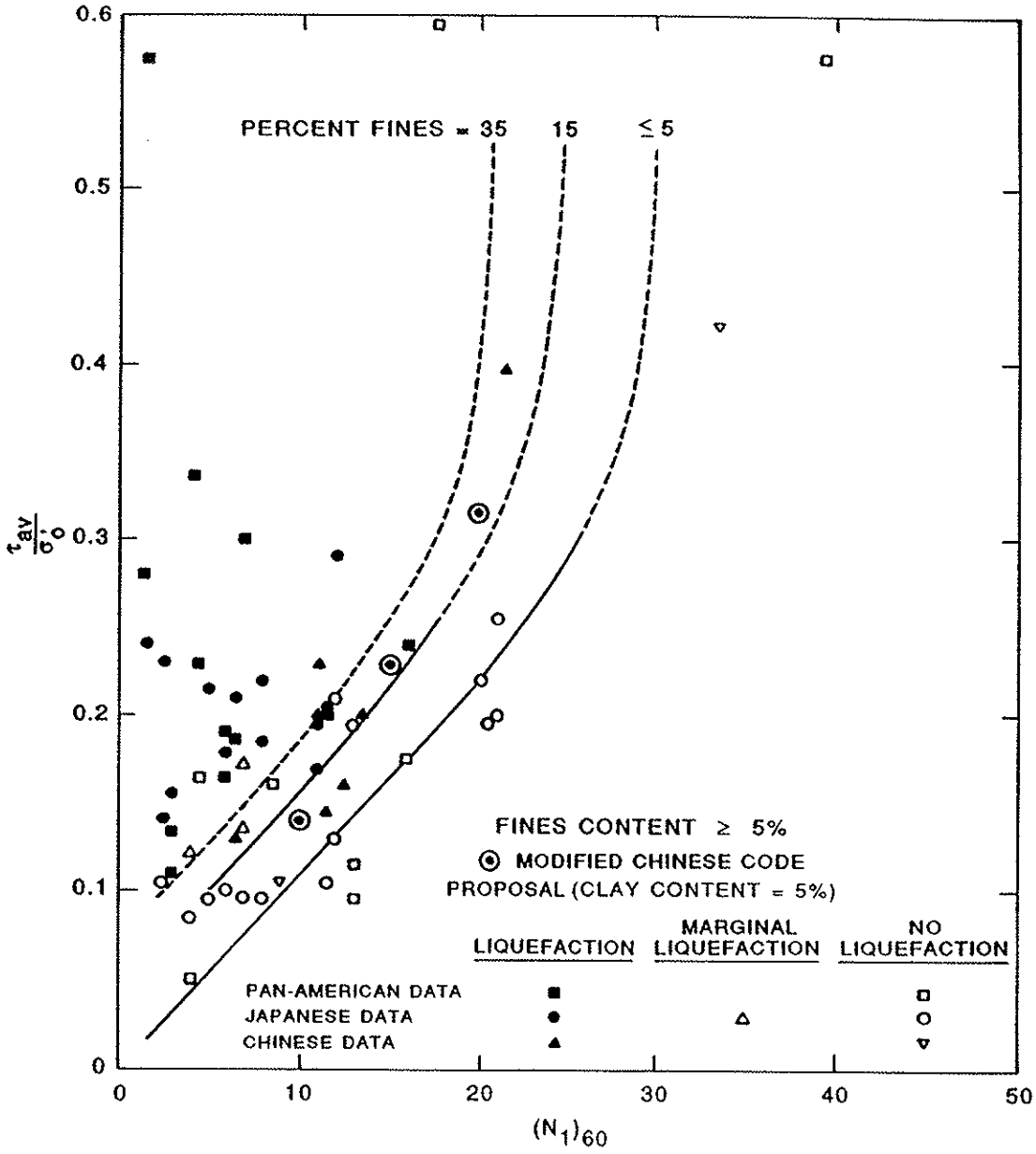

Figure 5.5 Relationships Between Stress Ratio Causing Liquefaction and $(N_1)_{60}$ Values for Sands for M 7.5 Earthquakes (Seed et al., 1985).

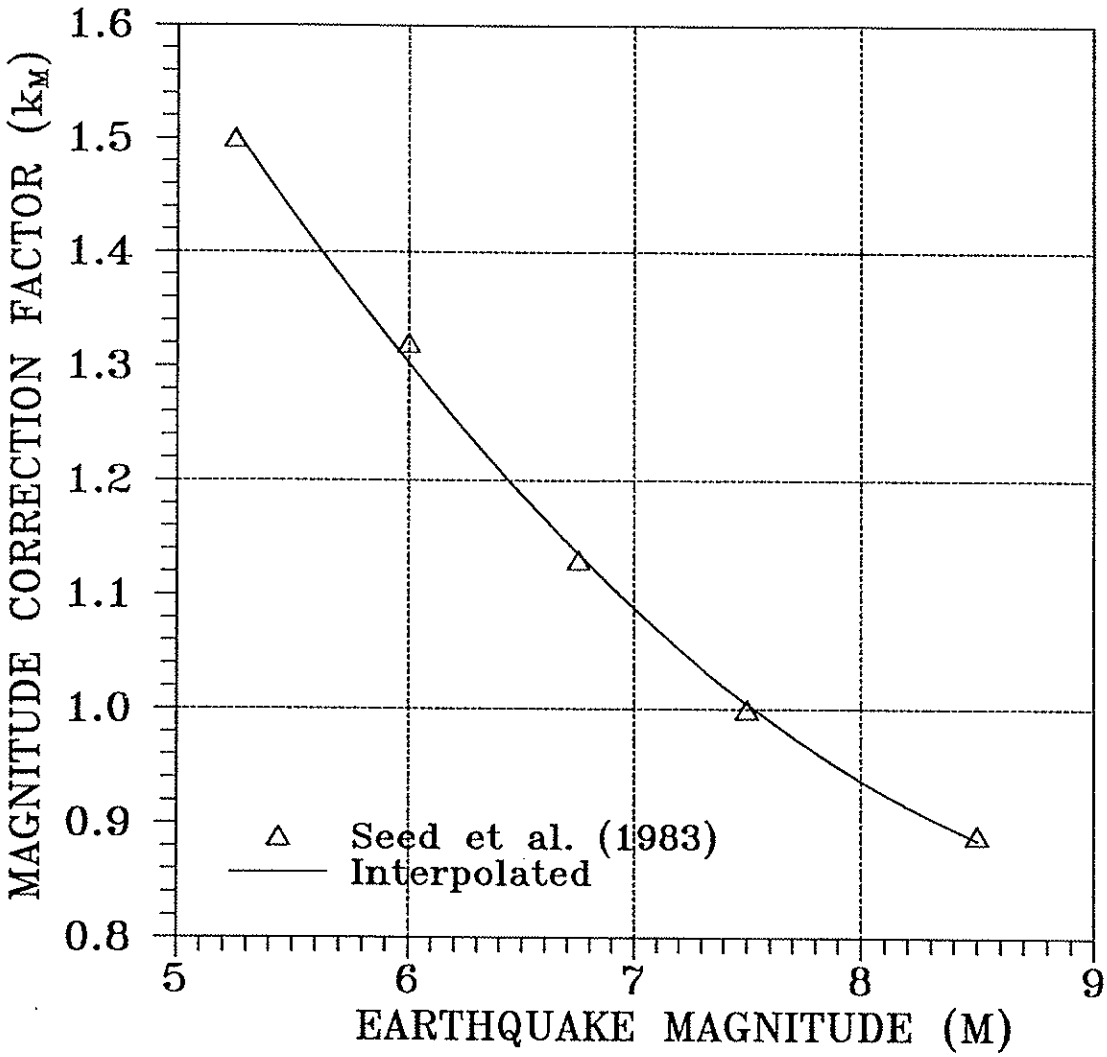

Figure 5.6 Curve for Estimation of Magnitude Correction Factor, k_M (after Seed et al., 1983).

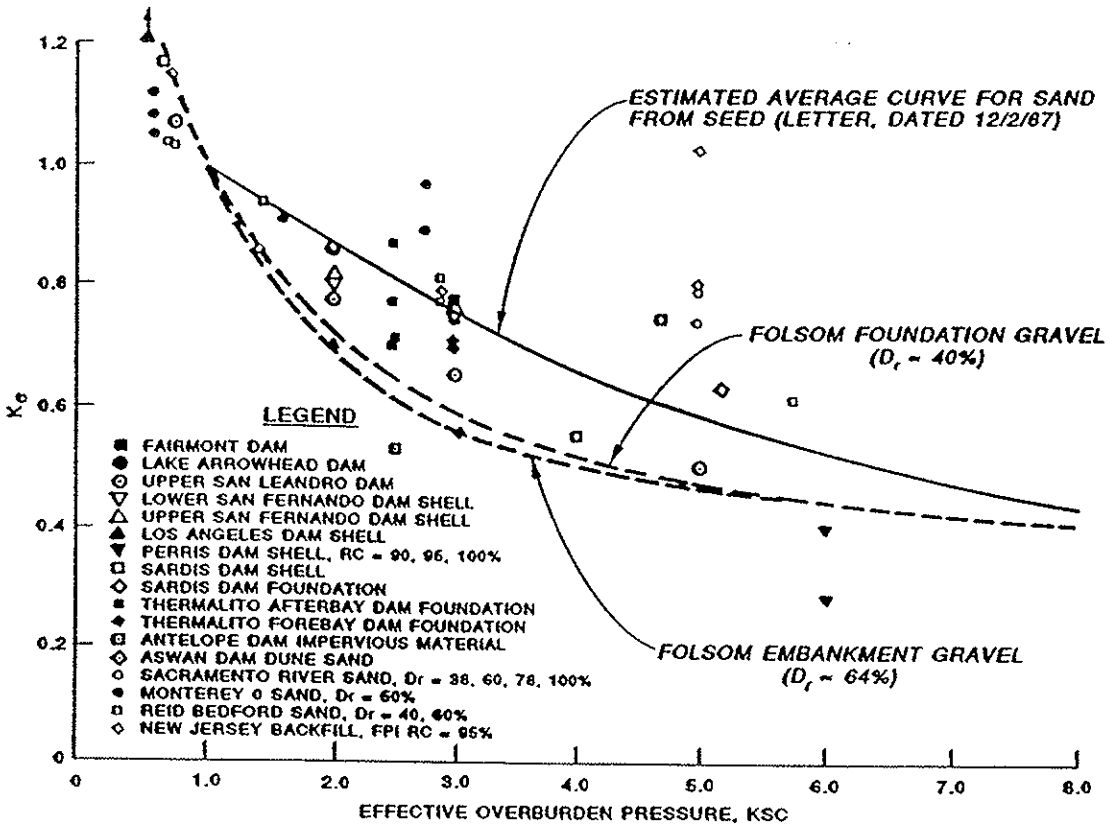

Figure 5.7 Curves for Estimation of Correction Factor k_σ (Harder 1988, and Hynes 1988, as Quoted in Marcuson et al., 1990)

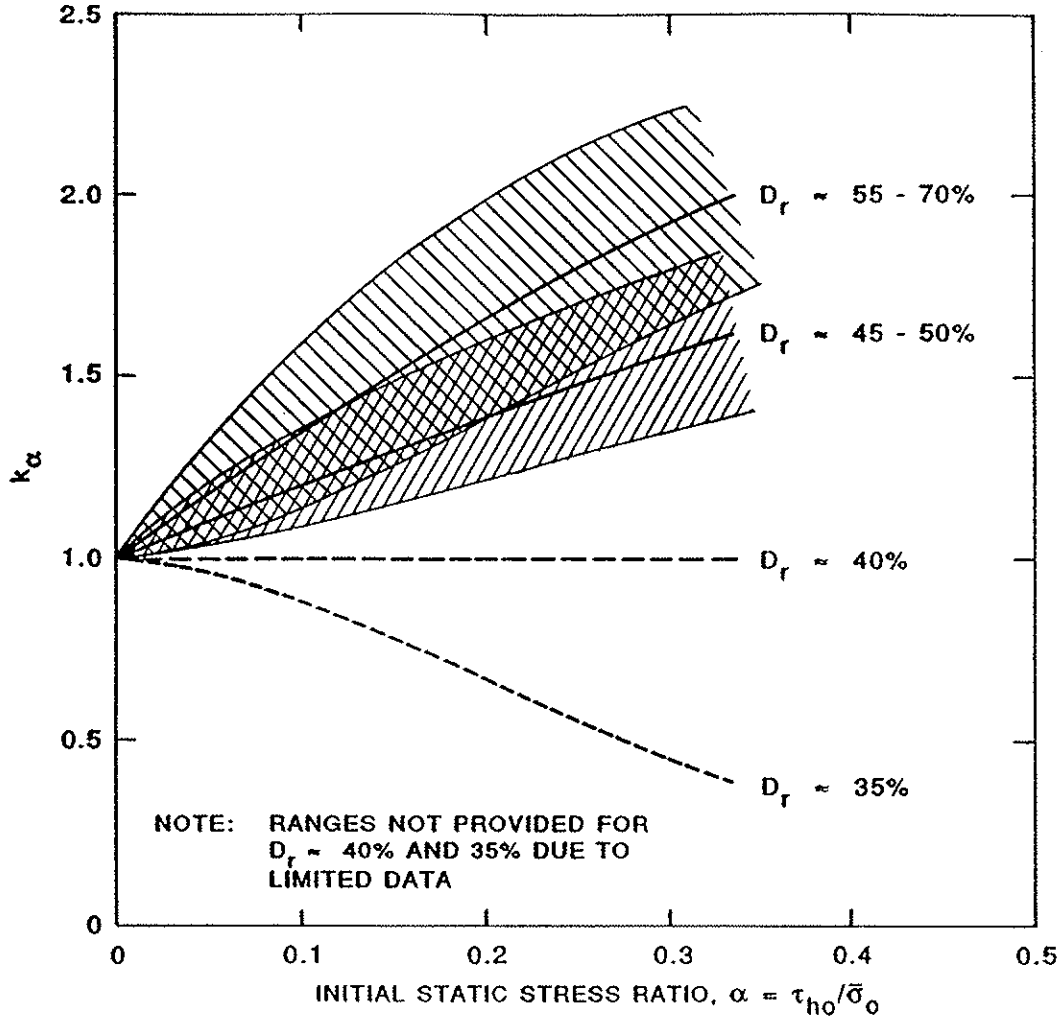

Figure 5.8 Curves for Estimation of Correction Factor k_α (Harder 1988, and Hynes 1988, as Quoted in Marcuson et al., 1990)

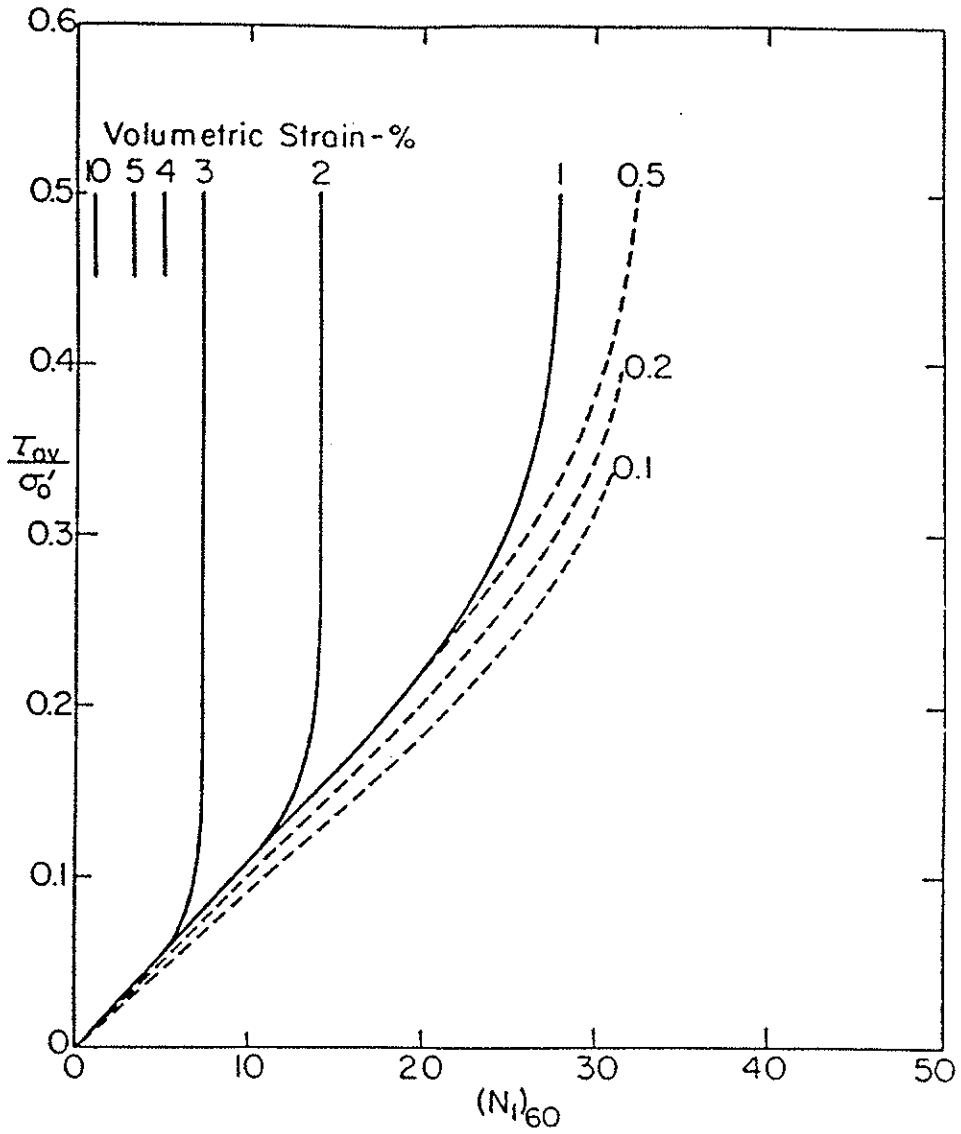

Figure 5.9 Curves for Estimation of Post-Liquefaction Volumetric Strain using SPT Data and Cyclic Stress Ratio (Tokimatsu and Seed, 1987).

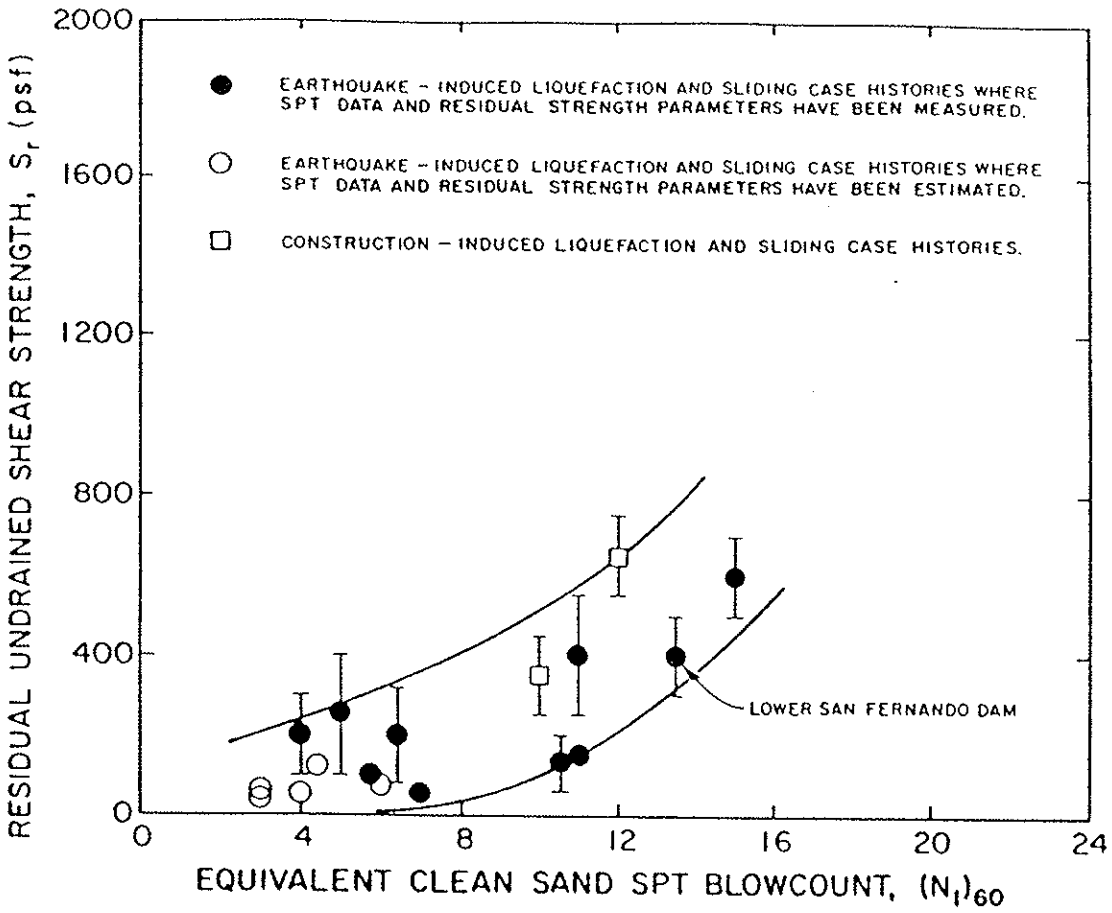

Figure 5.10 Relationship Between Corrected "Clean Sand" Blowcount $(N_1)_{60}$ and Undrained Residual Strength (S_r) from Case Studies (Seed et al., 1988).

SECTION 6

258.14 SEISMIC IMPACT ZONES: SLOPE STABILITY AND DEFORMATION ANALYSIS

The potentially large accelerations associated with seismic events can induce significant forces that may lead to permanent deformations within a MSW landfill. These deformations potentially can lead to impairment of the functions of the containment system. However, reports of significant seismic-related damage to MSW landfill containment systems are relatively rare. Several studies dealing with landfill behavior during the 1989 M 7.1 Loma Prieta earthquake report only minor damage to landfills, even for the landfills located in the epicentral region or founded on relatively weak San Francisco Bay mud (Orr and Finch, 1990; Buranek and Prasad, 1991; Sharma and Goyal, 1991; Johnson et al., 1991). Damage was mostly limited to cracking of earthen cover soils and disruption of surficial piping systems. No geomembrane-lined landfills were impacted by the Loma Prieta event. At least two modern, geosynthetic-lined landfills were impacted during the 1994 M 6.7 Northridge Earthquake. While preliminary studies indicate that no major damage occurred, the geosynthetic liner system was torn in at least two locations above the limit of waste placement at one of the landfills (EERC, 1994; Kavazanjian, 1994).

Numerous methods and procedures are currently available to evaluate static slope stability (Duncan, 1992). Most of the methods available are, in some form, suitable for seismic stability analyses. They can be used in conjunction with several different approaches for seismic analysis, of which the following two conventional methods represent the current state-of-practice: (1) pseudo-static factor of safety approach, and (2) permanent seismic deformation approach. Both of these conventional approaches to seismic stability assessment are based on the principles of limit equilibrium analysis.

In the pseudo-static factor of safety approach, a seismic coefficient is specified to represent the effect of the inertial forces imposed by the earthquake upon the potential failure mass and a factor of safety is defined in the conventional manner as the ratio of the ultimate shear strength of the slope elements to the maximum shear stresses induced in those elements by seismic and static loadings. The main drawback of the pseudo-static factor of safety approach lies in its inability to rationally relate the value of the seismic coefficient to the characteristics of the design earthquake. Use of the peak acceleration (expressed as a fraction of gravity) as the seismic coefficient in conjunction with a pseudo-static factor of safety of 1.0 has been shown to give excessively conservative assessments of slope performance in earthquakes.

In contrast to the pseudo-static factor of safety approach, the permanent seismic deformation approach involves the calculation of cumulative seismic deformations. The most commonly used method for calculating the permanent seismic deformation of slopes is termed the Newmark method (Newmark, 1965). In this approach, the potential failure mass is treated as a rigid body on a yielding base. The acceleration time history of the rigid body is assumed to correspond to the average acceleration time history of the failure mass. Deformations accumulate when the rigid body acceleration exceeds its yield acceleration. The yield acceleration is the horizontal acceleration that results in a factor of safety of 1.0 in a pseudo-static limit equilibrium analysis.

The calculation of permanent seismic deformations using the Newmark approach is depicted in Figure 6.1. Acceleration pulses in the time history that exceed the yield acceleration are double integrated to calculate cumulative relative displacement. In a Newmark analysis, relative displacement is often assumed to accumulate in only one direction, the downslope direction. With this assumption, the yield acceleration in the other (upslope) direction is implicitly assumed to be larger than the peak acceleration of the failure mass being analyzed.

In practice, both the pseudo-static factor of safety and permanent seismic deformation approaches are often combined in a unified seismic slope stability and deformation analysis. Such an analysis outlined in Section 6.2 of this guidance document.

6.1 Key Material Properties

To perform seismic slope stability analyses, estimates of the unit weight and (dynamic) shear strength parameters of various components of the landfill are needed. Unfortunately, a large amount of uncertainty often exists as to appropriate values for some of these parameters. Evaluation of the material properties of MSW required for a slope stability analysis can be a difficult task. This is due to the paucity of field and laboratory measurements of MSW properties, the cost and difficulty in making project-specific field measurements, and the heterogeneous nature of MSW. The following sections summarize the information currently available for estimating key material properties of MSW.

6.1.1 Unit Weight

Values of unit weight for MSW reported in the literature are summarized in Table 6.1 (Fassett et al., 1994). Initial values of MSW unit weight can be estimated from landfill gate receipts and survey elevations of the waste face. Current regulations in California require operators to achieve an initial density of at least 1,250 lbs per cubic yard (7.3 kN/m^3 or 46 lb/ft^3). Average

values of MSW unit weight can also be estimated based upon the total gate receipts over the life of a landfill and survey data. Average values for MSW unit weight cited by landfill operations and used in practice for landfill capacity estimates typically vary from 8.6 to 10.2 k/m^3 (55 to 65 lbs/ft^3) (Kavazanjian et al., 1994). Landfill-specific values of MSW unit weight will depend upon actual operational practice. For instance, significantly higher MSW unit weights have been reported for a landfill that used an unusually high percentage of daily cover soil (Richardson and Reynolds, 1991).

The MSW unit weights in Table 6.1 do not account for the increase in density with depth that occurs in MSW due to its compressibility or to changes that occur with time. Kavazanjian et al. (1994) have demonstrated that the variation of density with depth can have a significant influence on the results of static and dynamic stability and seismic response analyses. The dashed line on Figure 6.2 (Kavazanjian et al., 1994) shows the density-depth relationship developed for one southern California landfill on the basis of field measurements of density and laboratory measurements of waste compressibility (Earth Technology, 1988). Based upon the density-depth profile developed by Earth Technology (1988), the initial and average unit weights cited above, and representative compressibility values for MSW reported by Fassett et al. (1994), Kavazanjian et al. (1994) developed the MSW unit weight profile shown by the solid line on Figure 6.2 for use in stability and seismic response analyses of MSW landfills in the absence of landfill-specific data.

6.1.2 Interface Shear Resistance

The interface shear resistance between geosynthetic components (e.g., a geomembrane and geotextile interface) and between soil and geosynthetic components (e.g., a geomembrane and low permeability soil interface) from static laboratory tests are generally used for dynamic stability analyses. Typical values for peak and residual interface friction angles have been reported by Williams and Houlihan (1986, 1987), Seed and Boulanger (1990), Koerner (1991), and Byrne (1994). Byrne (1994) recommended that the interface friction angle used in dynamic analysis be evaluated on the basis of compatibility between the load-deformation curve from laboratory testing and the calculated seismic deformation.

Some investigations have reported slight differences between static and dynamic interface strengths (Kavazanjian et al., 1991). Others have reported that interface shear strengths appear to be independent of the frequency content and number of cycles of motion (Yegian and Lahlaf, 1992). However, considering the uncertainties inherent to other material properties, it appears

that the shear strength measured in static tests may be reasonably used to represent the dynamic interface shear strength in seismic stability and deformation analyses.

6.1.3 Low Permeability Soil

The dynamic shear strength of clay soils may be influenced by the amplitude of the cyclic deviator stress, the number of applied cycles, and the plasticity of the clay (Makdisi and Seed, 1978). In many cases, the static shear strength may be the same as or even greater than the shear strength for dynamic loading. Even for saturated, normally consolidated soft clays, the dynamic shear strength can be assumed to be equal to at least 80% of the static undrained strength with a high degree of confidence.

6.1.4 Granular Soil Shear Strength

The cyclic shear strength of a dry or unsaturated granular soil (sand or gravel) can be assumed to equal the static shear strength. In saturated sands, seismic loading can significantly alter the dynamic shear strength. Evaluation of the potential for shear strength reduction in a saturated sand subject to dynamic loading may require sophisticated cyclic laboratory testing. Alternatively, a residual shear strength may be assigned to the sand based upon either undrained laboratory tests or in situ test results. Use of residual shear strengths in a pseudo-static stability assessment can result in a very conservative assessment of the pseudo-static factor of safety and/or yield acceleration and is not recommended for most problems (Marcuson et al., 1990).

6.1.5 MSW Shear Strength

The available data on MSW shear strength is relatively limited. Available data includes laboratory test results on reconstituted samples and strength values backfigured from field load tests and case histories of landfill performance. Laboratory and field tests have consistently shown shear strengths in excess of a cohesion of 200 psf (10 kPa) and a friction angle of 20 degrees (Landva and Clark, 1990 and Richardson and Reynolds, 1991). Table 6.2 presents a compilation of the available data of MSW developed by GeoSyntec (1993). Table 6.3 presents a compilation of lower bound friction angles backfigured from observations of the satisfactory performance of steep side slopes at existing landfills by GeoSyntec (1993) based upon the assumption of a cohesion of 100 psf (5 kPa). Figure 6.3 presents a bi-linear strength envelope for MSW developed by Kavazanjian et al. (1994) based upon evaluation of the data in Tables 6.2 and 6.3.

Observations of the satisfactory performance of landfill slopes in major earthquakes indicates that the dynamic shear strength of MSW may be significantly greater than the static shear strength. Figure 6.4 (Siegel et al., 1990) shows combinations of cohesion, friction angle, and yield acceleration that resulted a pseudo-static factor of safety of 1.0 in back analyses of the satisfactory performance of the slopes of the OII landfill in a major earthquake.

6.1.6 Sensitivity Studies

It is strongly recommended that all stability analyses of MSW landfills be performed using parametric studies to clearly identify the sensitivity of the performance of the landfill to the material properties used in the analysis. If performance depends significantly on a given parameter, then additional laboratory or field testing may be required to better define appropriate properties for design.

6.2 Seismic Stability and Deformation Analysis

A prerequisite for performing a seismic slope stability and deformation analysis is performance of a static slope stability analysis. The seismic stability and deformation analysis is carried out using the same basic model(s) of landfill (waste mass and foundation) and containment system used in the static analysis. The following steps are used in a typical seismic slope stability and deformation analysis:

Step 1: Reinterpret the cross-sections analyzed in the static stability analysis and assign appropriate dynamic strength parameters. In cases where it is not clear whether drained or undrained shear strength parameters are appropriate for the dynamic analysis, follow guidelines presented in Duncan (1992).

Step 2: Evaluate the seismic coefficient, k_s. There are many different views on how to define k_s (e.g., Seed and Martin, 1966; Seed, 1979; Marcuson, 1981; Hynes and Franklin, 1984). The most reasonable definition appears to be one that regards the seismic coefficient as an empirical factor. This definition recognizes the limitations of the pseudo-static slope stability analysis in representing the actual effects of an earthquake on the slope. Unfortunately, this definition provides no guidance to selection of an appropriate value of k_s. Seed (1979) reports that slopes and embankments designed with a minimum pseudo-static factor of safety of 1.15 using a seismic coefficient of 0.15 have experienced "acceptable" deformations in earthquakes of magnitude less than 7.5 and intensity less than

0.75 g. However, Seed's definition of acceptable deformations appears to include deformations of over one meter in some cases.

Figure 6.5 shows the results of Newmark seismic deformation analyses performed by Hynes and Franklin (1984) using 387 strong motion records and 6 artificial accelerograms. Based upon this data and their experience with seismic response analyses of slopes and embankments, Hynes and Franklin (1984) concluded that slopes and embankments with a yield acceleration equal to half the peak ground acceleration would experience permanent seismic deformations of less than one 0.3 meters (1.0 foot) in any earthquake, even for embankments where amplification of motions occurs. In the absence of amplification, the Hynes and Franklin data suggest that deformations may remain small for yield accelerations less than one-third the peak ground acceleration. Based upon the work of Hynes and Franklin, it appears that the maximum value of k_S may be safely determined as $k_S = 0.5 \cdot a_{max}/g$, where a_{max} is peak horizontal acceleration at the ground surface for analyses of the liner system and at the top of the landfill for analyses of the cover system. a_{max} can be estimated either using the simplified methods presented in Section 4 of this guidance document or from the results of a seismic response analysis.

Step 3: Perform the pseudo-static stability analysis. If the minimum factor of safety, FS_{min}, exceeds 1.0, the seismic stability analysis is completed.

Step 4: If the pseudo-static factor of safety is less than 1.0, perform a Newmark deformation analysis. This is done with the following three steps:

1) Calculate the yield acceleration, k_y. The yield acceleration is usually calculated in pseudo-static analyses using a trial and error procedure in which the seismic coefficient is varied until $FS_{min} = 1.0$ is obtained.

2) Calculate the permanent seismic deformation. The permanent seismic deformation may be calculated using either simplified design charts (e.g., Hynes and Franklin, 1984; Makdisi and Seed, 1978) or a formal time-history analysis in which the excursions of the average acceleration time history above the yield acceleration are double integrated.

3) Compare the calculated permanent seismic deformation to the allowable maximum permanent displacement, u_{max}. Seed and Bonaparte (1992) report that u_{max} values of 0.15 to 0.3 meters (0.5 to 1.0 feet) are typically used in practice for design of geosynthetic liner systems. For cover systems, where permanent seismic deformations may be observed in post-earthquake inspections and damage to components can be repaired, larger permanent deformations may be considered acceptable. In fact, some regulatory agencies consider seismic deformations of the landfill cover system primarily a maintenance problem.

Several investigators have presented simplified charts based upon the results of Newmark deformation analyses for estimating permanent seismic deformations. Makdisi and Seed (1978) developed the chart shown in Figure 6.6 from the results of two-dimensional finite element analyses of embankments. This chart includes the effect of amplification of seismic motions by an embankment and provides upper and lower bounds on the permanent deformation as a function of magnitude. Hynes and Franklin (1984) developed the chart shown in Figure 6.5 from classical Newmark "sliding block on a plane" analyses. The Hynes and Franklin chart does not consider amplification or magnitude effects. Due to the uncertainties in using a simplified design chart and the characteristics and limitations discussed above, the use of the upper bound curves from Makdisi and Seed (Figure 6.6) for simplified analysis of the permanent seismic deformation potential of the waste mass and liner system. The *mean* + σ curve from Hynes and Franklin (Figure 6.5) is recommended for simplified permanent seismic deformation analysis of the cover system.

If a seismic response analysis has been performed, a formal Newmark seismic deformation analysis can be performed by using the acceleration or shear stress time histories from the response analysis. Jibson (1993) describes the analytical procedure for performing such an analysis. To evaluate the permanent displacement of the landfill mass, the average acceleration time history of mass above the critical failure plane (the failure surface with the lowest yield acceleration) should be used. The average acceleration time history may be calculated as the average of the acceleration time history of each layer above the interface weighted according to the unit weight and thickness of each layer. Alternatively, the average acceleration time history may be calculated from the shear stress at the interface divided by the total vertical stress above the interface, as described by Repetto et al. (1993). To calculate the permanent deformation of the landfill final cover, either the average acceleration time history of the cover or the shear stress time history at the cover-waste interface divided by the total vertical stress at the interface should be used in the Newmark analysis. Particularly for landfills in the eastern United States, where the earthquake acceleration time history may contain relatively enriched high frequencies,

the formal Newmark deformation analyses may yield significantly lower seismic deformations than simplified Newmark analyses using Figures 6.5 and 6.6.

6.3 Additional Considerations

Stability of the underlying foundation soil is an important consideration in evaluating the overall performance of the landfill, particularly if a layer (or layers) in the foundation is susceptible to liquefaction, as illustrated in Figure 6.7. The potential for a liquefaction induced flow failure may be analyzed using limit equilibrium analyses by employing residual shear strengths in the potentially liquefiable zones. In this type of post-earthquake stability assessment, the seismic coefficient should be set equal to zero (Marcuson et al., 1990). If the residual shear strength is conservatively assessed using minimum values of SPT blow counts (or CPT tip resistance) within the potentially liquefiable layer(s), a factor of safety of 1.1 may be considered as acceptable. Evaluation of seismic settlement potential, as described in Section 5.3, still must be conducted to assess the impact of liquefaction on the landfill.

In some situations, it may be convenient to treat the final cover of the landfill as an infinite slope. In these situations, the pseudo-static factor of safety and yield acceleration for the cover may be assessed using the following general equations for the stability of an infinite slope (Matasović, 1991):

$$FS = \frac{c/(\gamma \cdot z \cdot \cos^2\beta) + \tan\phi\left[1 - \gamma_w(z-d_w)/(\gamma \cdot z)\right] - k_s \cdot \tan\beta \cdot \tan\phi}{k_s + \tan\beta} \qquad (6.1)$$

$$k_y = \frac{c/(\gamma \cdot z \cdot \cos^2\beta) + \tan\phi\left[1 - \gamma_w(z-d_w)/(\gamma \cdot z)\right] - \tan\beta}{1 + \tan \cdot \beta \tan\phi} \qquad (6.2)$$

where FS = factor of safety, k_y = yield acceleration, k_s = seismic coefficient, γ =unit weight of slope material(s), γ_w= unit weight of water, c = cohesion, ϕ = angle of internal friction of the assumed failure interface or surface, z = depth to the assumed failure interface or surface, and d_w = depth to the water table (assumed parallel to the slope). The above equations yield the factor of safety and yield acceleration explicitly for both cohesive ($c \neq 0$) and cohesionless

soils (c = 0). If there is no downslope seepage, the depth to the water table, d_w, should be set equal to the depth to the assumed failure plane, z.

6.4 References

Bray, J.D., Augello, A.J., Repetto, P.C., Leonards, G.A., and Byrne, R.J. (1994), "Seismic Stability Procedures for Solid Waste Landfills," accepted for publication in the *Journal of Geotechnical Division*, ASCE.

Buranek, D. and Prasad, S. (1991), "Sanitary Landfill Performance During the Loma Prieta Earthquake," Proc. *2nd International Conference on Recent Advances in Geotechnical Earthquake Engineering and Soil Dynamics*, St. Louis, Missouri, pp. 1655-1660.

Byrne, R.J. (1994), "Design Issues with Strain-Softening Interfaces in Landfill Liners," Proc. *Waste Tech '94 Landfill Technology Conference*, National Solid Waste Management Association, Charleston, South Carolina, 26 p.

Duncan, J.M. (1992), "State-of-the-Art: Static Stability and Deformation Analysis," Proc. *Stability and Performance of Slopes and Embankments - II*, Vol. 1, pp. 222-266.

Earth Technology (1988), "In-Place Stability of Landfill Slopes, Puente Hills Landfill, Los Angeles, California," Report No. 88-614-1, The Earth Technology Corporation, Long Beach, California.

EERC (1994), "Preliminary Report on the Seismological and Engineering Aspects of the January 17, 1994 Northridge Earthquake," Earthquake Engineering Research Center, Report No. UCB/EERC-94-01, Berkeley, California.

Fassett, J.B., Leonards, G.A., and Repetto, P.C. (1994), "Geotechnical Properties of Municipal Solid Wastes and Their Use in Landfill Design," Proc. *WasteTech 94 - Landfill Technology Conference*, National Solid Waste Management Association, Charleston, South Carolina 32 p.

GeoSyntec Consultants (1993), "Report of Waste Discharge, Eagle Mountain Landfill and Recycling Center," Supplemental Volume 1, Report prepared for the Mine Reclamation Corporation, GeoSyntec Consultants, Huntington Beach, California.

Hynes, M.E. and Franklin, A.G. (1984), "Rationalizing the Seismic Coefficient Method," *Miscellaneous Paper GL-84-13*, U.S. Army Engineer Waterways Experiment Station, Vicksburg, Mississippi, 34 p.

Jibson, R.W. (1993), "Predicting Earthquake-Induced Landslide Displacements using Newmark's Sliding Block Analysis, *Transportation Research Record*, 1411, Transportation Research Board, National Research Council, Washington, D.C., pp. 9-17.

Johnson, M.E., Lew, M., Lundy, J. and Ray, M.E. (1991), "Investigation of Sanitary Landfill Performance During Strong Ground Motion from the Loma Prieta Earthquake of October 17, 1989," Proc. *2nd International Conference on Recent Advances in Geotechnical Earthquake Engineering and Soil Dynamics*, St. Louis, Missouri, pp. 1701-1708.

Kavazanjian, E., Jr., Hushmand, B., and Martin, G.R. (1991), "Frictional Base Isolation Using a Layered Soil-Synthetic Liner System," Proc. 3rd U.S. Conference on Lifeline Earthquake Engineering, *Technical Council on Lifeline Earthquake Engineering Monograph No. 4*, Los Angeles, California, pp. 1140-1151.

Kavazanjian, E. Jr. (1994), "Performance of a Geosynthetic Landfill Liner System in the 1994 Northridge Earthquake," An Interview, *Geotechnical Fabrics Report*, Vol. 12, No. 3, pp. 18-24.

Kavazanjian, E., Jr., Matasović, N., Bonaparte, R., and Schmertmann, G.R. (1994), "Evaluation of MSW Properties for Seismic Analysis," paper accepted for publication at *Geoenvironment 2000*, ASCE Specialty Conference, New Orleans, Louisiana, 22-24 February 1995.

Koerner, R.M. (1991), *Designing with Geosynthetics*, 2nd Edition, Prentice Hall, Englewood Cliffs, New Jersey, 652 p.

Landva, A.O. and Clark, J.I., (1990), "Geotechnics of Waste Fill," In *Geotechnics of Waste Fill - Theory and Practice*, ASTM STP 1070, pp. 86-103.

Makdisi, F.I., Seed, H.B. (1978), "Simplified Procedure for Estimating Dam and Embankment Earthquake-Induced Deformations," *Journal of Geotechnical Engineering Division*, ASCE Vol. 104, No. GT7, pp. 849-867.

Marcuson, W.F. (1981), "Earth Dams and Stability of Slopes Under Dynamic Loads," Moderators Report, Proc. *1st International Conference on Recent Advances in Geotechnical Earthquake Engineering and Soil Dynamics*, St. Louis, Missouri, Vol. 3, pp. 1175.

Marcuson, W.F., III, Hynes, M.E., and Franklin, A.G. (1990), "Evaluation and Use of Residual Strength in Seismic Safety Analysis of Embankments," *Earthquake Spectra*, Vol. 6, No. 3, pp. 529-572.

Matasović, N. (1991), "Selection of Method for Seismic Slope Stability Analysis," Proc. *2nd International Conference on Recent Advances in Geotechnical Earthquake Engineering and Soil Dynamics*, St. Louis, Missouri, Vol. 2, pp. 1057-1062.

Newmark, N.M. (1965), "Effects of Earthquakes on Dams and Embankments," *Geótechnique* 15, No. 2, pp. 139-160.

Orr, W.R. and Finch, M.O. (1990), "Solid Waste Landfill Performance During Loma Prieta Earthquake," *Geotechnics of Wastefills: Theory and Practice*, ASTM STP 1070, pp. 22-30.

Repetto, P.C., Bray, J.D., Byrne, R.J. and Augello, A.J. (1993), "Applicability of Wave Propagation Methods to the Seismic Analysis of Landfills," Proc. *Waste Tech '93*, Marina Del Rey, California, pp. 1.50-1.74.

Richardson, G. and Reynolds, D. (1991), "Geosynthetic Consideration in a Landfill on Compressible Clays," Proc. *Geosynthetics '91*, Industrial Fabrics Association, Minneapolis, Minnesota.

Seed, H.B. and Martin, G.R. (1966), "The Seismic Coefficient in Earth Dam Design," *Journal of Soil Mechanics and Foundations Division*, ASCE, Vol. 92, No. SM 3, pp. 25-58.

Seed, H.B. (1979), "Considerations in the Earthquake-Resistant Design of Earth and Rockfill Dams," *Géotechnique*, Vol. 29, No. 3, pp. 215-263.

Seed, R.B. and Boulanger, R.W. (1991), "Smooth HDPE-Clay Liner Interface Shear Strengths: Compaction Effects," *Journal of Geotechnical Engineering*, ASCE, Vol. 117, No. 4, pp. 686-693.

Seed, R.B., and Bonaparte, R. (1992), "Seismic Analysis and Design of Lined Waste Fills: Current Practice," Proc. *Stability and Performance of Slopes and Embankments - II*, Vol. 2, ASCE Geotechnical Special Publication No. 31, Berkeley, California, pp. 1521-1545.

Sharma, H.D. and Goyal, H.K. (1991), "Performance of a Hazardous Waste and Sanitary Landfill Subjected to Loma Prieta Earthquake," Proc. *2nd International Conference on Recent Advances in Geotechnical Earthquake Engineering and Soil Dynamics*, St. Louis, Missouri, pp. 1717-1725.

Siegel, R.A., Robertson, R.J., and Anderson, D.G. (1990), "Slope Stability Investigations at a Landfill in Southern California," *Geotechnics of Waste Fills-Theory and Practice, ASTM STP 1070*, Arvid Landva, G., David Knowles, editors, American Society for Testing and Materials, Philadelphia, Pennsylvania, pp. 259-284.

Singh, S. and Murphy, B.J. (1990), "Evaluation of the Stability of Sanitary Landfills," *Geotechnics of Waste Fills - Theory and Practice*, ASTM STP 1070, pp. 240-258.

Williams, N.D., and Houlihan, M.F. (1986), "Evaluation of Friction Coefficients Between Geotextiles, Geomembranes, and Related Products," Proc. *Third Conference on Geotextiles*, Vienna, Austria, pp. 891-896.

Williams, N.D., and Houlihan, M.F. (1987), "Evaluation of Interface Friction Properties Between Geosynthetics and Soils, "Proc. *Geosynthetics '87*, New Orleans, Louisiana, 23 p.

Yegian, M.K., and Lahlaf, A.M. (1992), "Dynamic Interface Shear Strength Properties of Geomembranes and Geotextiles," *Journal of Geotechnical Engineering*, ASCE, Vol. 118, No. 5, pp. 760-779.

Table 6.1 Unit Weight Data for MSW (Fassett et al., 1994).

REFERENCE	LOCATION	WASTE TYPE	WASTE AGE	PLACEMENT METHOD	MOISTURE CONTENT (%)	UNIT WEIGHT TOTAL (pcf)	UNIT WEIGHT DRY (pcf)	TEST METHOD	RELIABILITY	COMMENTS
Cambell, 1982	London	MSW		Thin layers; Cat 816		63		Full-Scale Field Test	Fair	Do not have details on measurement technique.
	"	MSW		5 ft lifts Cat 816		41		"	"	
	Northhampton	MSW		6.5 ft lifts L61D Loader		41		"	"	
	"	MSW		'Minimal'		29		"	"	
	Sussex	MSW		Pulverised 'Minimal'		43		"	"	
	Northhampton	MSW		5 ft lifts Cat 816		49		"	"	
	"	MSW		"		49		"	"	
	"	MSW		Thin layers; Cat 816		59		"	"	
	"	MSW		5 ft lifts Cat 955 Dozer		42		"	"	
Earth Technolgy, 1988	Los Angeles, CA	MSW			30.8 55.3	80.6 82.8	61.8 53.3	Plastic Tubes	Good	Depth about 50 ft.
Franklin & Assoc., 1990	U.S.	MSW				30		Estimate	Poor	Estimate based on component densities & relative vol.
Galante et al., 1991	S.E. PA	79% MSW 16% Sludge 5% Misc.	Fresh	Cat 826; 8-10 ft lifts		63-70		Lined Test Pits	Very Good	
Ham, et al., 1978	Madison, WI	MSW	Fresh	Cat 950B 4 ft lifts	38.2	41	30	Surveyed	Good	Density values are for waste only; no daily cover included.
Landva et al., 1984	Calgary					78-91		Test Pits	Good	Testing done in 1983-84.
	Edmonton					64-81		"	"	
	"					57-69		"	"	
	Mississauga					68-85		"	"	
	Red Deer					73-82		"	"	
	Vancouver					54-77		"	"	
	Waterloo					66-82		"	"	
	Winnipeg					54-73		"	"	
Merz & Stone, 1962	Pomona, CA	Soil:MSW (by vol.)								
	Cell 1	0:1	Fresh	(i) 1 18 ft lift; wetted to refusal	167.1	58.6 (Refuse only)	22	Surveyed	Good	
	Cell 2	1:6	Fresh	(ii) 4 4 ft lifts; Stand. Compact'n	51.9	45.3	29.8	Surveyed	Good	Compaction is sub-standard today
	Cell 3	1:4.8	Fresh	(iii) same as (ii) but no H2O added	32.5	38.6	29.1	Surveyed	Good	
	Cell 4	0:1	Fresh	(iv) 1 18 ft lift; min compaction	79.5	22.7 (Refuse only)	12.65	Surveyed	Good	

Table 6.1: (continued)

REFERENCE	LOCATION	WASTE TYPE	WASTE AGE	PLACEMENT METHOD	MOISTURE CONTENT (%)	UNIT WEIGHT TOTAL (pcf)	UNIT WEIGHT DRY (pcf)	TEST METHOD	RELIABILITY	COMMENTS
	Cell 5	1:4.1	Fresh, mixed with soil	(v) 1 18 ft lift; Stand. compact'n	41.7	46.5	32.9	Surveyed	Good	
Natarajan & Rao, 1977	Bombay, India	MSW				Ave=84 S.D=15	Ave=50 S.D=23	"Undisturbed" Samples	Good	6 Samples
Oweis & Khera, 1986	NJ	MSW MSW	Fresh 'Older'			42 62 70-80		Based on pore press. in subs Same Volume Estimates	Fair Poor Poor	Ave over 100 ft depth
Pacey, 1982	Mt. View, CA	MSW	Fresh " " " " "		51 47 43 35 41 35	48 47 44 43 43 44	32 32 31 32 30 33	Full-Scale Field Test " " " " "	Good " " " " "	Six 100 x 100 ft, 50 ft deep Test Cells.
Pfeffer, 1992		MSW	Fresh	1-1.5 ft lifts D-9 Dozer	23.6 35.4 53.2	45 44 49	34 28 22	Full-Scale Field Test " "	Good " "	Test reported in 1969; do not know how dry unit weight was calculated.
Richardson & Reynolds, 1991	Central Maine	MSW	1-2 yrs			Ave=96		12 Test Pits	Good	
Sargunan et al., 1986	Madras, India	MSW	10-50	Uncompacted	30-48	34-43		"In-situ Tests"(?)	Fair	
Schumaker, 1972 (From Oweis & Khera, 1986)				Poor Moderate Good		18.5 29.6-37 99.6			Fair " "	Do not have details on measurement technique.
Sharma et al., 1990	Richmond, CA	MSW & Liquids	?-40			46		Surveyed	Fair	MSW to daily cover ratio = 6:1
Siegel et al., 1990	S. CA	MSW	6-40 yrs		10-45		60-108	13 cm Acrylic Tubes	Fair	Samples depths = 15-82 ft Soil content = 20 to 95%
Stone, 1975		MSW No soil	Fresh	Stand. Compact'n no Soil added	29-48	35-46	26-34	Surveyed	Fair	
Stone & Friedland, 1969	U.S.					Ave=45 S.D.=18		National survey	Poor	Results of survey of 103 U.S. Operators.

TABLE 6.2: COMPILATION OF THE AVAILABLE SHEAR STRENGTH DATA ON MSW
SOURCE: GEOSYNTEC (1993)

REFERENCE	TYPE OF DATA	RESULTS	COMMENTS
Oweis (1985)	Laboratory tests on baled waste	ϕ = 15° to 25° c = 1400 psf (67 kPa)	No data on waste types, density, or test methods is provided. Results correspond to a limiting strain of 15 to 20%.
Oweis (1985)	Field load test at landfill in southern California	ϕ = 10° and c = 1000 psf (48 kPa) to ϕ = 26° and c = 0	Values represent lower-bound strengths as the slope did not fail. Results are for relatively low normal stresses. Assumed unit weight of MSW is 45 pcf (7 kN/m^3).
Oweis (1985) and Dvirnoff and Munion (1986)	Back calculation based on failure of a landfill foundation on marsh clays and silts	ϕ = 10° and c = 500 psf (24 kPa) to ϕ = 30° and c = 0	Values unreliable due to uncertainty in the back analysis and strain incompatibility between waste and foundation.
Pagotto and Rimoldi (1987)	**Back calculation from the results of plate bearing tests**	**ϕ = 22° and c = 600 psf (29 kPa)**	**No data on waste types, test procedures, or test results are provided.**
Earth Technology (1988)	Small-scale triaxial tests on wastes from LACSD Puente Hills landfill	ϕ = 24° and c = 2,600 psf (124 kPa) to ϕ = 35°	Strength with cohesive component associated with cover soil dominant waste; cohesionless strength for refuse dominated waste.
Landva and Clark (1990)	**Laboratory direct shear tests on municipal solid waste**	ϕ = 24° and c = 450 psf (22 kPa) to **ϕ = 39° and c = 400 psf (19 kPa)**	**Normal stresses up to about 10,000 psf (480 kPa). Shear box size was approximately 11 in. (275 mm) by 17 in. (425 mm).** Lower value corresponds to shredded waste, not used.
Singh and Murphy (1990)	Laboratory tests performed by others	ϕ = 0 and c = 700 psf (34 kPa) to ϕ = 42° and c = 0	Strength values bracket a range of results compiled from work of various researchers and consulting organizations.
Seigel et al. (1990)	Small-scale direct shear tests on wastes from OII	ϕ = 39° to ϕ = 53°	Confining pressures from 2,000 to 12,000 psf (100 to 570 kPa). Lower value of ϕ is based upon conservative interpretation.
Richardson and Reynolds (1991)	**Large direct shear tests performed in situ**	**ϕ = 18° to 43°and c = 200 psf (10 kPa)**	**Normal stresses from 200 to 800 psf (10 to 40 kPa). Unit weight of waste and cover soil estimated to be 96 pcf (15 kN/m^3).**

TABLE 6.3: LOWER BOUND FRICTION ANGLES BACKFIGURED FROM OBSERVATIONS OF STEEP LANDFILL SLOPES SOURCE: GEOSYNTEC (1993)

LANDFILL (Location)	AVERAGE SLOPE		MAXIMUM SLOPE		WASTE STRENGTH (ϕ, c = 100 psf)		
	Height, ft (m)	Angle, H:V	Height, ft (m)	Angle, H:V	FS = 1.0	FS = 1.1	FS = 1.2
Lopez Canyon (California)	400 (120)	2.5:1	120 (35)	1.7:1	25°	27°	29°
Operating Industries, Inc. (California)	250 (75)	2:1	75 (20)	1.6:1	28°	30°	34°
Town of Babylon (New York)	90 (30)	1.9:1	45 (10)	1.25:1	30°	34°	38°
Private Facility (Ohio)	130 (40)	2:1	35 (10)	1.2:1	30°	34°	37°

Notes: (1) FS = Assumed factor of safety for back-analysis to estimate ϕ. Back-analyses were performed assuming c = 100 psf (5 kPa).
(2) Data for Lopez Canyon, Town of Babylon, and Private Facility Landfills obtained from GeoSyntec Consultants project files. Data for Operating Industries, Inc. Landfill obtained from Siegel et al. (1990).

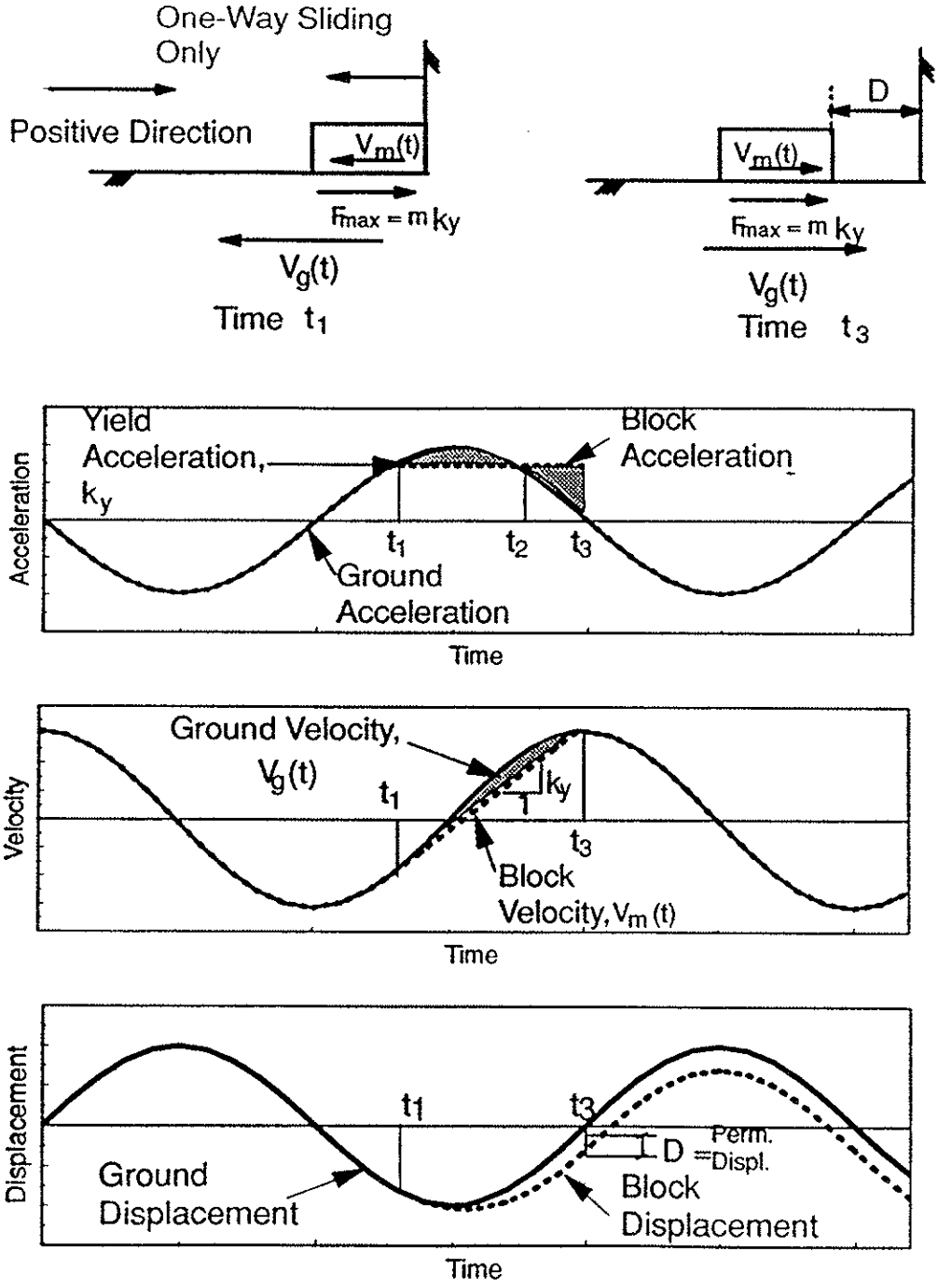

Figure 6.1 Fundamental Principles of the Newmark Seismic Deformation Analysis (after Bray et al., 1994).

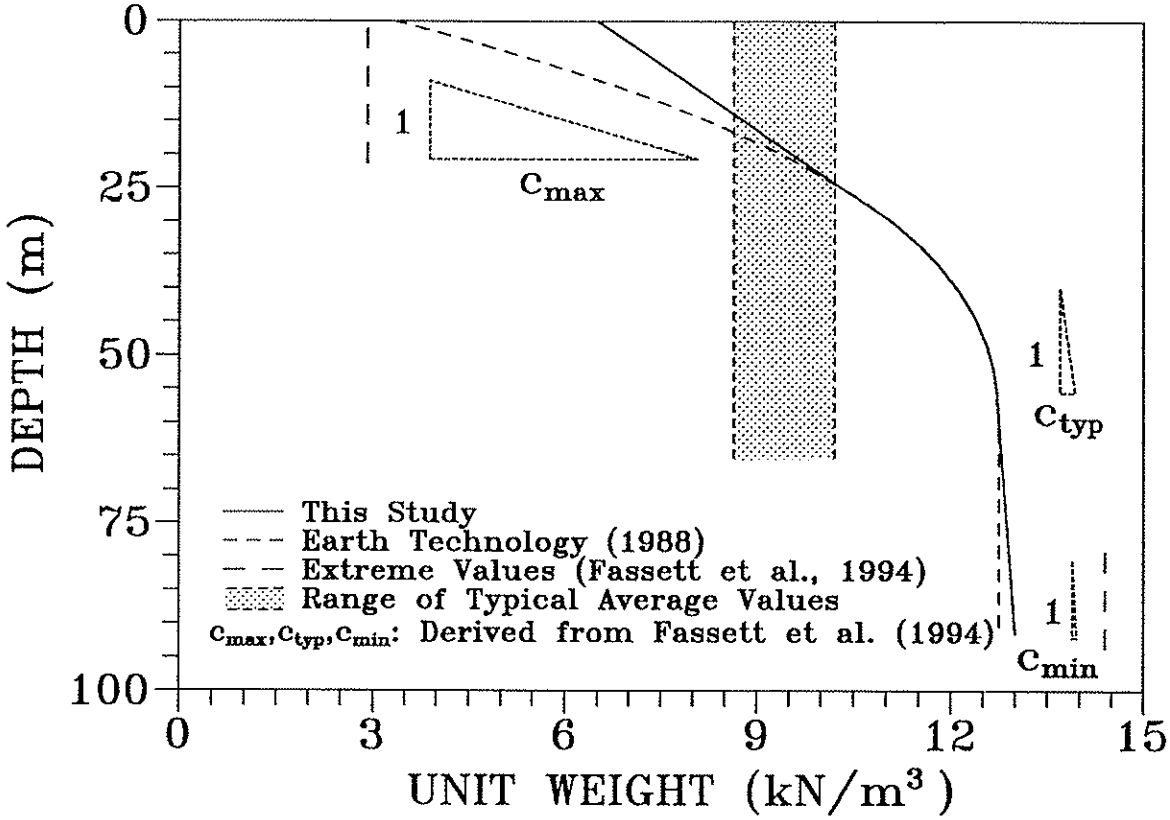

Figure 6.2 Unit Weight Profile for MSW (Kavazanjian et al., 1994).

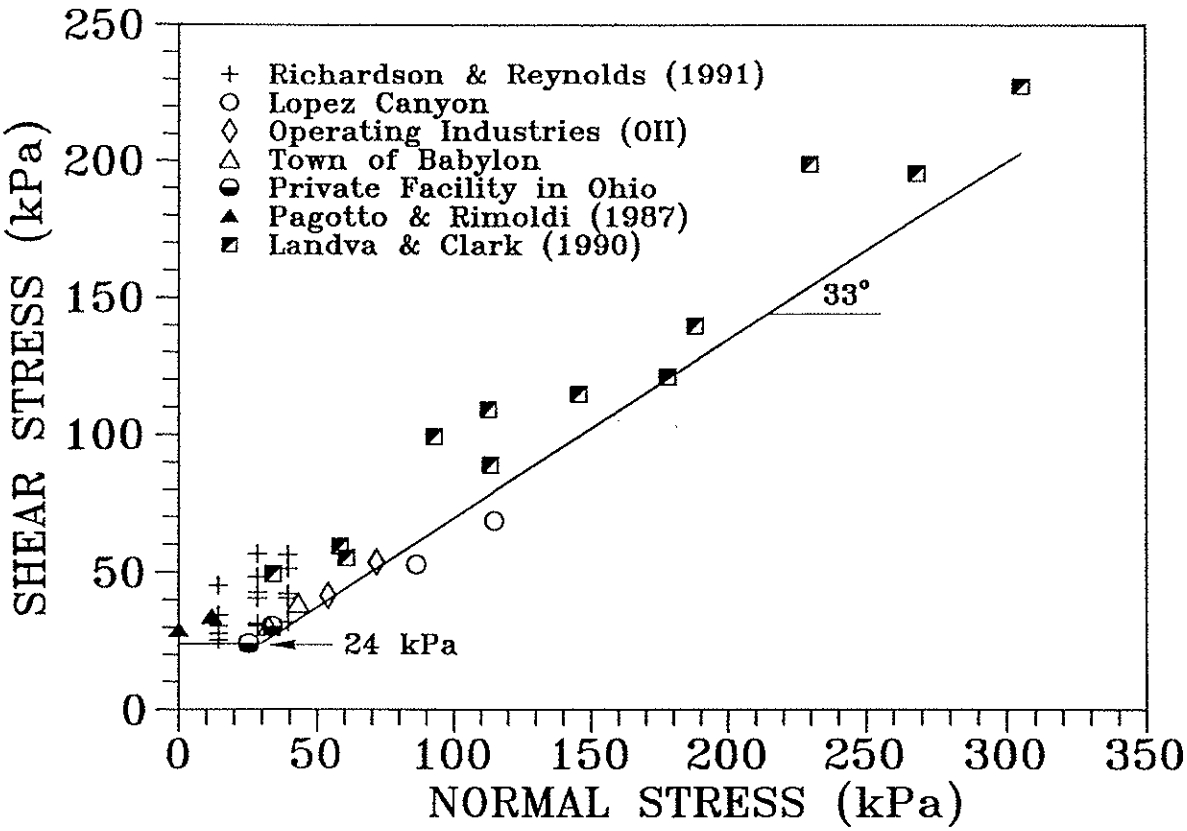

Figure 6.3 Bi-Linear Shear Strength Envelope for MSW (Kavazanjian et al., 1994).

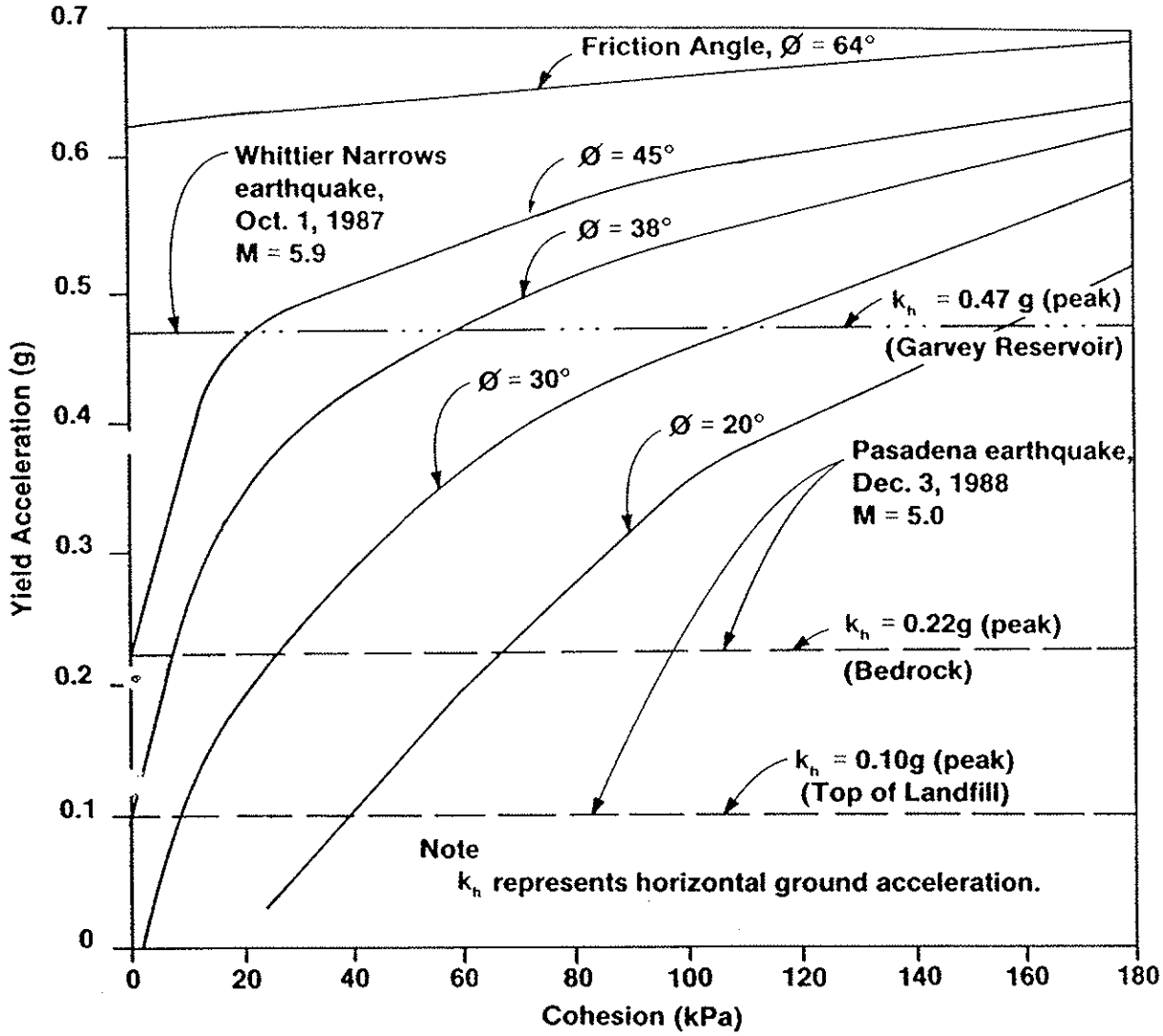

Figure 6.4 Yield Acceleration as a Function of Shear Strength Parameters for the OII Landfill (Siegel et al., 1990).

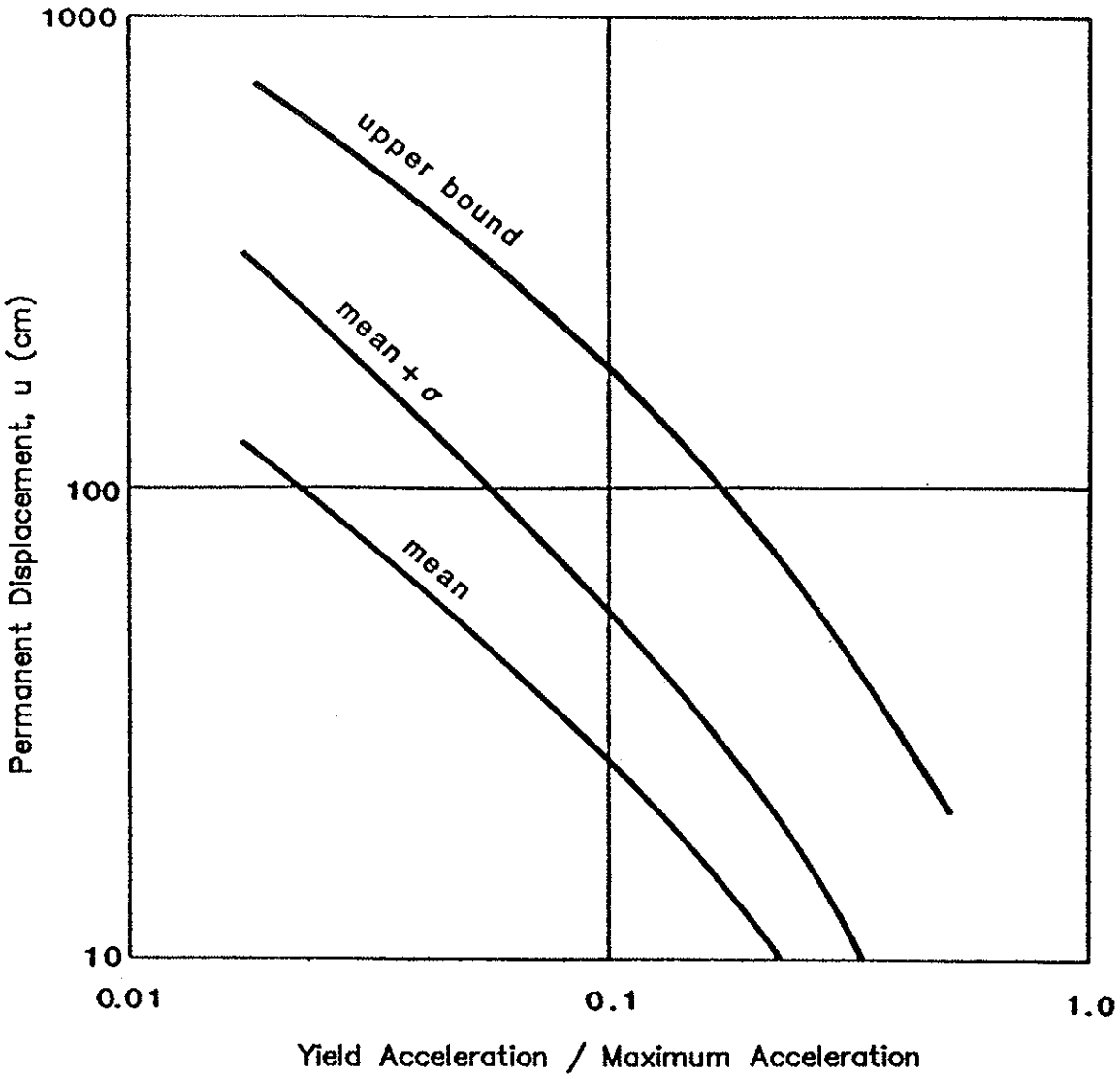

Figure 6.5 Hynes and Franklin Permanent Seismic Displacement Chart (Hynes and Franklin, 1984).

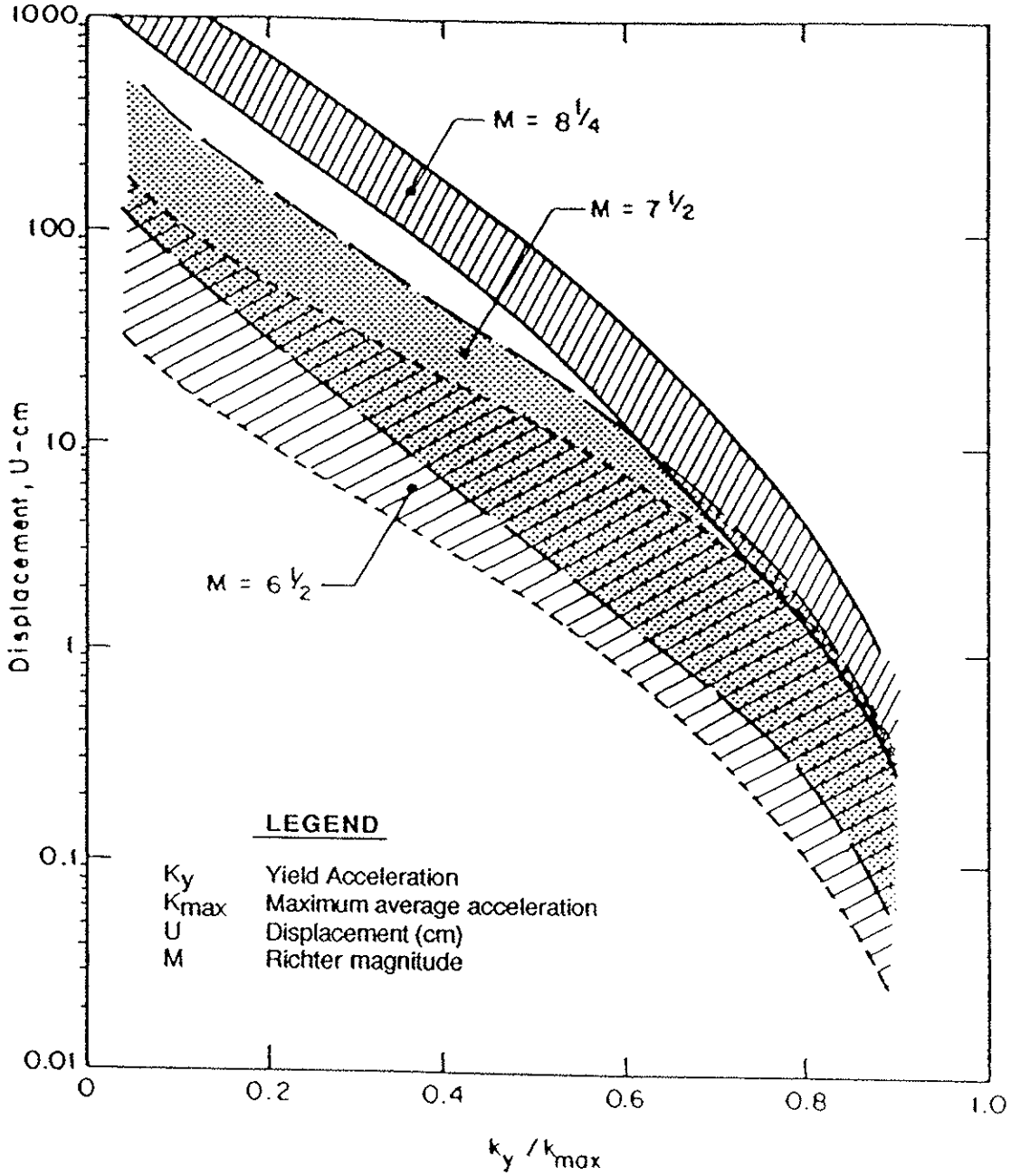

Figure 6.6 Makdisi and Seed Permanent Displacement Chart (Makdisi and Seed, 1978).

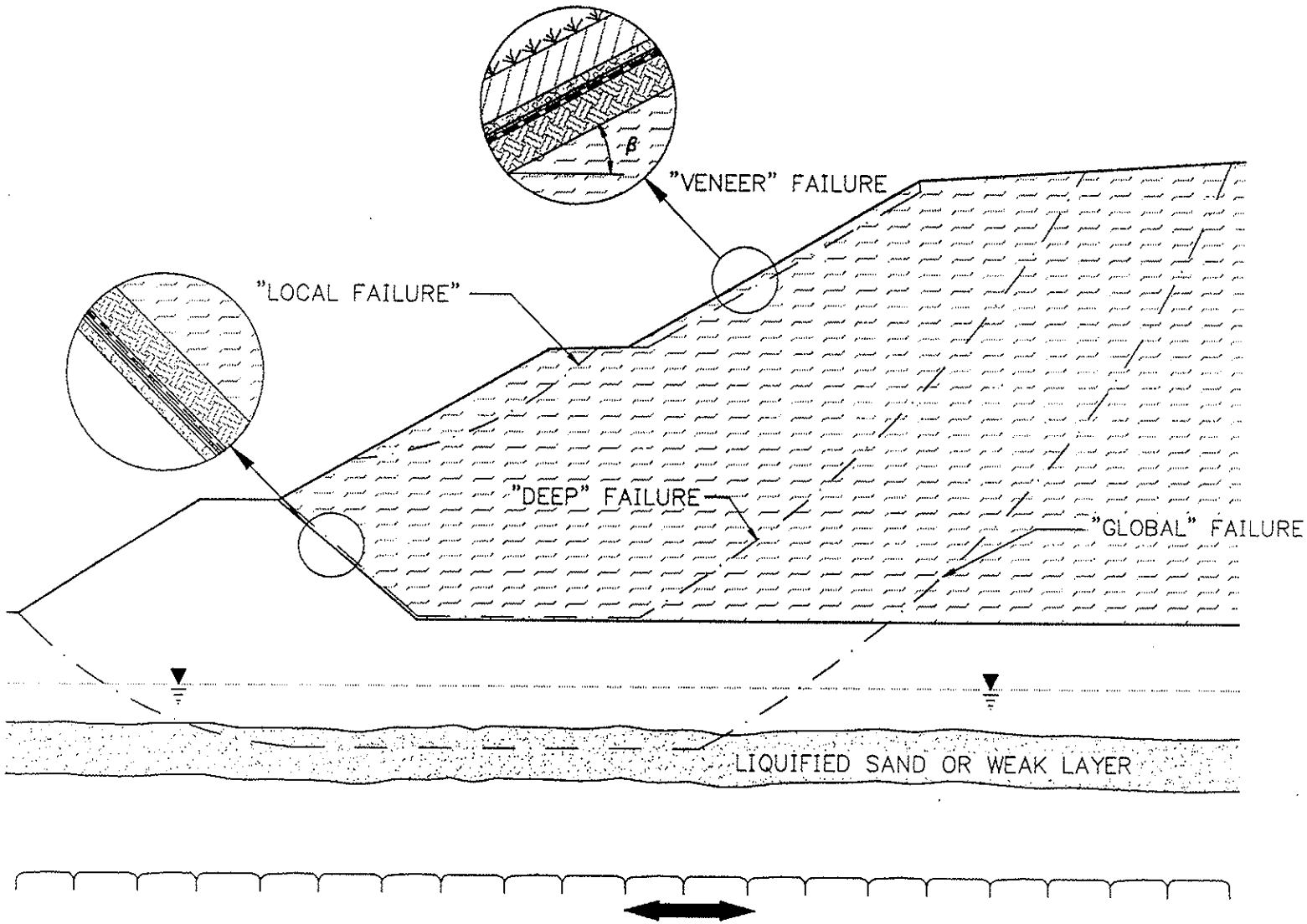

Figure 6.7 Modes of Instability of a MSW Landfill.

APPENDIX A LIQUEFACTION POTENTIAL

EXAMPLE 1 - MSWLF on Level Site - Initial Screening

EXAMPLE 2 - MSWLF on Level Site - Global Stability

APPENDIX A EXAMPLE PROBLEM - LIQUEFACTION POTENTIAL

EXAMPLE 1: This example evaluates the potential for liquefaction at the site of a proposed above grade MSWLF. The subgrade is composed of fine sands and the water table is near surface. The analysis neglects the additional normal stresses that will result from the landfill itself. This is conservative.

GIVEN:
- PEAK BEDROCK ACCELERATION = 0.22 g
- MAXIMUM MAGNITUDE = 6.2
- LEVEL SITE STRATIGRAPHY
- SOIL PROPERTIES - SEE PAGE 4 OF CALCS

2120
TABLE 3.1

DEFINE ZONES OF CONCERN

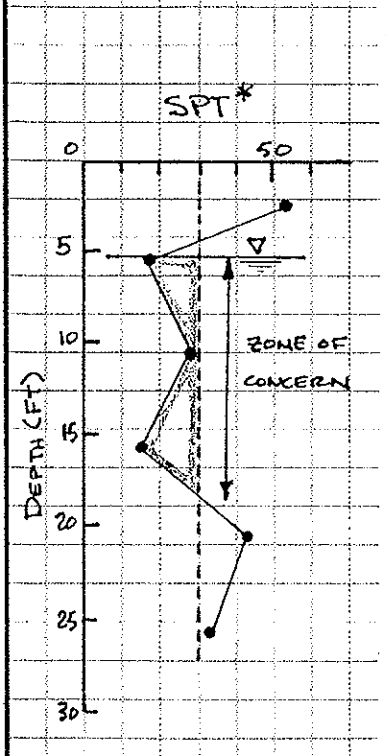

Log of Boring G-3

Equipment Mobile B-61

Elevation +10 ft *Date* 01/23/93

* Blows/foot	Depth (ft)	Sample	
	0		LIGHT BROWN CALCAREOUS SAND WITH SILT (SP-SM), very dense to medium dense, fine, moist, some shells.
54	5		Water level at 5.3 feet, 14:30, 1/23/93. Becomes saturated.
19	10		Becomes medium.
29	15		LIGHT BROWN CALCAREOUS SAND (SP), medium dense to dense, medium to coarse, saturated.
17	20		Becomes light gray-brown.
43	25		End of boring at 26.5 feet.
33	30		

ZONE OF CONCERN CRITERIA
- SPT < 30
- SATURATED

* SPTs GIVE ARE ASSUMED TO BE NORMALIZED, E.G. (N_{60})

APPENDIX A EXAMPLE PROBLEM - LIQUEFACTION POTENTIAL

EXAMPLE 1: The resistance of the existing soil strata is evaluated using the Simplified Procedure as outlined in Section 5. On this page the CSR capacity of the existing subgrade is calculated.

STEP 1 - COMPUTE CSR REQUIRED TO LIQUEFY STRATA

1.1 DETERMINE INITIAL σ_o AND σ_o'

ASSUME WATER LEVEL AT 5.3FT DEPTH IS SEASONAL HIGH

DEPTH-FT	σ_o-PSF	σ_o'-PSF	
5	520	520	SOIL UNIT WEIGHTS
10	1106	812	FROM PAGE 4 CALCS
15	1696	1090	
20	2286	1368	

1.3 NORMALIZE SPT → $(N_1)_{60}$ — Eq 5.3

DEPTH-FT	C_N	N_1	$(N_1)_{60}$
5	1.6	19	30
10	1.5	29	43
15	1.3	17	22
20	1.1	43	47

1.4 DETERMINE CSR — Eq 5.4

DEPTH-FT	$(N_1)_{60}$	CSR*	
5	30	0.5	*USE 5% FINES
10	43	>0.5	
15	22	0.25	
20	7	>0.5	

APPENDIX A EXAMPLE PROBLEM - LIQUEFACTION POTENTIAL

EXAMPLE 1: The CSR generated by the design earthquake is evaluated. The acceleration at the surface of the site is estimated using the general amplification/attenuation relationships from Figure 4.2.

1.5 CALCULATE CORRECTED CSR

$CSR_L = CSR \times K_M \times K_\alpha$ (K_α: 1-LEVEL GROUND)

DEPTH-FT	CSR	K_M^*	CSR_L
5+	0.5	1.25	0.625
15	0.25	1.25	0.312

*Fig 5.5

STEP 2 - COMPUTE CSR_{EQ} RESULTING FROM EARTHQUAKE

2.1 DEFINE STRESS REDUCTION FACTOR, r_d — Fig 5.7

DEPTH-FT	r_d
5+	0.98
15	0.96

2.2 CALCULATE CSR_{EQ}

- SOLVE FOR $\ddot{a}_{max}$ AT GROUND SURFACE (DEEP COHESIONLESS SOIL) — Fig 4.2

  $\Rightarrow \ddot{a}_{GRD} = 0.18g$

- SOLVE FOR CSR_{EQ} — EQ. 5.1

DEPTH-FT	r_d	σ_o/σ_o'	CSR_{EQ}
5+	0.98	1.0	0.114
15	0.95	1.55	0.172

APPENDIX A EXAMPLE PROBLEM - LIQUEFACTION POTENTIAL

EXAMPLE 1: The Factor of Safety against liquefaction calculated for the two critical depths is greater than 1.0, so the site has limited liquefaction potential.

STEP 3 - COMPUTE FS AGAINST LIQUEFACTION

DEPTH, ft	CSR_{EQ}	CSR_L	$FS = CSR_L / CSR_{EQ}$
5+	0.114	0.625	5.5
15	0.172	0.312	1.8

∴ NO LIQUEFACTION OCCURS

ATTACHMENT - SOIL DATA

UNIT WEIGHTS

$\gamma_{SAT} = 118$ PCF

$\gamma_{DRY} = 104$ PCF

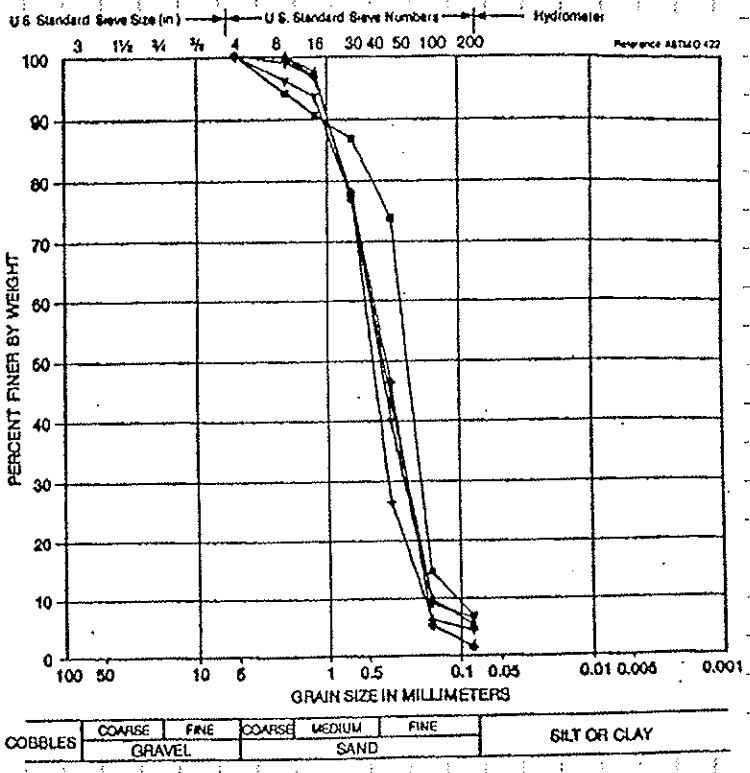

APPENDIX A EXAMPLE PROBLEM - LIQUEFACTION POTENTIAL

EXAMPLE 2: A potentially liquefiable sand layer is located approximately 30 feet below the landfill. Analyses have shown that in the case of liquefaction neither the integrity of overlying soil will be disrupted nor excessive settlement will occur. However, there is a concern that global stability of the landfill might be disrupted, as shown in the enclosed diagram. Evaluate the post-earthquake global stability of the landfill assuming that the underlying sand layer has liquefied.

Given:
- Site stratigraphy and landfill geometry.
- Results of liquefaction analysis.
- Average corrected SPT blow count in liquefiable layer = 12.

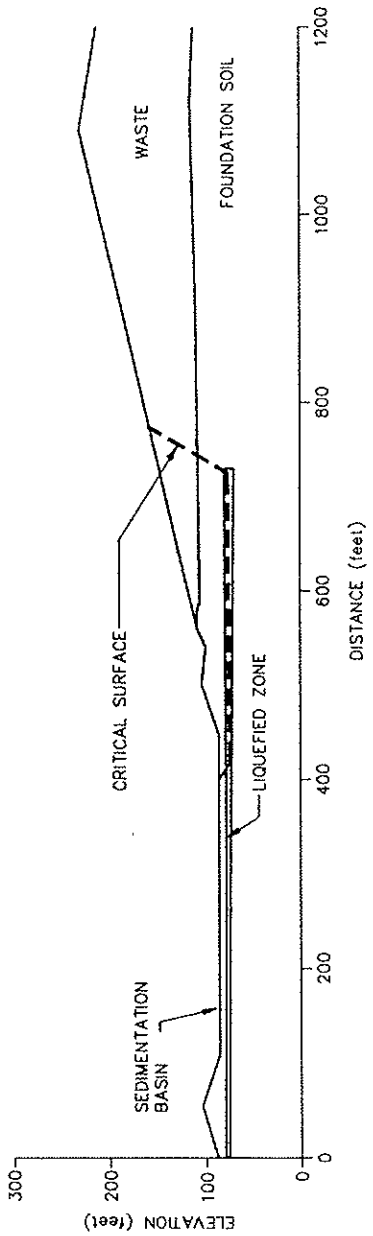

The residual shear strength for the liquefied soil was estimated on the basis of the empirical relationship between corrected SPT blow counts and residual shear strength for sands developed by Seed et al. (1988), and reiterated by Marcuson et al. (1990). Based on average corrected SPT blow count of 12 for the loose layer (liquefied zone), the relationship indicated lower bound residual strength of 200 psf. The shear strength parameters for the underlying sand layer were therefore taken as friction angle of zero and a cohesion of 200 psf for the post-earthquake stability assessment. Slope stability analysis performed using the residual shear strength yielded a factor of safety of 1.1 which was deemed acceptable.

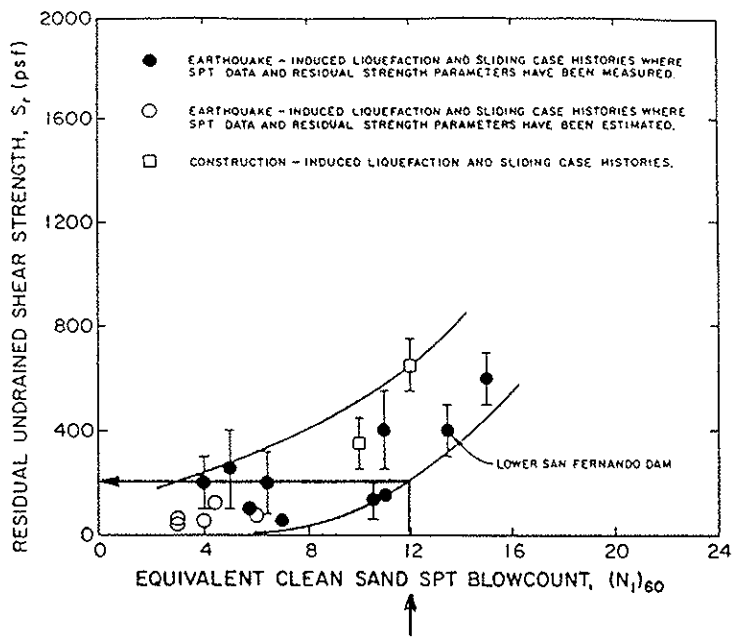

APPENDIX B SEISMIC SLOPE STABILITY

EXAMPLE 1 - MSWLF on Ridge

EXAMPLE 2 - MSWLF Above Grade

EXAMPLE 3 - MSWLF on Soft Subgrade

EXAMPLE 4 - MSWLF Displacement Analysis

APPENDIX B EXAMPLE PROBLEM - SEISMIC SLOPE STABILITY

EXAMPLE 1: This example reviews the seismic stability of a MSWLF placed on a ridge. The subgrade stratigraphy at the site has approximately 10-ft of soil profile over the rock forming the ridge. Two important assumptions are made at this point: 1-the peak bedrock acceleration acts on the bottom of the liner, and 2- due to the ridge, the seismic coefficient is assumed to equal the peak bedrock acceleration.

GIVEN: • DESIGN EARTHQUAKE → $\ddot{a}_{PEAK} = 0.11g$ (250 YR, 90%) USGS 2120

• MATERIAL PROPERTIES:

• MUNICIPAL SOLID WASTE	γ=65 PCF	ϕ=20°	c=200 PSF
• LODGEMENT TILL	γ=120 PCF	ϕ=28°	c=500 PSF
• DECOMPOSED ROCK	γ=125 PCF	ϕ=20°	c=1000 PSF

• COORDINATES FOR ANALYSIS

#	X	$\bar{X}$*	Y
1	1250	(1250)	1980
2	1500	(1000)	2050
3	1650	(850)	2050
4	2450	(50)	1820
5	2150	(350)	1870
6	1600	(900)	1945
7	2500	(0)	1818
8	1050	(1450)	1980

*MIRRORED FOR STABL

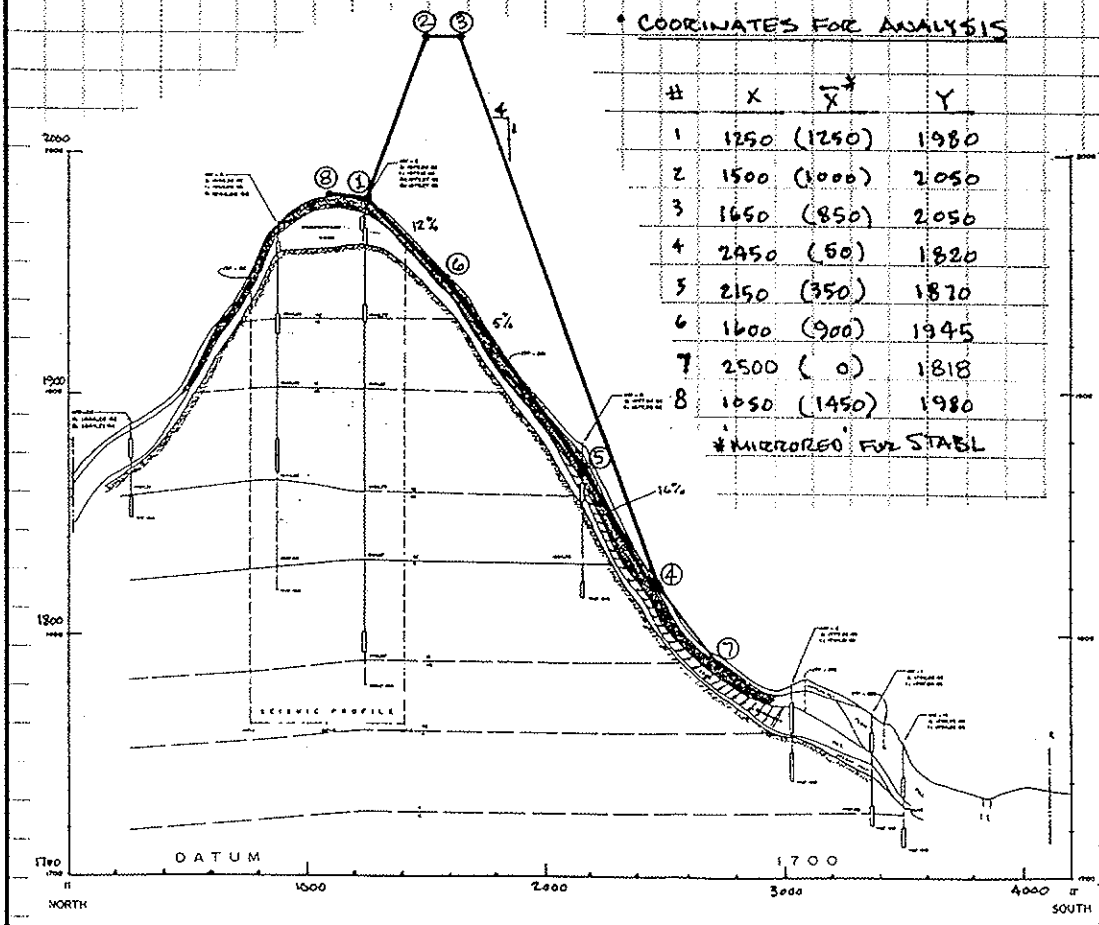

STRATIGRAPHIC PROFILE

APPENDIX B EXAMPLE PROBLEM - SEISMIC SLOPE STABILITY

EXAMPLE 1: The seismic stability of the unlined landfill is evaluated for a range of seismic coefficients. The STABL model is setup to force the failure surface to bottom in the MSW due to the higher strengths of the natural soils and the geometry. While a general analysis will confirm this assumption, potential failure surfaces through the subgrade should not be discounted without analysis.

EVALUATE MSWLF STABILITY W/O LINER SYSTEM

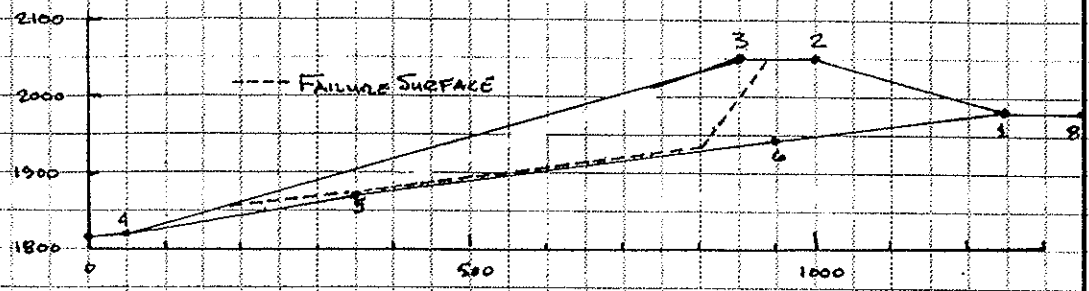

STABL INPUT FILE

```
PROFILE
EXAMPLE #1  RIDGE TOP SITE W/O LINER
8 5
0. 1818. 50. 1820. 2
50. 1820. 850. 2050. 1
850. 2050. 1000. 2050. 1
1000. 2050. 1250. 1980. 1
1250. 1980. 1450. 1980. 2
50. 1820. 350. 1870. 2
350. 1870. 900. 1945. 2
900. 1945. 1250. 1980. 2
SOIL
2
65. 65. 200. 20. 0. 0. 0
120. 120. 500. 25. 0. 0. 0
EQUAKE
0.11 0. 0.
BLOCK
25 2 50.
50. 1820. 350. 1870. .0
351. 1870. 900. 1945. .0
```

0.11 g

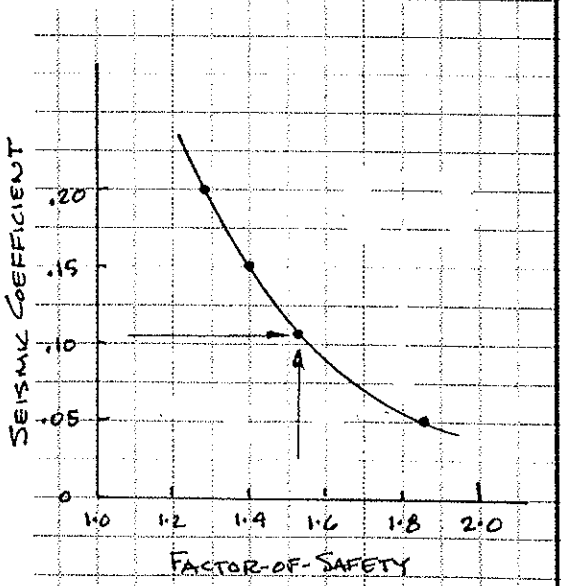

FS = 1.52

APPENDIX B EXAMPLE PROBLEM - SEISMIC SLOPE STABILITY

EXAMPLE 1: The STABL model was modified to allow the addition of 'soil' types to represent the liner system. In the example shown, two liner types are included so that textured and smooth sheet could be incorporated at the same time. The shear strength of the liner 'soils' should be obtained from interface friction testing of the liner interfaces.

EVALUATE MSWLF STABILITY W/ LINER SYSTEM

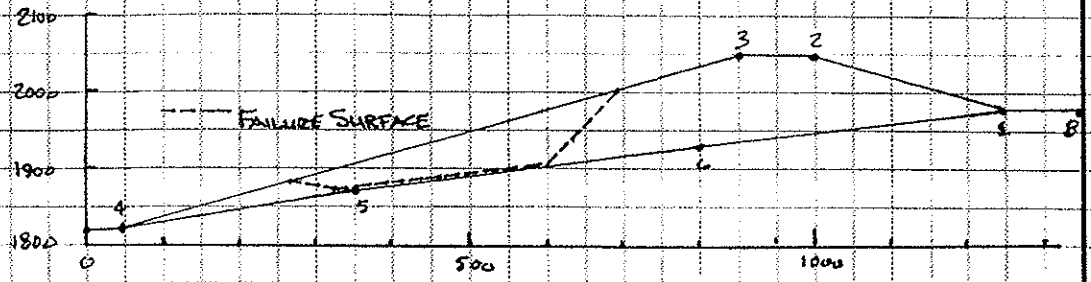

STABL INPUT FILE

```
PROFILE
EXAMPLE #1  RIDGE TOP SITE W/ LINER
11 5
0. 1818. 50. 1820. 2
50. 1820. 850. 2050. 1
850. 2050. 1000. 2050. 1
1000. 2050. 1250. 1980. 1
1250. 1980. 1450. 1980. 2
50. 1819.5 350. 1870. 4
350. 1870. 900. 1945. 3
900. 1945. 1250. 1979.5 4
50. 1819. 350. 1869.5 2
350. 1869.5 900. 1944.5 2
900. 1944.5 1250. 1979.5 2
SOIL
4
65. 65. 200. 20. 0. 0. 0
120. 120. 500. 25. 0. 0. 0
60. 60. 0. 10. 0. 0. 0
60. 60. 0. 20. 0. 0. 0
EQUAKE
0.055 0. 0.
BLOCK
25 2 50.
50. 1819.5 350. 1870. .0
351. 1869.5 900. 1945. 0.
```

LINER

0.055g

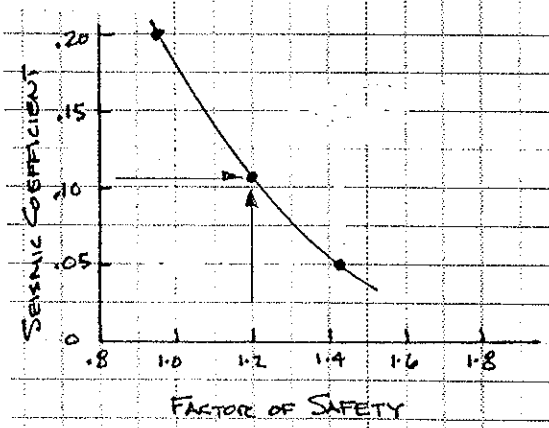

a_y = 0.16 YIELD

FS = 1.2

NOTE THAT TWO 'LINER' TYPES HAVE BEEN USED. THIS ALLOWS COMBINATIONS OF SMOOTH AND TEXTURED SHEET TO BE TRIED. IN THE EXAMPLE TEXTURED WAS USED ON ④-⑤ AND ⑥-①. HOWEVER THE FAILURE SURFACE DID NOT GO THRU THESE ZONES.

APPENDIX B EXAMPLE PROBLEM - SEISMIC SLOPE STABILITY

EXAMPLE 2: This landfill is built upon a relatively shallow layer of stiff basal till such that the peak surface acceleration can be assumed to equal the peak bedrock acceleration. The site is approximately level so that the seismic coefficient is assumed to equal 0.5 times the peak ground surface acceleration or 0.125g.

GIVEN: • DESIGN EARTHQUAKE → a_{MAX} = 0.25g (250 yr, 90%) USGS 2120

∴ SEISMIC COEFFICIENT = 0.125g 0.125g

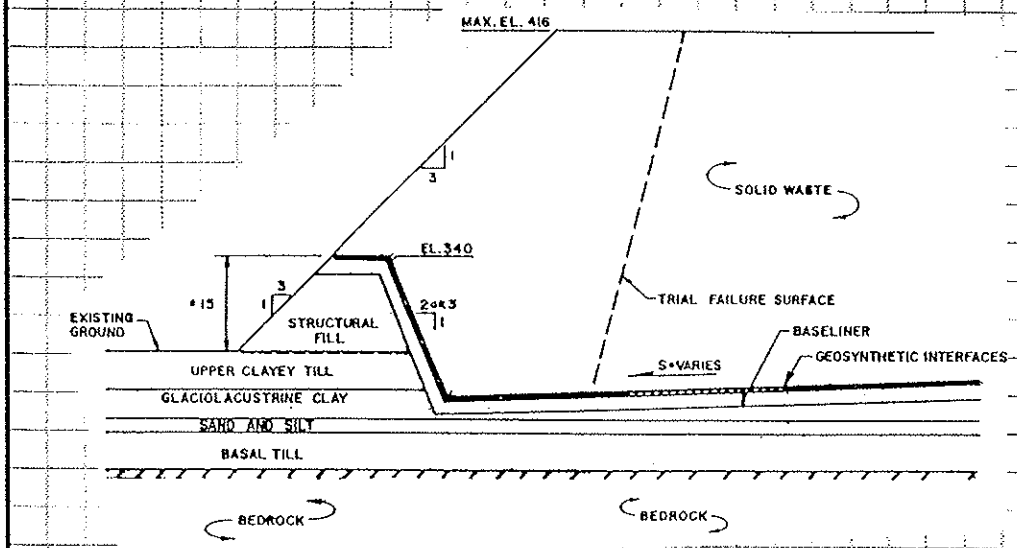

MATERIAL ENGINEERING PROPERTIES

Item	Moist Unit Weight (pcf)	Saturated Unit Weight (pcf)	Total Stress Analysis (Short Term)		Effective Stress Analysis (Long Term)	
			Cohesion (psf)	Friction Angle (Degrees)	Cohesion (psf)	Friction Angle (Degrees)
NYSDOT No. 2 Stone	110	110	0	30°	0	30°
Solid Waste	65	75	300	33°	300	33°
Soil Liner	125	130	1000	0	0	25°
Upper Clayey Till	135	138	1800	0	0	32°
Glaciolacustrine Clay	120	120	350-1500*	0	0	23°
Sand and Silt	130	138	0	32°	0	32°
Basal Till	135	140	0	34°	0	34°

Note: Refer to Table 3-4 for geosynthetic interface friction angle.

* $S_u = \sigma'_{vc} 0.34(OCR)^{0.7}$

APPENDIX B EXAMPLE PROBLEM - SEISMIC SLOPE STABILITY

EXAMPLE 2: The STABL model used in this example is much more detailed than that used in Example 1. Each layer of the liner is included in the model. The model can be simplified by replacing the multiple layer liner with a single layer having the lowest interface friction properties. This complete model allows evaluation of the influence of pore water (or leachate) pressures within individual layers on the overall stability.

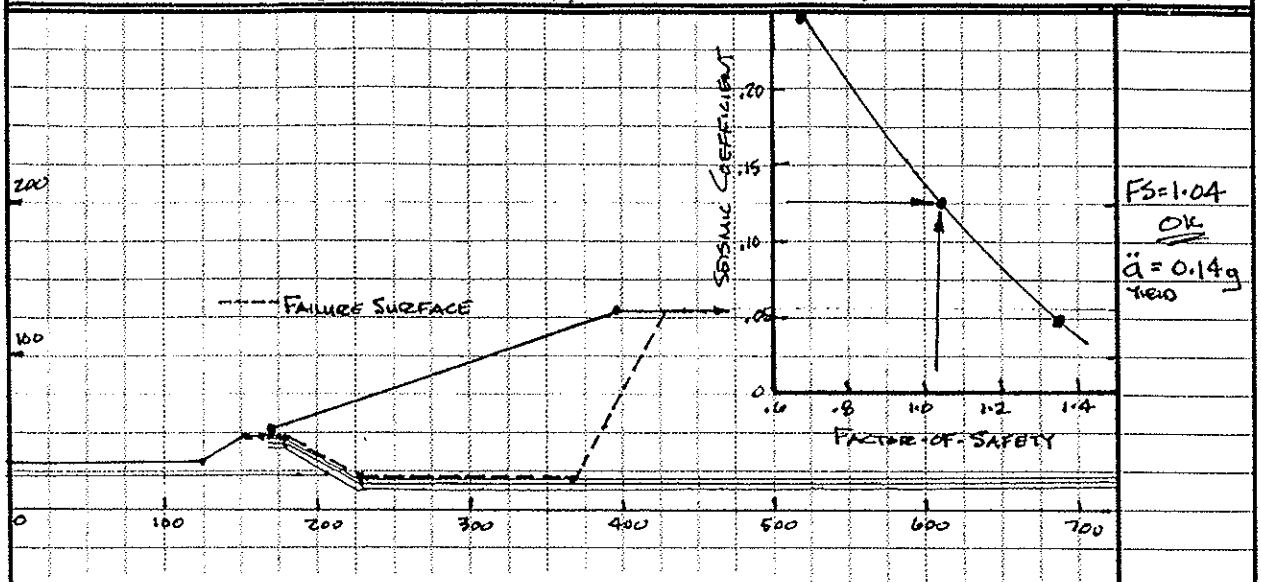


```
PROFILE
EXAMPLE #2 CLAY FOUNDATION WITH TOE BERM
21 6
0. 35. 119.5 35. 5
119.5 35. 158.5 48. 5
158.5 48. 163.9 49.8 4
163.9 49.8 164.5 50. 3
164.5 50. 392.5 126. 2
392.5 126. 850. 126. 2
164.5 50. 174.5 50. 3
174.5 50. 230.5 22. 3
230.5 22. 850. 25.1 3
163.9 49.8 174.5 49.8 4
174.5 49.8 230.5 21.8 4
230.5 21.8 850. 24.9 4
158.5 48. 174.5 48. 5
174.5 48. 222.5 24. 5
222.5 24. 232.5 19. 6
232.5 19. 850. 22.1 6
0. 24. 222.5 24. 6
0. 17. 246.5 17. 7
246.5 17. 850. 16. 7
0. 14. 450. 12. 8
450. 12. 850. 10.5 8
```

```
SOIL
8
110. 110. 0. 30. 0. 0. 0
65. 75. 300. 33. 0. 0. 0
.1 .1 .0 10. 0. 0. 0 ← HDPE/GEONET
125. 130. 1000. 0. 0. 0. 0
135. 138. 1800. 0. 0. 0. 0
120. 120. 600. 0. 0. 0. 0
130. 138. 0. 32. 0. 0. 0
135. 140. 0. 34. 0. 0. 0
EQUAKE
0.25 0. 0. ← (0.25g)
LIMITS
3 3
0. 8. 300. 8.
300. 8. 500. 6.
500. 6. 850. 4.
BLOCK
50 3 40.
174.5 49.95 174.5 49.95 0.
230.5 21.9 230.5 21.9 0.
325.0 22.37 425. 22.87 .8
```

APPENDIX B EXAMPLE PROBLEM - SEISMIC SLOPE STABILITY

EXAMPLE 3: The global seismic analysis shows that the governing failure during an earthquake is the result of a global failure. Increasing the global factor of safety may require reduction of the landfill exterior slope or reduction of the waste height.

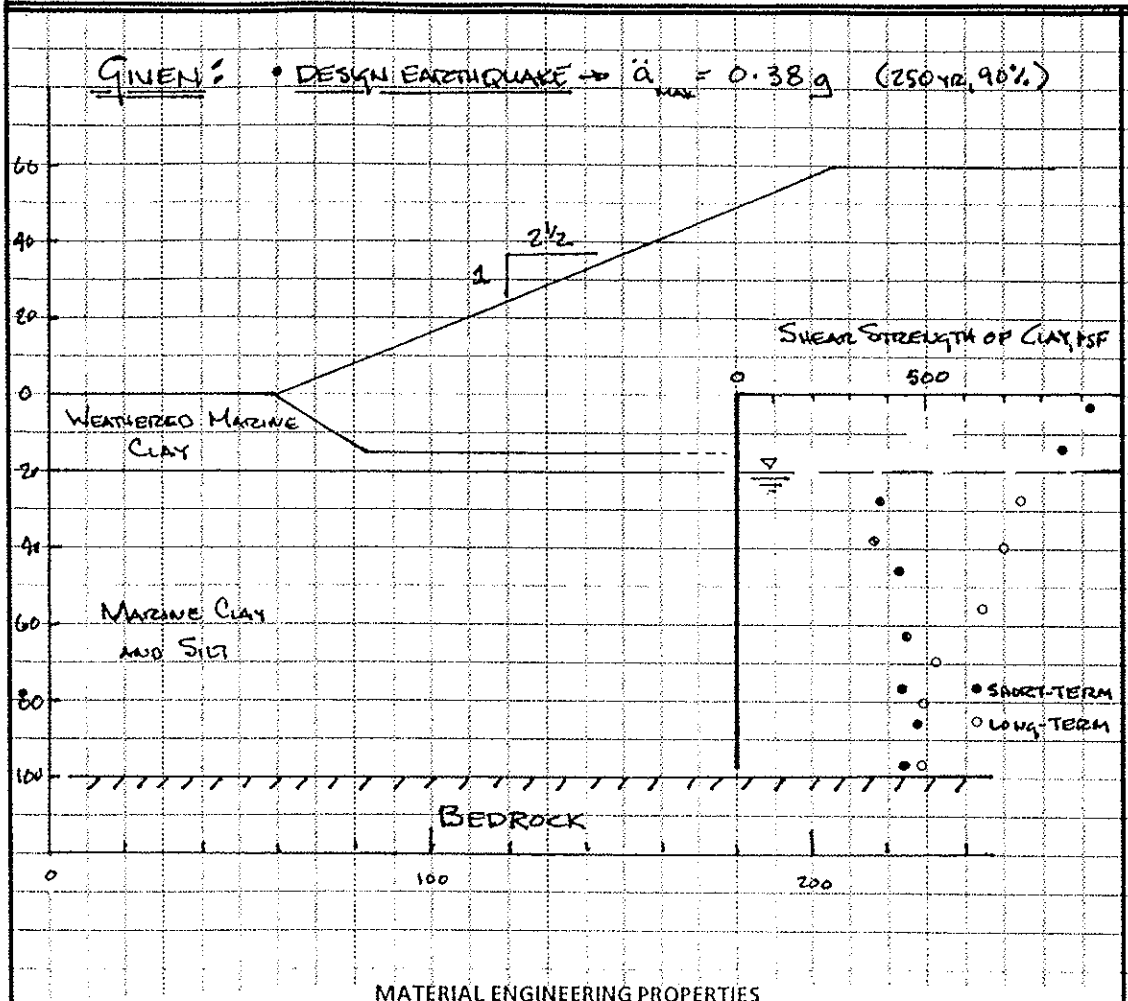

MATERIAL ENGINEERING PROPERTIES

Item	Moist Unit Weight (pcf)	Saturated Unit Weight (pcf)	Total Stress Analysis (Short Term) $_{INITIAL}$		Total Stress Analysis (Long Term)*	
			Cohesion (psf)	Friction Angle (Degrees)	Cohesion (psf)	Friction Angle (Degrees)
Municipal Solid Waste	60	–	200	30°	200	30°
Weathered Clay	100	–	1000	0	1000	0
Marine Clay, 60+	–	90	400	0	400	0
Marine Clay, 20-60'		95	400	0	750	0
Liner	50	50	0	10	0	10

* CU TEST

SEISMIC DESIGN OF MUNICIPAL SOLID WASTE LANDFILLS Pg 1 of 4

APPENDIX B EXAMPLE PROBLEM - SEISMIC SLOPE STABILITY

EXAMPLE 3: This landfill is sited on a thick deposit of normally consolidated marine clays. The static slope stability must evaluated the impact of the rate of waste placement, e.g. the marine clays increase in strength as they consolidate under the weight of the MSWLF.

STATIC SLOPE STABILITY

CASE 1: WASTE PLACED FASTER THAN UNDERLYING CLAY CAN DRAIN. ⇒ $FS_{MIN} = 1.14$ NG ≠ FS=1.14

CASE 2: WASTE PLACEMENT STAGED TO ALLOW COMPLETE DRAINAGE OF UNDERLYING CLAY. ⇒ $FS_{MIN} = 1.43$ OK = FS=1.43

∴ WASTE PLACEMENT MUST BE STAGED !!

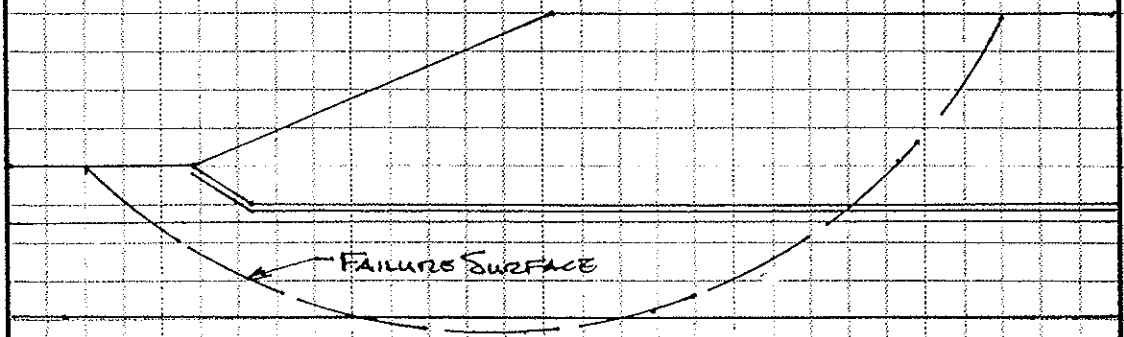

STABL DATA FILE

```
PROFILE
EXAMPLE #3 STATIC STABILITY
9 3
0. 100. 160. 100. 3
160. 100. 325. 160. 1
325. 160. 500. 160. 1
160. 100. 182. 82. 2
182. 82. 500. 82. 2
160. 99. 182. 81. 3
182. 81. 500. 81. 3
0. 80. 500. 80. 4
0. 40. 500. 40. 5
SOIL
5
60. 60. 200. 30. 0. 0. 0
50. 50. 0. 10. 0. 0. 0
100. 100. 1000. 0. 0. 0. 0
90. 90. 400. 0. 0. 0. 0
90. 90. 400. 0. 0. 0. 0
LIMITS
1 1
0. 0. 500. 0. 0.
CIRCLE
20 10
120. 300. 0. 500. 0. 10. 0. 0.
```

750 FOR CASE 2

APPENDIX B EXAMPLE PROBLEM - SEISMIC SLOPE STABILITY

EXAMPLE 3

The static analysis indicates that the critical global failure surface passes through the soft marine clays and is significantly influenced by the rate of waste placement. This means that the waste must be placed at a rate that will allow the consolidation generated pore water pressures to dissipate.

SEISMIC SLOPE STABILITY - BLOCK FAILURE AT LINER

GIVEN: • PEAK BEDROCK ACCELERATION = 0.38g
• SOFT SOIL SITE
• REFERENCE FIGURE 4.2

⇒ PEAK GROUND SURFACE ACCELERATION ≈ 0.39g
SEISMIC COEFFICIENT ≈ 0.20g

0.35g
K_s 0.2g

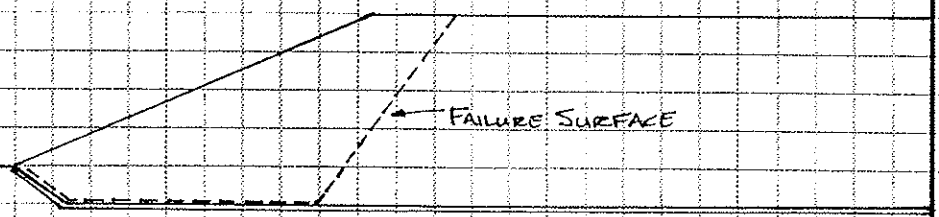


```
SOIL
5
60. 60. 200. 30. 0. 0. 0
50. 50. 0. 10. 0. 0. 0
100. 100. 1000. 0. 0. 0. 0
90. 90. 400. 0. 0. 0. 0
90. 90. 750. 0. 0. 0. 0
EQUAKE
0.20 0. 0.
LIMITS
1 1
0. 100. 160. 100.
BLOCK
50 3 10.
80. 100. 160. 100. 0.
160.5 99.5 182. 81.5 0.
182.5 81.5 500. 81.5 0.
```

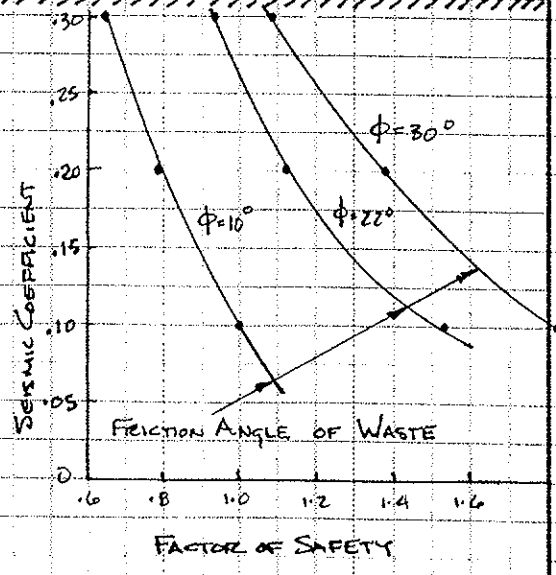

FS=1.1
$\ddot{a}_{req'd}$ = 0.26g

APPENDIX B EXAMPLE PROBLEM - SEISMIC SLOPE STABILITY

EXAMPLE 3: The pseudo-static seismic analysis indicates a block sliding factor-of-safety, FS, of 1.1 assuming ϕ = 30 degrees in the MSW. The influence of the assumed MSW internal angle of friction on the FS is shown below. The assumed MSW properties can influence the FS as significantly as the seismic coefficient.

SEISMIC SLOPE STABILITY - GLOBAL FAILURE

GIVEN: SEISMIC COEFFICIENT = 0.2g

Pg 3 GALES

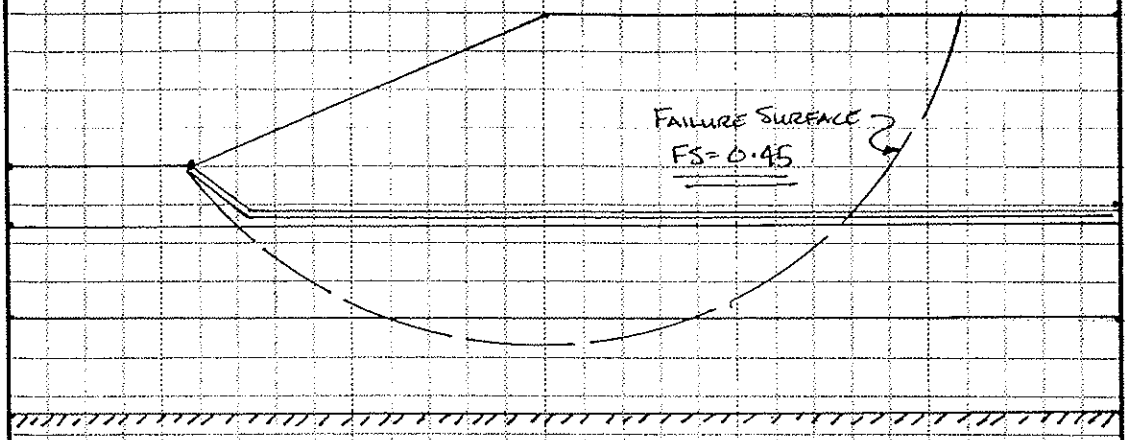

FS=0.45
NG

```
PROFILE
EXAMPLE #3 Seismic Analysis - Longterm
9 3
0. 100. 160. 100. 3
160. 100. 325. 160. 1
325. 160. 500. 160. 1
160. 100. 182. 82. 2
182. 82. 500. 82. 2
160. 99. 182. 81. 3
182. 81. 500. 81. 3
0. 80. 500. 80. 4
0. 40. 500. 40. 5
SOIL
5
60. 60. 200. 30. 0. 0. 0
50. 50. 0. 10. 0. 0. 0
100. 100. 1000. 0. 0. 0. 0
90. 90. 400. 0. 0. 0. 0
90. 90. 750. 0. 0. 0. 0
EQUAKE
0.20 0. 0.
LIMITS
1 1
0. 0. 500. 0. 0.
CIRCLE
20 10
120. 300. 0. 500. 0. 10. 0. 0.
```

APPENDIX B EXAMPLE PROBLEM - SEISMIC SLOPE STABILITY
EXAMPLE 4: MSWLF Displacement Analysis

Background

An MSW landfill is founded on 40 m (130 ft) of silt and clay soil with an average shear wave velocity of 200 m/s (660 ft/s). The landfill has a geomembrane in the base liner and cover. The weak layer in the base liner is anticipated to be at the filter geotextile / operations layer interface. The weak layer in the cover is anticipated to be at the filter geotextile / vegetative layer interface. Stability analyses show yield acceleration (horizontal acceleration for FS = 1.0) equal to k_y = 0.10 g for base liner and k_y = 0.07 g for the cover. Algermissen map (USGS Map MF-2120) shows the MHA for a hypothetical bedrock outcrop at the site equals 0.12 g. The regional seismicity source zone map (Fig. 3.2) reveals the maximum earthquake magnitude to be M 6.4.

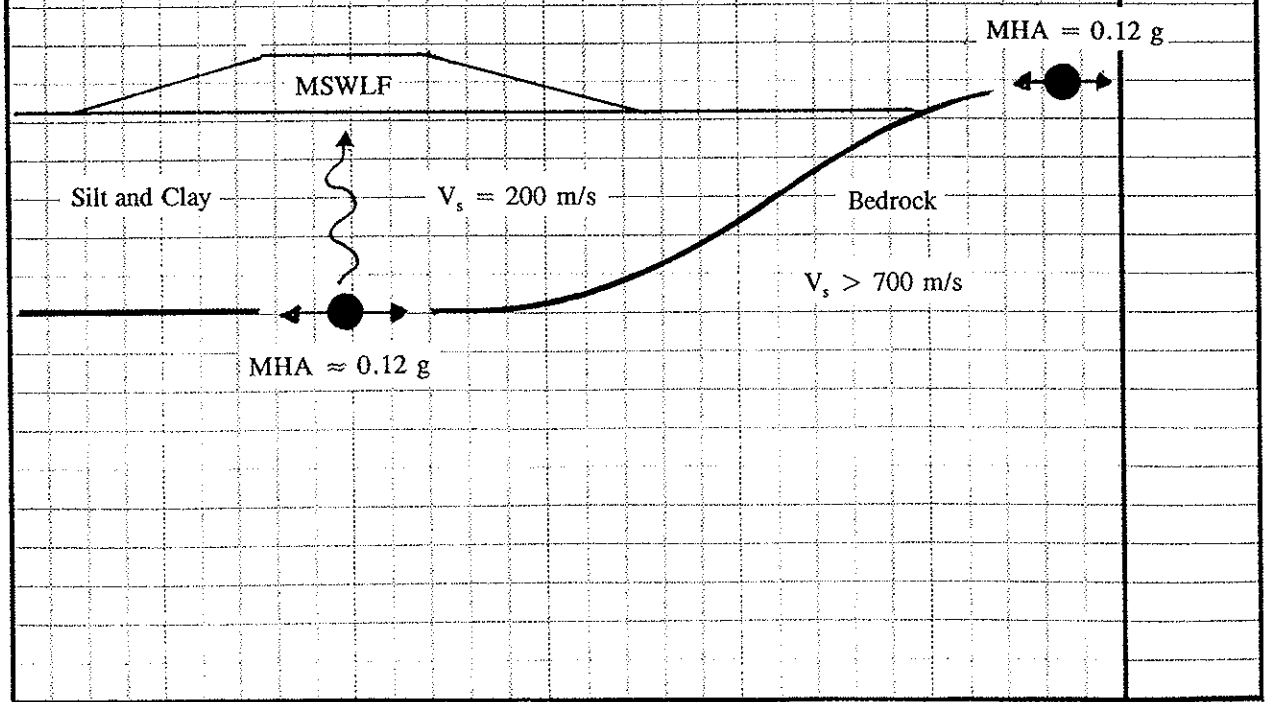

APPENDIX B EXAMPLE PROBLEM - SEISMIC SLOPE STABILITY
EXAMPLE 4: MSWLF Displacement Analysis

Liner Stability Evaluation

Step 1 Find the free-field peak ground acceleration (PGA) at the ground surface using Seed and Idriss (1982) charts.
From Fig. 4.4b (or from Fig. 4.5), for MHA = 0.12 g, PGA ≈ 0.23 g.

Step 2 Compare PGA to k_y.
k_y is less than PGA. Therefore, a deformation analysis is required.

Step 3 Estimate liner deformation (i.e., the maximum permanent displacement, u_{max}), as function of PGA and k_y using Makdisi and Seed (1978) charts.
Using upper bound of the M 6.5 area in Fig. 6.6, for k_y / PGA = 0.41 and M 6.5, a value for u_{max} of approximately 20 cm (8 in.) is estimated.

Step 4 Determine if the estimated u_{max} value is acceptable.
The landfill is an area fill with essentially a flat base and no penetrations through liner. The weakest interface (interface for which k_y is calculated) is between the operations layer and geotextile. Therefore, based upon engineering judgement, the calculated deformation of 20 cm (8 in.) is considered acceptable.

Cover Stability Evaluation

Step 1 Find the maximum acceleration (a_{max}) at the top of the landfill using the Idriss (1990) chart.
Using the recommended median relationship from Fig. 4.4b (or from Fig. 4.5) and the PGA of 0.23 g from Step 1 of the liner stability evaluation, an a_{max} value of approximately 0.32 g is estimated at the top of the landfill.

Step 2 Compare a_{max} to k_y.
Since k_y for cover is less than 0.5 · a_{max}, a seismic deformation analysis is required.

Step 3 Estimate cover deformation as function of a_{max} and k_y using Hynes and Franklin (1984) charts.
Using mean + σ curve from Fig. 6.5, for k_y / a_{max} = 0.22, the u_{max} value of approximately 20 cm (8 in.) is estimated.

Step 4 Determine if estimated u_{max} value is acceptable.
The critical (lowest yield acceleration) surface in the cover is anticipated at the filter geotextile / vegetative layer interface on the side slopes. Since all vertical gas wells that penetrate the composite cover are on the horizontal deck, the estimated cover deformation of 20 cm (8 in.) is considered acceptable.

United States
Environmental Protection Agency
Center for Environmental Research Information
Cincinnati, OH 45268

Official Business
Penalty for Private Use
$300

EPA/600/R-95/051

Please make all necessary changes on the below label, detach or copy, and return to the address in the upper left-hand corner.

If you do not wish to receive these reports CHECK HERE ☐; detach, or copy this cover, and return to the address in the upper left-hand corner.

BULK RATE
POSTAGE & FEES PAID
EPA
PERMIT No. G-35